Tsunami deposits of the Caribbean – Towards an improved coastal hazard assessment

Max Engel, Jan Oetjen, Simon Matthias May, Helmut Brückner

PII: S0012-8252(16)30375-0
DOI: doi: 10.1016/j.earscirev.2016.10.010
Reference: EARTH 2336

To appear in: *Earth Science Reviews*

Received date: 13 April 2016
Revised date: 25 October 2016
Accepted date: 26 October 2016

Tsunami deposits of the Caribbean – towards an improved coastal hazard assessment

Max Engel[1], Jan Oetjen[1,2], Simon Matthias May[1], Helmut Brückner[1]

[1]Institute of Geography, University of Cologne, Albertus-Magnus-Platz, 50923 Köln, Germany

[2]Institute of Hydraulic Engineering and Water Resources Management, RWTH Aachen, Mies-van-der-Rohe-Str. 17, 52056 Aachen, Germany

Abstract

Coasts worldwide experience considerable population pressure and the demand for reliable hazard management, such as of tsunamis, increases. Tsunami hazard assessment requires information on long-term patterns of frequency and magnitude, which are best explained by inverse power-law functions. In areas with a short historical documentation, long-term patterns must therefore be based on geological traces. The Caribbean tsunami hazard is exemplified by more than 80 events triggered by earthquakes, volcanic activity, or mass wasting within the region or in the far-field during the last 520 years. Most of these tsunamis had regional or local impacts. Based on two numerical hydrodynamic models of tsunamis spawning at the Muertos Thrust Belt (MTB) and the South Caribbean Deformed Belt (SCBD), which are two scenarios only marginally considered so far, we show that pan-Caribbean tsunamis can also be taken into account. We furthermore review almost 60 sites for possible geological evidence of tsunamis in the Caribbean including fine-grained subsurface deposits and subaerial coarse clasts, and re-evaluate their implications for tsunami hazard assessment against state-of-the-art models of onshore sediment deposition by tsunamis and extreme storms. The records span the mid- to late Holocene, with very few exceptions from of Pleistocene age.

Only a limited number of reliable palaeotsunami records with consistent and robust age control were identified, hampering inter-island or interregional correlation of deposits of the same event. Distinguishing between storm and tsunami transport of solitary boulders is very difficult in most cases, whereas those clasts arranged as ridges or incorporated into polymodal ridge complexes, which line many windward coasts of the Caribbean, can mainly be attributed to long-term formation during strong storms, overprinting potential tsunami signatures. The quantification of tsunami flooding parameters such as flow depth, inundation distance or flow velocities, by applying inverse and forward numerical models of sediment transport is still very limited and needs to be extended in the future. Likewise, sediment-derived hazard implications still await implementation in spatial planning. As extreme-wave deposits are clearly understudied in the

Caribbean, there is great potential for coastal hazard assessment to be developed and improved. Thus, further studies using common standards of high-resolution methods of bedform and stratigraphical documentation and robust chronological models with independent age control, combined with refined inverse and forward models of sediment transport and deposition are required to reconstruct reliable patterns of magnitude and frequency of palaeotsunamis in the Caribbean and to map hazard-prone areas. To date, known palaeotsunami deposits from the Caribbean probably represent only a fraction of actually happened prehistoric tsunamis and, therefore, do not reflect major tsunami inundations of the past adequately.

Keywords: Tsunami deposit; Storm deposit; Palaeo-tsunami research; Holocene; Coastal hazard management; Caribbean Basin

1. Introduction

Coasts around the globe experience high population growth, resulting in an increasing number of humans exposed to hazards associated with the sea and continental margins (Brückner, 2000; Adger et al., 2005). With more than 700 islands and 55,383 km of coastline (UNEP, 2004), and most of its population, infrastructure, and tourist facilities concentrated in close proximity to the sea (McGregor and Potter, 1997; von Hillebrandt-Andrade, 2013), the Caribbean region is disproportionally vulnerable to coastal hazards (Fitzpatrick, 2012).

The traditional triad of rapid-onset hazards in the Caribbean, as perceived some decades ago and summarized in Tomblin (1981), comprises earthquakes, volcanism and hurricanes. This was once more exemplified by the devastating earthquake of Haiti in 2010 with a death toll of more than 230,000 (Bilham, 2010; Fritz et al., 2013), the eruption of Mount Pelée on Martinique in 1902, which destroyed the former principal town of the island and killed around 28,000 inhabitants (Tanguy, 1994), and the Great Hurricane of 1780 with a similar number of fatalities along the Lesser Antilles island arc (Rappaport and Fernandez-Partagas, 1997).

However, history tells that the Caribbean is also highly susceptible to the hazard of tsunamis, which is closely linked to the high seismic activity and volcanism, coastal and submarine landslides, and teletsunamis generated in the open Atlantic Ocean. Even though 127 potential tsunamis were revealed for the Caribbean by O'Loughlin and Lander (2003) based on historical accounts (Fig. 1), the Caribbean is still lacking well-founded information regarding long-term occurrence patterns of high-magnitude tsunamis (Rowe et al., 2009). However, a regional early warning system has been installed for the Caribbean and adjacent regions, relying on more than

115 seismic stations, 55 sea-level stations, five DART buoys, detailed local evacuation maps, as well as several community engagement programs (von Hillebrandt-Andrade, 2013).

→ Fig. 1 (Tectonic overview)

Similar to other types of natural hazards (Korup and Clague, 2009; Corral et al., 2010), frequency-magnitude patterns of tsunamis can be explained best by inverse power-law functions, but without upper truncation (Burroughs and Tebbens, 2005). The tsunami record of the Caribbean (1498–2014) (NGDC/WDS, 2015) is mainly compiled of a rather low number of non-verifiable eyewitness observations on tsunami height, which usually do not distinguish between wave height, flow depth and run-up height. While this record matches the power-law function inadequately, the fit of the larger, global dataset for the same time period is much better (Fig. 2a). By disregarding run-up measurements and unspecific eyewitness records and only considering tide-gauge measurements as well as flow depth and tsunami height derived from post-tsunami measurements from the global dataset, the confidence level rises to >0.95 (Fig. 2b), therefore corroborating the inverse power-law relationship.

→ Fig. 2 (Frequency-magnitude relationships)

The spatial distribution of tsunami hazard in the Caribbean based on historical accounts and instrumental data is irregular, focusing on the Greater Antilles islands of Jamaica, Hispanola, and Puerto Rico, followed by the Lesser Antilles island arc (Zahibo and Pelinovsky, 2001; Parsons and Geist, 2009) (Fig. 3). Nevertheless, a number of uncertainties are associated with these data:

- Information on historical tsunamis or earthquakes is mainly based on colonial reports. These reports have to be considered incomplete, since population density was lower and thus events may have occurred unnoticed. Civil authorities only noted events if they severely affected the economic activities of the colony (O'Loughlin and Lander, 2003).
- The quality and reliability of sources on tsunami occurrence varies greatly, partly due to the fact that the concept of tsunamis and their trigger mechanisms were not well understood in the past (O'Loughlin and Lander, 2003).
- Historical documentation of Caribbean tsunamis covers the last 517 years, which is exceeded by recurrence intervals of highest-magnitude tsunamis in other parts of the world (Jankaew et al., 2008; Brill et al., 2012; Sawai et al., 2012).

The effects of tsunamis along the Caribbean coasts prior to the era of historical and instrumental documentation can only be traced by their telltale deposits stored in a variety of sedimentary archives. These records often cover several millennia and have the potential to significantly add to the development of coastal hazard assessment by providing insight into approaching directions of tsunamis and long-term occurrence patterns (Scheffers and Kelletat, 2006; Weiss and Bourgeois, 2012; Switzer et al., 2014), even though they may be biased by limited sediment preservation potentials (Szczuciński, 2012; Spiske et al., 2013) or very dynamic coastal environments influencing patterns of onshore deposition by extreme waves over short time (May et al., 2015a). Tsunami deposits help to delineate areas prone to tsunami flooding, which is essential to analyse exposure and vulnerability, calculate potential losses and develop site-specific mitigation concepts (Fig. 4). Against this background, this paper aims at providing a first comprehensive review of deposits which are potentially related to tsunami-induced flooding in the Caribbean region. We furthermore present new hydrodynamic models for major tsunamis potentially related to these deposits and compile implications for regional coastal hazard assessment.

→ Fig. 3 (Sectors and tsunami/hurricane hazard)

2. Tsunamis and their onshore deposits

Telltale deposits of tsunamis usually comprise a coarser spectrum than their vertically confining background sediments. They can be found both onshore (Peters and Jaffe, 2010; Brill et al., 2012; Goff et al., 2012; Spiske et al., 2013) and offshore (Sugawara et al., 2008; Feldens et al., 2012; Tamura et al., 2015) and are separated into fine-grained (clay, silt, sand, pebble) (Goff et al., 2012) and coarse-clast (pebble, cobble, boulder, block) (Goto et al., 2010; Etienne et al., 2011) deposits, depending on sediment sources, coastal geomorphology, flow patterns, and local preservation potential. Fine-grained tsunami deposits are usually left and preserved in sediment sequences of coastal lakes (Minoura et al., 1994), lagoons (Minoura and Nakaya, 1991), floodplains (Nanayama et al., 2000; Jaffe et al., 2003) or swales associated with beach and barrier coasts (Jankaew et al., 2008; Brill et al., 2012), muddy coasts (Jaffe et al., 2003; Spiske et al., 2013) or deltas (Bourgeois and Johnson, 2001) and estuaries (Lario et al., 2010). Coarse-clast deposits are found along (mostly emerging) rocky shores (Scheffers and Kelletat, 2003; Bourgeois and MacInnes, 2010; Etienne et al., 2011) and adjacent lowlands (Goto et al., 2010), on coral reef flats (Goto et al., 2010; Terry et al., 2013; Lau et al., 2014), but also on beaches, for instance in case of beachrock clasts (Terry et al., 2013), or inside shallow salt ponds and salt flats backing coral reefs (Atwater et al., 2012). In the Caribbean, morpho-sedimentary archives can be separated into intertidal to highly elevated carbonate platforms including reef flats and karst sinkholes, as well as mangrove swamps, lagoons, coastal lakes and backbarrier mudflats (see categories A–F in Fig. 4), exemplified by the Lac Bai area on the south Caribbean island of Bonaire (Fig. 5).

2.1. Fine-grained tsunami deposits

Common features of tsunami deposits include erosional basal contacts, buried plants or soils, basal load structures, rip-up clasts, landward fining, cross bedding, multimodal grain size distribution, poor sorting, heavy mineral lamination, heavy metal contamination (limited to recent examples), macro- and microfossil remains representing a broad range of habitats and states of preservation, high amounts of reworked benthic marine diatoms, a basal traction carpet, one or several fining-upward sequences with mud caps coinciding with the number of tsunami waves or even representing backwash, potentially intercalated with ungraded sections, abrupt changes in pollen concentration and composition, or a marine geochemical signature. Their thickness usually ranges from millimeters to several decimeters (see details in Table 1). Many of the features are highly site-dependent and determined by the hydraulic characteristics of the tsunami, available sediment sources, local topography and bathymetry, and post-depositional changes (Kortekaas and Dawson, 2007; Morton et al., 2007; Sugawara et al., 2008; Mamo et al., 2009; Lario et al., 2010; Peters and Jaffe, 2010; Engel and Brückner, 2011; Moore et al., 2011; Goff et al., 2012; Szczuciński, 2012).

Preservation of tsunami deposits mostly depends on the mineralogical composition, the onshore geomorphic setting, rainfall regime, vertical tectonic movement and anthropogenic impact (Spiske et al., 2013). Tsunami deposits exposed subaerially in tropical carbonate environments, which prevail in the Caribbean, seem to have a limited potential of preservation due to reworking, carbonate dissolution and bioturbation (Nichol and Kench, 2008; Szczuciński, 2012).

Even though tsunamis differ significantly in hydraulic characteristics from other extreme inundation processes such as storm surges, both their deposits show many similarities, which often impedes unequivocal interpretation (Table 1). It is generally accepted that the presence of distinct sub-units created by runup and backwash is associated with tsunamis, and that tsunami deposits lack foreset bedding (Nanayama et al., 2000), which is very common in subaqueous storm-induced washover deposits (Sedgwick and Davis, 2003; Brill et al., 2016). Internal mud drapes, often vertically confining graded tsunamigenic sand beds, have not been reported from storm deposits (Komatsubara and Fujiwara, 2007; Morton et al., 2007). Furthermore, the landward extent of tsunami deposits tends to be larger compared to storms (Morton et al., 2007; Brill et al., 2016), and they often have a larger source area comprising deeper waters, which might be reflected by a broader range of microfaunal remains (Mamo et al., 2009; Uchida et al., 2010;

Goff et al., 2012). Thus, identifying the origin of a candidate tsunami deposit requires consideration of a broad variety of factors, including the “tsunami potential” of a region. It is most valuable to have reference deposits from either modern or historically well documented tsunami or severe storm events, to ensure the best deduction as to a deposit's origin (Engel and Brückner, 2011).

2.2. Coarse-clast tsunami deposits

The size and pattern of boulder accumulations of tsunamis are mostly determined by flow velocity, availability of material, surface roughness, the pre-transport setting, coastal topography, rock density, shape and particle-particle interaction (Bourgeois and MacInnes, 2010; Etienne et al., 2011; Weiss, 2012; Terry et al., 2013). In carbonate reef settings and steep offshore bathymetries, as typically found in the Caribbean, tsunami gravel and boulder fields show rather abrupt landward boundaries instead of exponential landward fining as observed for boulder fields created by tropical cyclones (Goto et al., 2010; Etienne et al., 2011; Watt et al., 2012a; Lau et al., 2014). The formation of polymodal ridge complexes or ramparts, respectively, a common landform built up during strong storms, has not been directly observed for tsunamis (Etienne and Paris, 2010; Etienne et al., 2011; Richmond et al., 2011) though it was suggested in some places (Scheffers and Kelletat, 2003) (Table 2). The main axis of large boulders tends to arrange perpendicular to the flow direction and can be used to infer the approaching angle and a possible event source (Terry et al., 2013). Several studies assume that the capacity of a tsunami to transport very large boulders is significantly higher than in storms (Nott, 2003; Barbano et al., 2010; Benner et al., 2010; Engel and May, 2012), whereas this view has recently been challenged (Weiss, 2012). In particular, the coarse-clast record of Typhoon Haiyan (7–9 November 2013) on Eastern Samar (Philippines) showed that infragravity waves created by the interaction of groups of high and steep storm waves with fringing reefs reach transport capacities similar to tsunamis (May et al., 2015b). In cliff-top positions, vertical jets may support the transport of very large boulders during storms (Cox et al., 2016)

→ Fig. 4 (Coastal hazard management process)

→ Fig. 5 (Examples of morpho-sedimentary archives)

2.3. The challenges of dating event deposits

In order to use deposits to establish long-term frequency patterns of tsunamis, they need to be dated accurately. Age estimates of fine-grained Holocene tsunami deposits are usually derived from ^{14}C dating. Where quartz or feldspar is dominant and luminescence properties are suitable, optically stimulated luminescence (OSL) can be used (e.g., Brill et al., 2012), even for deposits from the last interglacial. In subrecent contexts, ^{137}Cs has been applied successfully (e.g., Barra et al., 2004). Method-specific uncertainties, such as the reworking of dated organisms and/or varying reservoir effects in time and space in the case of ^{14}C (e.g., May et al., 2015a; Adomat and Gischler, 2016) or partial bleaching in the case of OSL (e.g., Bishop et al., 2005; Brill et al., 2012), still complicate the establishment of chronostratigraphies. Embedded into a stratigraphic sequence, dating of fine-grained tsunami deposits can also be supported by reliably dated volcanic ash layers (e.g., Sawai et al., 2012) or diagnostic archaeological remains (e.g., Rajendran et al., 2011).

Since subaerial boulder deposits lack stratigraphic contexts in most cases, it is much more difficult to date the timing of their transport. Marine organisms attached to boulders, such as boring molluscs, vermetids or serpulids, are dated by ^{14}C (e.g., Barbano et al., 2010; Biolchi et al., 2016), but only provide maximum ages and are prone to uncertainties imposed by diagenetic processes (Douka et al., 2010). Along reef-dominated coasts, U/Th is preferred over ^{14}C or electron spin resonance (ESR) for dating coral material (Schellmann et al., 2011; Scheffers et al., 2014). In temperate regions, lichenometry has been applied for relative age dating on decadal scales (Hall et al., 2006). Attempts to directly date boulder transport onshore by surface exposure dating (^{36}Cl) are currently being developed (e.g., Rixhon et al., 2016), whereas Sato et al. (2014) revealed cautiously optimistic results through the application of palaeomagnetic dating. Hearty (1997) used amino acid racemisation (AAR) on carbonate boulders, though this approach permits only relative age estimations for the age of the substrate. In the near future, OSL surface exposure dating (Sohbati et al., 2012) might represent an alternative tool for dating boulder transport in the Holocene.

2.4. Deposits of recent extreme-wave events in the Caribbean

In the Caribbean, no sedimentological post-tsunami documentation has ever been carried out. Zahibo et al. (2005) and Le Friant et al. (2008) conducted field surveys following the small 21 November 2004 tsunami generated by shallow normal faulting between Basse-Terre (Guadeloupe) and Dominica. Besides observations on water-level changes, run-up and inundation on Les Saintes and southern Basse-Terre based on debris and eyewitness interviews, no account is made for sedimentation or erosion features. Similarly, Fritz et al. (2013) only recorded characteristics and inundation patterns of the twin tsunamis following the 12 January 2010 Haiti Earthquake. Geomorphic and sedimentary impacts of the 11 October 1918 tsunami in the Mona Passage west of Puerto Rico are briefly touched upon by Reid and Taber (1919, p. 111), who describe the beach near Point Agujereada as “turned into a sandy waste” by a 5.5–6 m-high wave. Rectangular blocks (>1 t) shifted for several tens of metres inland and slightly downslope by a >4 m wave southwest of Aguadilla.

Sedimentary effects of recent strong storms representing the most important alternative mechanism of episodic coastal deposition and erosion are much better documented. Atwater et al. (2014) surveyed effects of Hurricane Earl (30 Aug 2010, Saffir-Simpson hurricane scale [SSH] category 4) on Anegada, British Virgin Islands. They found limited sediment deposition, mostly in the form of small washover fans along the south coast and redistribution of microbial detritus in salt ponds, which stands in stark contrast with extensive deposits of palaeo-wave events on the island. The hurricane waves induced only limited reworking at pre-existing coral rubble ridges on the north shore (Spiske and Halley, 2014). Based on further monitoring, Spiske (2016) inferred, however, that these intertidal to supratidal ridges also experience modification during tropical storms and low-category hurricanes.

→ Table 1 (Sand-dominated tsunami and storm deposits)

→ Table 2 (Coarse clast tsunami and storm deposits)

All around the coast of Jamaica, pre-existing clasts were shifted during Hurricane Dean (19 August 2007, SSH category 4), including one cliff-top boulder of 80 t, which moved horizontally for a few metres (Khan et al., 2010). Caron (2012) surveyed effects of Hurricanes Omar (16 Oct 2008) and Earl on a beach of southwest St. Bartholomew, where massive erosion of sand- and granule-sized sediment occurred and previously covered beachrock became exposed.

After Hurricane Lenny (16 November 1999, SSH category 4), Scheffers (2005) found coral-rubble ridges consisting to 20–30% of freshly broken material, up to 1 m high and 8 m wide, with small lobate washover structures, piled up by the storm waves on the leeward coast of Bonaire (Leeward Antilles). A new coral-rubble spit was created and later modified by Hurricane Ivan (15–16 September 2004, SSH category 5), which created wave heights of up to 12 m at the coast of Bonaire (Scheffers, 2005; Scheffers and Scheffers, 2006) and other Caribbean islands (Stewart, 2004), as well as maximum wave heights of up to 28 m measured by buoys on the shelf of the Gulf of Mexico (Wang et al., 2005). At Playa Funchi, northeast Bonaire, Lenny created a 1.5 m high and 26 m wide ridge with separate units indicating inflow and return flow by the orientation of imbricated clasts (Spiske and Jaffe, 2009). Hurricane Ivan induced erosion of pre-existing polymodal ridges in the southeast, as well as flattening or seaward steepening of pre-exisiting ridges in the northwest. Sands were redistributed to sand sheets and single boulders of up to 25 t were dislodged on top of the elevated palaeo-reef platform in the northeast, whereas other boulders of up to 6 t were detached and moved in saltation mode (Scheffers and Scheffers, 2006).

3. Physical setting and tsunami triggers of the Caribbean

The geographical entity of the Caribbean comprises the Caribbean Plate and adjacent coastal areas (Fig. 1). It includes the Greater Antilles (Cuba, Jamaica, Hispaniola, Puerto Rico) and the more eastern and southern Lesser Antilles, the Bahamas and Turks and Caicos Islands, as well as the coastlines of eastern Central America, northern Colombia and northern Venezuela (UNEP, 2004). The Caribbean Sea is the Atlantic Ocean's largest marginal sea ($1.52 \cdot 10^6$ km^2), has a mostly microtidal regime and an average depth of 4400 m (Gallegos, 1996).

3.1. Triggers of tectonic tsunamis

3.1.1. Historical scenarios

The Caribbean Basin is characterized by very active geodynamics. Eastward migration of the Caribbean Plate (CP) relative to the North (NAP) and South (SAP) American Plates (Cenozoic offset c. 1000 km) creates the Lesser Antilles subduction zone (LASZ) in the east and complex patterns of strike-slip processes in the north and south (Fig. 1) (Meschede and Frisch, 1998). Neotectonic uplift during the Holocene is generally moderate (Fairbanks, 1989; Milne and Peros, 2013). At the LASZ, the NAP and SAP are subducted at a rate of c. 2 cm a^{-1}. Seismic activity occurs where the plates interact during subduction, deeper down along the dipping slab, and within the CP (Harbitz et al., 2012). The maximum magnitude of an earthquake at the LASZ in historical times is estimated at 7.5–8, released by the 8 February 1843 megathrust intraplate earthquake between Antigua and Grand-Terre (Guadeloupe) (Feuillet et al., 2011). In general, the seismic hazard is considered to be moderate to large as the age and density of the oceanic lithosphere and the rather slow subduction rate lower the expected maximum magnitudes (Harbitz et al., 2012). However, Hayes et al. (2014) found that sufficient strain is accumulated in the LASZ offshore of Guadeloupe for a tsunamigenic earthquake of $M_w \sim 8.2 \pm 0.4$. In the southeast basin, the Motagua/Swan Islands Fault System has generated earthquakes of M 7–8 and associated tsunamis in the Gulf of Honduras on 9 August 1956 and c. AD 900 inferred from coseismically uplifted coastal landforms (Cox et al., 2008).

Further scenarios, which are (i) commonly associated with the Caribbean tsunami hazard, (ii) based on the historical record, and (iii) were reconstructed by means of numerical hydrodynamic models in the past (Zahibo et al., 2003; Lopez-Venegas et al., 2008; ten Brink et al., 2008; Barkan and ten Brink, 2010; Harbitz et al., 2012) include:

- Devastating shallow earthquakes through strike-slip faulting along the northern boundary of the CP, exemplified by the 12 January 2010 Haiti earthquake (Bilham, 2010; Fritz et al., 2013).
- Oblique convergence at the tip of a strike-slip fault, in particular near Hispanola and Puerto Rico (Grindlay et al., 2005; Harbitz et al., 2012).
- Strike-slip faults or parallel normal fault systems along the steep submarine slopes of the northern CP boundary potentially activating tsunami-triggering slumps, such as during the 11 October 1918 tsunami in the opening Mona Passage (Moya and Mercado, 2006; Hornbach et al., 2008b; López-Venegas et al., 2008). Faults are created due to a difference in migration rates between the Hispanola (slower) and the Puerto Rico-Virgin Islands-Aves Island (faster) areas (Mann et al., 2002).
- Complex tectonic deformation patterns between the Virgin Islands and the Lesser Antilles island arc, resulting in one of the strongest historical tsunamis of the Caribbean in November 1867 (Zahibo et al., 2003; Barkan and ten Brink, 2010).
- The CP-SAP boundary, which is a >100 km transpressional boundary running on- and offshore. Its main source of seismicity is the dextral strike-slip El Pilar fault. Earthquakes generated along the submarine fault segments reached M_s 7.1–7.3 in 1530 and 1853 (Audemard, 2007) and M_w 7.6–7.7 in 1900 (Colón et al., 2015). However, the resulting regional tsunamis (O'Loughlin and Lander, 2003; Harbitz et al., 2012) may have been enhanced through submarine landslides along the offshore fault segment (ten Brink et al., 2008).

3.1.2. Numerical modelling of scenarios unprecedented in historical times

Only recently, earthquakes along the active Muertos thrust belt (MTB) extending south of eastern Hispanola and Puerto Rico were identified as a potential, major tsunamigenic source (Fig. 1). The low-angle subduction thrust belt, a deformation zone of 250 km width, is a direct result of oblique CP-NAP convergence inducing a complex pattern of transtension, transpression, and microplate tectonics (Granja Bruña et al., 2014), as well as collision with the southeastern Bahamas platform (Mann et al., 2002). High-magnitude earthquakes and related tsunamis are anticipated by Granja Bruña et al. (2014), if the active thrust faults of the MTB rupture along their entire length.

The South Caribbean Deformed Belt (SCDB) represents an underthrust margin of the Colombian Plain, the largest abyssal zone of the Caribbean (Draper et al., 1994), and separates the Leeward

Antilles terrane from the CP (Fig. 1). Similar to the MTB in the north, oblique CP-SAP convergence drives the deformation process, focused along the northern margin of the SCDB (Donovan, 1994). Its potential tsunami hazard remains ambiguous and only very few shallow, minor offshore earthquakes have been recorded between 1976 and 2007. Nevertheless, ten Brink et al. (2008) suggest a low-probability, "worst-case" scenario of >500 km tsunamigenic thrust faulting along the SCDB, a scenario adapted for the Caribbean-wide tsunami warning exercise in 2013 (UNESCO, 2012).

We created hydrodynamic models of both the MTB and SCDB tsunami scenarios using Delft Dashboard and Delft3D-Flow (4.01.00) software. Both models have the same rectangular numerical grid of 597,723 cells (1027 x 583 cells, cell size 5 km x 5 km) and bathymetric setting (GEBCO08). The grid expands over nearly the whole Caribbean Sea from 6°41'42"N, -87°42'54' E to 24°11'6"N, -56°54'18"E. Boundary conditions along the four open boundaries are set to Riemann conditions. The tsunami wave is generated utilizing the Delft Dashboard tsunami toolbox and the Okada model (Okada, 1985). It is further based on rupture parameters mainly adapted from ten Brink et al. (2009) for the MTB, and from ten Brink et al. (2008) and UNESCO (2012) for the SCDB (Table 3). The computational time step is set to 0.01 min. Outputs are derived for 1 and 2 min, respectively, at all 138 observation points. The MTB model output indicates a moderate tsunami hazard with coastal wave heights mostly below 0.5 m and a maximum of 0.8 m on Aruba (Fig. 6). In contrast, a tsunami generated at the SCDB poses a hazard both for the central northern and central southern Caribbean shores. Wave heights at the coast would reach up to 4.6 m on southern Hispanola, up to 3.5 m at the Venezuelan coast, and up to 3.2 m along the windward ABC Islands (Fig. 7).

→ Fig. 6 (Tsunami scenario MTB)

→ Fig. 7 (Tsunami scenario SCDB)

3.2. Volcanism, volcanic edifice failure and landslides

Volcanic tsunamis are triggered by volcano-tectonic earthquakes, volcano edifice collapse, pyroclastic flows, underwater explosion and shock waves. They are less frequent than seismic tsunamis (Paris, 2015). Twenty-one active volcanoes occur along the Lesser Antilles island arc. Tsunamis of short periods but pronounced local impact may be generated in the region by direct explosive activity, onshore or underwater, either by associated atmospheric pressure disturbances, or pyroclastic flows, lahars, or debris avalanches entering the ocean (Pararas-

Carayannis, 2004). The submarine Kick 'em Jenny volcano, which is currently situated c. 150 m below the water surface off the Grenadine Islands, currently represents the greatest hazard. Eleven eruptions were recorded since 1939 which triggered several local tsunamis (Smith and Shepherd, 1995; Pararas-Carayannis, 2004). Possible violent eruptions in the future may reach run-ups of up to 8 m on northern Grenada and the Grenadines (Smith and Shepherd, 1995).

Large submarine structures of volcanic debris mostly resulting from volcanic flank failure of late Quaternary age frame several active volcanic islands, such as Montserrat, Martinique, St. Lucia, St. Vincent or Dominica, and possibly have triggered major tsunamis during downslope transport (Deplus et al., 2001; Le Friant et al., 2009, Lebas et al., 2011; Watt et al., 2012b; Brunet et al., 2015). Massive amphitheatre-shaped scarps identified at the southern margin of the Puerto Rico Trench indicate, according to Grindlay et al. (2005), the occurrence of giant submarine slumps and tsunamis comparable to the early Holocene Storegga event off Norway. Further substantial mass wasting deposits have been identified along the coasts of Trinidad and Venezuela (Moscardelli et al., 2010). On Curaçao, a large and partly subaerial mass failure event created the c. 1 km wide Caracasbaai and apparently induced a large tsunami at the end of Marine Isotope Stage (MIS) 5e (Hornbach et al., 2008a, 2010). Recently, Leslie and Mann (2016) pointed to three massive Neogene-Pleistocene mass-transport deposits offshore northern Columbia potentially indicating an additional threat of major tsunamis for the southwest and north Caribbean. Alfaro and Holz (2014) identified mud diapirism and gas hydrates to foster slope destabilisation in this area.

3.3. Teletsunamis

The hazard of teletsunamis generated in the open Atlantic Ocean became evident after the 1755 Lisbon Earthquake, which generated run-ups of up to 6.4 m on the northern Lesser Antilles island arc (ten Brink et al., 2008; Barkan et al., 2009; Harbitz et al., 2012). Scenarios of potential wave heights reaching more than 20 m on the coast of northern South America and up to 10 m along the Lesser Antilles island arc following a possible future collapse of the Cumbre Vieja volcano on La Palma, Canary Islands (Ward and Day, 2001), have been challenged by Hunt et al. (2013), who demonstrate that failures of such volcanic edifices usually occur in several stages and not as one giant slide. A recent study, however, indicates a potential hazard of megatsunamis for the Atlantic basin based on observations of large boulders high up on the slopes of Santiago (Cape Verde Islands), which supposedly were dislocated after a giant late Pleistocene volcanic flank collapse on the adjacent island of Fogo (Ramalho et al., 2015).

4. Alternative processes causing elevated coastal deposits in the Caribbean

4.1. Hurricanes

The Caribbean basin is located in the tropics of the northern hemisphere, influenced by the trade winds, and, for most parts, experiences pronounced wet and dry seasons and constantly high temperatures (Blume, 1962). High atmospheric and sea surface temperatures (SST) further east in the open Atlantic basin during the second half of the year in combination with decreasing wind shear support the transformation of easterly waves into warm-core tropical cyclones, which track westwards. A significant percentage of them cross the Caribbean as high-category hurricanes (Goldenberg and Shapiro, 1996; Hobgood, 2005). The highest hurricane frequencies are temporally associated with La Niña conditions (Caviedes, 1991), and, geographically, with the Bahamas, the southeast USA coast, Puerto Rico, the Virgin Islands, and the northern part of the Lesser Antilles island arc (Fig. 3). Frequencies decrease in a southwestern direction in roughly concentric half-circles. Nevertheless, as about ten hurricanes enter the Caribbean each year (Reading, 1990; Walsh and Reading, 1991), high-category hurricanes and associated storm surges, high waves and coastal flooding have to be taken into account for almost any coastal section of the circum-Caribbean when interpreting elevated coastal deposits. Information on fluctuations of hurricane frequencies for both the historical era (Reading, 1990; Caviedes, 1991; Walsh and Reading, 1991; Chenoweth and Divine, 2008) and the last millennia (e.g. Donnelly and Woodruff, 2007; McCloskey and Liu, 2013a; see synthesis in Adomat and Gischler, 2016) is controversial, whereas the last decades seem to have seen an increase in mean intensities and frequencies of high-category hurricanes in the North Atlantic basin related to elevated SST and associated atmospheric dynamics (Knutson et al., 2010).

4.2. Relative sea-level (RSL) changes

Relative sea level (RSL) is defined as “the level of the sea with respect to land” at a certain location (Lambeck, 2002, p. 33). Understanding RSL histories is crucial to the interpretation of the palaeotsunami record (Morton et al., 2006), as marine deposits located in elevated positions today might have been formed in an intertidal position several millennia ago where RSL falls. In the Caribbean, RSL was 121±5 m below current mean sea level (b.s.l) during the Last Glacial Maximum 20 ka BP (Fairbanks, 1989). RSL rose quickly after 15 ka BP until the early Holocene (Fairbanks, 1989; Toscano and Macintyre, 2003). A slowdown of global ice ablation around 7 ka BP stimulated the influence of regional (e.g., glacioisostatic adjustment, gravitational effects inducing deformation of the Earth, upper/lower mantle viscosity) and local (lithosome compaction, vertical neotectonic displacement) factors, and diverging RSL histories evolved (Jackson, 2013; Milne and Peros, 2013). While RSL rose between 1 mm yr^{-1} in the eastern Caribbean basin and 2.5 mm yr^{-1} in the southwestern part from 7000–4000 years ago, rates dropped below 0.5 mm yr^{-1} in the past 500 years (Jackson, 2013). However, no RSL higher than today has been reported for the Holocene of the Caribbean basin (Fairbanks, 1989; Toscano and Macintyre, 2003; Jackson, 2013; Milne and Peros, 2013). Therefore, elevated marine deposits of Holocene age can generally be attributed to extreme-wave conditions.

5. Tsunami deposits of the Caribbean

By reviewing almost 59 published coastal sedimentary records for potential fine-grained (Table 4) and coarse-clast (Table 5) tsunami deposits, we divided the Caribbean basin into five different sectors (Fig. 3). The sedimentary evidence was classified into six categories following the interpretation given in the original source:

- 0 = no allochthonous deposits or disturbances present in the stratigraphy;
- 1 = allochthonous deposits or other disturbances are ascribed to storm impact or gradual coastal changes. Tsunamis are excluded by the authors;
- 2 = allochthonous deposits are ascribed to storm rather than tsunami, but the latter is not entirely excluded;
- 3 = allochthonous deposits are ascribed to either storm or tsunami;
- 4 = allochthonous deposits are ascribed to tsunami rather than storm, but the latter is not entirely excluded;
- 5 = allochthonous deposits are ascribed to tsunami and storm is excluded.

Only evidence placed into categories 3 to 5 is presented and discussed here in detail.

The precision and scope in documentation of the traces of extreme-wave events in fine-grained sedimentary archives varies strongly. Literature sources range from short abstracts to highly technical reports. Studies focusing on palaeoclimate or palaeoecology, i.e. long-term or periodic sedimentation patterns, often provide only limited information on layers of episodic high-energy sedimentation and assign a lower priority to their interpretation (e.g., Dix et al., 1999; Donnelly and Woodruff, 2007; Dalman and Park, 2012; Brooks et al., 2015; Caffrey et al., 2015).

Documentation and process-related interpretation of the coarse-clast record, mostly located on rock platforms from the intertidal level to elevations of up to 20 m, usually focuses on extreme-wave events and coastal hazard assessment. Coarse-clast features have regularly been used to infer palaeotsunamis, even though intense discussions arose in some cases and diverging conclusions on the origin of the deposits exist (e.g., Grand Cayman, ABC Islands) (Jones and Hunter, 1992; Scheffers, 2002b, 2004, 2005; Morton et al., 2008a; Spiske et al., 2008; Rowe et al., 2009; Khan et al., 2010).

5.1. NW sector

A wedge-shaped berm supposedly deposited around 1500 years ago is the only sedimentary feature from the NW sector linked with a tsunami (Shaw and Benson, 2015, Site 36 on Fig. 3). It has a thick base layer of unstructured coarse sand and floating coarse clasts with overlying whitish and densely packed, reddish brown sand, gravel, and boulders. The berm extends about 50 km along the east coast of the Yucatán Peninsula. It reaches >4 m above mean sea level on headlands, where it is covered by numerous imbricated boulders with a-axes of up to 1 m length on the seaward side. At headlands, it reaches up to 150 m inland, where it gradually becomes finer, whereas behind low-lying beaches, berm deposits can be found up to 400 m from the shore. Gaps in the berm are attributed to channelized tsunami backflow (Shaw and Benson, 2015).

5.2. N sector

5.2.1. Grand Cayman

On Grand Cayman, Jones and Hunter (1992) describe boulders with a-axes of up to 5.5 m weighing up to 40 t (Site 37, Fig. 3). They are located at a distance of up to 100 m from the shoreline on an elevated carbonate platform. At Blowholes (southeast Grand Cayman), boulders are believed to have been shifted onshore c. 330 years ago based on ^{14}C ages of coral attached to a boulder, and were not moved since then. Boulders gather landward of shore-perpendicular indentations on the carbonate platform, where waves seem to become funnelled. Storm waves or tsunamis are equally considered as being capable of dislodgement (Jones and Hunter, 1992). Robinson et al. (2006) and Rowe et al. (2009) revisited the sites after Hurricane Ivan in 2004 and found many clasts relocated and partly overturned as indicated by exposed fresh, white surfaces and downward facing grass patches. Besides solitary boulders and boulder clusters, coastal deposition on Grand Cayman is dominated by pebble and boulder ramparts and mixed sand-to-boulder ridges, in particular along the south coast (Rigby and Roberts, 1976; Hernandez-Avila et al., 1977; Jones and Hunter, 1992).

5.2.2. Jamaica

Very similar patterns were found in Jamaica (Site 39, Fig. 3). Boulders at Galina (northeast Jamaica) derive from the cliff edge, weigh up to 120 t, and are clustered in a zone 80–160 m from the shore (Robinson et al., 2006), fining landward (Rowe et al., 2009). The boulders are backed by a ridge of polymodal debris, sand and mollusc shells, which is covered by boulders and separates the boulder field from the densely vegetated area inland (Robinson et al., 2006; Morton et al., 2008a; Rowe et al., 2009; Miller et al., 2014). While Robinson et al. (2006) describe their internal architecture as chaotic, Morton et al. (2008a) found particle sorting and distinct stratification in ridge exposures. At other sites, boulders of up to 200 t were found gathering inland of shoreline indentations (Robinson et al., 2006). Based on eyewitness reports and surveys after the passage of Hurricane Dean in 2007, where Khan et al. (2010) identified a limestone clast of 80 t having shifted laterally for 2 m at an elevation of 12 m above current mean sea level (a.s.l.) near Manchioneal, east Jamaica, it is anticipated that most boulders have a complex heritage of dislocation potentially covering the last 4000–5000 years and that hurricane-induced waves may be capable of shifting even the largest boulders horizontally for a short distance. Displacement by tsunami is not excluded, in particular in the case of the largest boulders, but no direct evidence exists so far (Rowe et al., 2009; Khan et al., 2010).

In addition to the coarse clast records, fine-grained deposits of extreme-wave overwash were identified in sediment cores from the enclosed lagoon of Manatee Bay on the Jamaican south coast (Site 10, Fig. 3). Whether the bioclastic carbonate sands deriving from the offshore coastal zone represent storms or tsunamis is uncertain (Palmer and Burn, 2012).

5.2.3. Bahamas

Near Glass Window on northern Eleuthera, Bahamas (Site 40, Fig. 3), Hearty (1997) was the first to investigate very large oolitic-peloidal boulders weighing up to 2330 t (Hearty, 1997), later corrected to 958 t by Viret (2008). The boulders rest on aeolianite covered by oolitic entisols at elevations of up to 20 m a.s.l. High-angle bedding, a lack of possible alternative transport mechanisms, and absence of source areas higher than the boulders are cited as evidence for transport by extreme waves. Based on stratigraphic evidence, fossil soils and inverse amino acid racemisation (AAR) ages, transport at the end of MIS 5e was inferred (Hearty, 1997; Viret, 2008; Kindler et al., 2010). Along with the heavily disputed "chevron ridges" (Hearty et al., 1998, 2002; Kindler and Strasser, 2000; Kelletat et al., 2004), the giant boulders were used as evidence for "larger and more frequent cyclonic storms in the North Atlantic than those seen today" (Hearty and Neumann, 2001, p. 1892; Hansen et al., 2016, p. 3784). Others inferred tsunami deposition during MIS 5e based on numerical modelling of a local submarine slope failure event and the assumption that storm waves have a limited transport capacity (Samankassou et al., 2008; Hasler et al., 2010).

At the east coast on southern Eleuthera (Site 41, Fig. 3), low ridges of beachrock and aeolianite slabs with a-axes of up to 3 m have formed low, imbricated ridges at elevations of up to 3 m a.s.l. overgrown by trees. Kelletat et al. (2004) assume that these ridges have remained stable for centuries. Angular boulders weighing up to 5 t are also found on the leeward side on top of an elevated carbonate platform. Further north, boulders of up to 30 t and a bimodal deposit of carbonate sand, shells and coral branches were documented behind a 15 m-high cliff and inland sloping platform. Soil formation within the sand, mature vegetation cover, and two ^{14}C ages indicate formation at least several hundred years ago. The Whale Point peninsula in the north also shows an almost continuous shore-parallel bimodal deposit and boulders of up to >300 t, with shore-parallel a-axes, mostly imbricated, arranged into ridges or fields, and separated from the shoreline by a sediment-free, 80–100 m-wide zone. Very similar findings were made on Long Island (Site 42, Fig. 3). All deposits are ascribed to two palaeotsunamis generated in the open Atlantic Ocean around 3000 and 500 years ago (Kelletat et al., 2004).

5.2.4. Dominican Republic

Coastal lagoons at Bahia de Ocoa, Dominican Republic (Site 15, Fig. 3), reveal overwash fans and three coarse sand deposits in multiple cores at varying depths, with the beach and shoreface as source areas. The overwash deposits, for which a tsunami origin is possible, also contain organic-rich clasts (Fuentes and Huérfano-Moreno, 2013). At Playa Cosón, northeast coast (Site 17, Fig. 3), a light carbonate sand layer extending up to 260 m inland was found vertically confined by non-carbonate silty clay and a thin top layer of sandy loam. It is dominated by shallow-marine foraminifera, whereas low numbers of bathyal and abyssal taxa occur as well (Scheucher et al., 2011). At Puerto Viejo, southwest coast (Site 16, Fig. 3), carbonate sand with gravel components unconformably overlies carbonate-containing loamy clay. It occurs at depths of up to 85 cm and mostly contains shallow-marine benthic foraminifera (one taxon preferring bathyal/abyssal depths), as well as an unusually high amount of planktonic taxa (c. 30%). The deposits were tentatively associated with the 8 August 1946 tsunami (Playa Cosón) and the 18 October 1751 tsunami (Puerto Viejo) (Scheucher et al., 2011).

5.2.5. Puerto Rico

In sediment cores from Aguada Plain at Carrizales, Aguada Swamp at Espinar and Aguadilla Swamp, northwest Puerto Rico (Site 18, Fig. 3), Moya and Mercado (2006) found several thin marine overwash deposits within background sediments of mud to very fine sand, all of which were linked to tsunamis. Behind the beach on coastal plains and in swamps up to c. 100 m away from the shore, thin laminated layers containing *Halimeda* sp. fragments and hematite suggest the beach as the main source area. A correlation of layers is possible between cores from one site, but also across sites. Two ^{14}C ages allow maximum age estimates of about 2770–2350 BP and 680–540 BP to be inferred for the corresponding events, whereas the uppermost deposit (<40 cm below surface in several cores) is associated with the tsunami of 11 October 1918. Morton et al. (2006) revisited the area and reported a layer of grey sand at a depth of 127–137 cm with basal concentrations of heavy minerals within a sequence of sandy mud in a mangrove wetland. Further to the east, they identified two thin strata of grey sand – the upper one showing shallow marine gastropods on top – within background muds in a wetland environment behind a breached eolianite ridge and narrow coastal plain. At Punta Cucharas, south coast (Site 19, Fig. 3), a grey sand-and-shell layer with a thickness of only 2 cm was found 1 m below a tidal flat. Depositional processes remain uncertain (Morton et al., 2006).

→ Fig. 8 (Examples of tsunami deposits)

The coastal boulder record of northwest Puerto Rico (Site 44, Fig. 3) comprises isolated rocks with a-axes of up to 1 m at a distance of 70 m from the beach inside a small creek at Punta Borinquen and a large coral (a-axis = 1.2 m) behind a breached, active coastal dune east of Punta Agujereada. Based on limited storm surge potential in the area, due to a very narrow shelf, and a strong impact of the 11 October 1918 tsunami in the Mona Passage (Reid and Taber, 1919; Lopez-Venegas et al., 2008), Moya and Mercado (2006) assume that these boulders were deposited by tsunami waves. At Isla Mona (Site 45, Fig. 3), offshore of northwestern Puerto Rico, limited information is available on several large reefrock clasts (a-axes up to 5 m) dislodged from the Holocene reef onto late Pleistocene coastal flats along the southwestern coast either during tsunamis or hurricanes. U/Th dating indicates deposition sometime after 4176 years ago (Taggart et al., 1993; Gonzalez et al., 1997).

5.2.6. British Virgin Islands

On Anegada (Site 23, Fig. 3), a multi-proxy study on disturbed beach ridges and back-barrier sediments points to an extreme-wave impact between 1600 and 1850 cal AD. Candidate events include the Antilles tsunami of 1690, the Lisbon teletsunami of 1755, a previously undocumented tsunami, or a storm surge with a magnitude greater than the most severe hurricane of the past decades. The event caused overwash and breaching of sandy barriers and deposition of a sand-and-shell sheet (Fig. 8-II), now covered by carbonate mud, as well as boulders and cobbles distributed over a large area. The sand deposit thins and fines inland to a distance of up to 1.5 km from the breached ridges. The overwash process and associated erosion and sedimentation seems to have transformed marine inlets into hypersaline, restricted ponds (Atwater et al., 2012). The taphonomy of shells and encrusting reefal foraminifera (*Homotrema rubrum*) indicates that source areas of the sand-and-shell sheet comprise pre-existing storm wrack deposits (sorted beach) and the reef (Pilarczyk and Reinhardt, 2012; Reinhardt et al., 2012). Two fields of cobbles and boulders (c. 300 and 800 m away from the coast) (Site 47, Fig. 3), embedded in the sand-and-shell deposit (Atwater et al., 2012), derive from adjacent inland outcrops of Pleistocene limestone.

The wide scatter of boulders and absence of ridge-like structures, their distribution far inland, and the application of sediment transport and coastal inundation modelling indicate that the boulder fields were likely created by a regional tsunami following a high-magnitude, Puerto Rico Trench outer-rise earthquake (Buckley et al., 2012; Watt et al., 2012a). Furthermore, ^{14}C ages derived from outer bands of large coral heads transported inland at several sites on Anegada (Fig. 8-I) cluster around 1200–1450 cal AD. Their dislocation is associated with breaches cut into beach ridges and points to a Medieval tsunami according to Weil Accardo et al. (2012) and Atwater et al. (2013b, 2014). Papers in preparation compile further sedimentary evidence and re-evaluate the tsunami hypothesis for the deposits of 1200–1450 cal AD and 1600–1850 cal AD (B. Atwater, pers. comm.).

5.3. E sector

The Lesser Antilles island arc was subjected to extensive, pioneering surveys of coarse-clast high-energy wave deposits, most of which were interpreted as tsunamigenic. They comprise:

- Boulder ridges and fields on elevated carbonate platforms (up to 15 m a.s.l.) on Anguilla and Scrub Island (Site 48, Fig. 3), in particular along the southeast and east coasts. The sediment-free zone between the coast and the coarse-clast deposits is used as evidence for hurricanes to predominantly induce erosion. Based on ^{14}C ages, two strong tsunamis approaching from the open Atlantic are inferred for around 500 and 1600 years ago (Scheffers, 2006b; Scheffers and Kelletat, 2006).
- Boulders weighing up to 10 t on St. Martin (Site 49, Fig. 3) and a “tsunami boulder spit” at an offshore volcanic island ^{14}C-dated to 500 BP (Scheffers, 2006b; Scheffers and Kelletat, 2006).
- Boulders up to 5 t scattered at elevations of 2–5 m a.s.l., 30–40 m inland, and a mixed deposit of sand, shells and coral rubble along with boulders of up to 30 t (up to 10 m a.s.l.) at the east coast of Grand Terre, Guadeloupe (Site 50, Fig. 3), indicating tsunami impact 2400 years ago based on pedogenesis and ^{14}C data (Scheffers et al., 2005).
- Well-rounded basaltic components floating in a volcanic ash matrix at elevations of up to 50 m a.s.l. with exposures of 100 m and a thickness of at least several metres on St. Lucia (Site 51, Fig. 3), interpreted as deposits of middle Pleistocene tsunamis (Scheffers et al., 2005).
- Large singular boulders – one of them weighing up to 170 t is overturned and located 13 m a.s.l. and 30 m away from the cliff edge –, boulder ridges, boulder imbrication and unstable settings with vertical a-axes on Barbados (Site 52, Fig. 3), attributed to two

tsunamis approaching from the open Atlantic Ocean at around 1500 and 4500 BP (Schellmann and Radtke, 2004; Scheffers, 2006b; Scheffers and Kelletat, 2006).

- Well-rounded cobbles and boulders in a sand matrix between 0–3 m a.s.l., presumably of Pleistocene age, are covered by tephra at the northwest coast of Grenada (Site 53, Fig. 3). Near Halifax Harbour, west coast, a 200 m-long, 2–4 m-high boulder ridge, consisting of weathered clasts of up to 10 t, is related to a late Holocene local tsunami supposedly induced by an eruption of the Kick 'em Jenny volcano (Scheffers et al., 2005).

5.4. S sector

5.4.1. Venezuela

A first multiproxy study from Laguna los Patos, Cumaná (Site 30, Fig. 3), provides evidence for marine incursions based on geochemical signatures, grain size and the erosive base of layers in the uppermost part of the studied sediment core. The signatures were interpreted to have probably been induced by historical tsunamis (Leal et al., 2014). Oropeza et al., (2015) present silty sand layers, some of which show landward directed ripples and salt lenses from three lagoons of the Araya Peninsula, eastern Venezuela (Site 29, Fig. 3), which are interpreted as possible traces of tsunami flooding. Another candidate tsunami deposit is reported from the islet of Cayo Sal off the coast of western Venezuela (Site 31, Fig. 3), where a massive, *ex-situ* deposit of skeletal muddy sand is associated with an inversion of the sediment core's age model (Weiss, 1979). ^{14}C data indicate an event of the last 600 years.

Schubert (1994) documents coral branches of pebble to boulder size distributed over a terrace of Mesozoic metamorphic rocks (15–18 m a.s.l.) west of Puerto Colombia, Venezuela (Site 55, Fig. 3). The coral material has an age of 1300 years based on U/Th and ^{14}C data. Deposition of the clasts is ascribed to a tsunami, mainly based on comparison with intertidal to supratidal, storm-built polymodal ridges on La Orchila Island (Schubert and Valastro, 1976). Tsunamis are assumed to be induced by either strong, local submarine earthquakes, by offshore slumping, or a combination of both (Schubert, 1994).

5.4.2. ABC Islands (Aruba, Bonaire, Curaçao)

The core record from several onshore coastal depressions (e.g., Fig. 8-III) along the entire coast of Bonaire (Sites 32, 56, Fig. 3), further off the coast of western Venezuela, contains layers of reworked marine and littoral deposits, and those mixed with terrestrial deposits as indication of past extreme-wave events. Their sedimentary characteristics comprise one or more normally graded or non-graded sequences separated by mud caps, rip-up clasts, horizons enriched with heavy minerals, foraminifera reflecting a dominant shallow-marine sediment source with minor percentages from deeper waters, low-density particles (wood, plant material, light shells) rafted on top, and erosive basal contacts (some features visible in Fig. 8-III) (Engel et al., 2010, 2012, 2013). Source areas of the deposits were identified as shallow areas off the coast, whereas locally, terrestrial sediment was incorporated as well. Following the lines of evidence in Engel et al. (2012, 2013), the oldest potential tsunami deposit was identified on Klein Bonaire (3.6 ka BP). A well-preserved one from Boka Bartol with a maximum age of 3.3 ka BP (Fig. 8-III) has counterparts on the leeward coast (Klein Bonaire, Saliña Tam, possibly between Saliña Tern and Punt'i Wekua) and the windward coast (Playa Grandi, possibly Boka Washikemba) and represents the best documented potential palaeotsunami on Bonaire. A post-2 ka BP tsunami left massive deposits at Lagun (Engel et al., 2010) and Saliña Tam. Sediments laid down by another younger unspecified extreme-wave event (1300–500 BP) were found between Saliña Tam and Punt'i Wekua, and at Boka Washikemba (Engel et al., 2010, 2012).

The ABC Islands also have an intensely studied record of coarse-clast deposits. Coastal "ridges [...] of loose blocks" (Fig. 9-I–V) have long been associated with a higher mid-Holocene sea level (de Bousonjé, 1974) or storms (Zonneveld et al., 1977) without generating too much attention. Since the late 1990s, the ridges (Fig. 9-I–IV), ramparts (*sensu* Focke, 1978; Scheffers, 2005) or ridge complexes (Fig. 9-V) (*sensu* Morton et al., 2008a), respectively, as well as singular boulders and boulder fields (Fig. 8-IV) were subjected to systematic investigations (Scheffers, 2002a,b; 2004, 2005; Scheffers et al., 2006, 2009, 2014; Radtke et al., 2003; Morton et al., 2006, 2008a; Spiske et al., 2008; Pignatelli et al., 2010; Watt et al., 2010; Engel and May, 2012). Narrow ridges of unimodal, mostly rounded coral fragments (mostly branches of *Acropora cervicornis*) based in intertidal position or close to sea level, with a height of up to 4 m, steep flanks, avalanching features (Fig. 9-I–IV,VI) and – where those features are low – distinct washover lobes at their landward sides, dominate the leeward coasts of all three islands (Scheffers, 2002b) and are deposited and modified by storm waves (Scheffers, 2002b; Morton et al., 2008a; Scheffers et al., 2014). Along the windward coasts (eastern and northern exposure), up to 400 m wide polymodal ridge complexes of corals boulders (mostly large branches of *Acropora palmata*), Pleistocene reefrock, shells, and sand with a steep seaward slope, tapering out inland at a very low angle prevail on top of elevated Pleistocene platforms (Fig. 9-V,VI). Scheffers (2002b, 2004, 2005, 2006a) associated their formation with palaeotsunamis generated at the LASZ, the CP-SAP boundary or the open Atlantic Ocean based on their large inland extent, coarseness of the particles, wide particle size distributions, the seemingly chaotic internal structure, and large ripple marks identified on aerial imagery. However, Morton et al. (2006, 2008a) showed that textural sorting, imbrications of platy particles, stratigraphic organization, and even initial palaeosols may be found within the wide ramparts (Fig. 8-V). They concluded, based on comparison with ridge-like features elsewhere, that the ramparts were the result of multiple extreme-wave events over millennial scales and that they were not indicative of a certain hydrodynamic process, but only reflect the range of available source material. Based on age clusters of an initial ESR (Radtke et al., 2003) and ^{14}C dataset derived from coral branches of the ramparts, Scheffers (2002b, 2004) and Scheffers et al. (2009) inferred three tsunami impacts at around 500, 1500, and 3500 BP.

Diverging conclusions also existed on the origin of the largest singular boulders on Bonaire (Fig. 8-IV) (Scheffers, 2004; Spiske et al., 2008), whereas later a general consensus was reached that the largest boulders carry significant characteristics of tsunami dislodgement (Scheffers, 2002b, 2005; Pignatelli et al., 2010; Watt et al., 2010; Engel and May, 2012). The application of initiation of motion criteria after Nott (2003) and Nandasena et al. (2011) indicates that transport by storm-induced waves is unlikely for the largest boulders of up to 150 t. At the most extensive boulder fields of Bonaire, boulders and blocks are located on top of an elevated Pleistocene reef platform (3.5–5 m a.s.l.) at a distance of 40–120 m from the coast (Pignatelli et al., 2010; Engel and May, 2012), whereas recent category 5 hurricanes such as Ivan in 2004 only shifted small clasts close to the shore (Scheffers and Scheffers, 2006).

On Curaçao and Aruba, the subaerial coarse-clast record is similar to Bonaire with a smaller spatial extent (Sites 57–58, Fig. 3). Several tsunamis were inferred by Scheffers (2002b, 2004). A palaeoenvironmental record from St. Michiel lagoon on Curaçao (Site 33, Fig. 3) indicates closure by a barrier of coral rubble at around 3500 BP (or later) based on an abrupt transition from an open marine to a euryhaline biofacies. Rapid formation of the barrier by a potential tsunami was taken into account by Klosowska (2003) without further analysis or discussion. An underwater sediment core from Spaanse Waters bay (Site 34, Fig. 3) contains a ”chaotic mixed layer” dated to 460–310 cal BP (or younger). It contains rock components, terrestrial plant remains, mollusc shells and older reef material, and was linked to a tsunami by Hornbach et al. (2008a: p. 44). A short core from Fuik Bay reveals three layers – the lowermost one dated to 500–320 cal BP – containing shell fragments, which were linked to either storm or tsunami events (Hornbach et al., 2008a).

6. Discussion

6.1. Review of extreme-wave deposits

In this chapter, the Caribbean records of potential tsunami deposits are re-evaluated based on state-of-the-art models of extreme-wave deposition as summarized in Tables 1 and 2.

6.1.1. Fine sediments

At Carrizales, Puerto Rico, successful correlation of the two layers in a 25 m-long trench, the identification of more well-preserved shells and coral fragments on the trench scale, and the fact that, according to survivors, the trench site was flooded by the 11 October 1918 tsunami, the tsunami hypothesis is reasonable. At Espinar, distinct laminated sub-units and the observation of tsunami flooding in 1918 are the strongest arguments *pro* tsunami deposition. The sites chosen by Moya and Mercado (2006) are promising for using tsunami deposits to reconstruct frequency-magnitude patterns of tsunamis in the wider area of the Mona Passage, but more detailed multidisciplinary analyses of the event layers and more dating are required to verify their tsunami origin, to infer hydrodynamic characteristics of the marine incursion and to foster an event chronology.

The record from Anegada seems reliable as well, as the widespread presence of *ex-situ* articulated bivalves and angular fragmentation in the sand-and-shell deposit (Reinhardt et al., 2012) and its sheet-like distribution up to more than 1 km inland are congruent with models of tsunami-laid sediments. Minor depositional effects of strong hurricanes of the past decades (Atwater et al., 2012) and a relatively high seismic tsunami potential (Parsons and Geist, 2009) further support this evaluation.

The sediments from around Bonaire also meet several criteria associated with the occurrence of tsunamis as listed above, and age control points to up to four major events (Fig. 10). However, due to the lack of recent local tsunami deposits for comparison, storm surges and waves exceeding those of modern hurricanes in the southern Caribbean cannot entirely be ruled out as a possible source. Whereas the SCDB tsunami scenario (Fig. 7) would probably create sufficient inundation to match the spatial distribution of fine-grained candidate tsunami deposits identified so far on Bonaire, the largest historical scenarios of the southern Caribbean seem to have only moderately affected the island (Oetjen et al., 2015).

→ Fig. 9 (Examples of storm deposits)

The records from the Dominican Republic (Scheucher et al., 2011; Fuentes and Huérfano-Moreno, 2013), Manatee Bay, Jamaica (Palmer and Burns, 2012), and Curaçao (Klosowska, 2003; Hornbach et al., 2008a) require more details on sediment texture, composition and spatial extent before their depositional process can be properly evaluated. To date, only conference abstracts are available. All sites are exposed to potential regional tsunami sources and thus, further in-depth research is advocated. Similarly, the records from Venezuela (Weiss, 1979; Leal et al., 2014;

Oropeza et al., 2015) only provide first insights. Based on the large number of local historical tsunamis which the sediments could be linked with, the tsunami hypothesis seems reasonable.

6.1.2. Coarse sediments

6.1.2.1. Solitary boulders and boulder clusters

Boulders are well known from both storm and tsunami deposition (Table 2) (Etienne et al., 2011; Richmond et al., 2011). On Grand Cayman (Jones and Hunter, 1992; Robinson et al., 2006) and Jamaica (Robinson et al., 2006; Khan et al., 2010), they primarily indicate the impact of storm waves and surge, as the strong storms seem to be capable to shift even some of the largest boulders (Robinson et al., 2006; Rowe et al., 2009; Khan et al., 2010). Even though tsunamis cannot be excluded, their effects might have been overprinted by the much more frequent high-category hurricanes as convincingly summarized by Khan et al. (2010).

Coastal boulders on Eleuthera are much bigger and older (MIS 5e) than anywhere else in the Caribbean. Considering the entire spectrum of evidence, the boulders may either relate to late Pleistocene tsunamis (most likely generated in the near-field), major hurricanes, or a combination of both (Engel et al., 2015). Similarly, the large singular boulders at Whale Point peninsula described by Kelletat et al. (2004) show consistencies with both tsunami and storm-wave deposition. The latter process should not be ruled out according to potentially high storm surges during hurricanes of around 4.5 m, and a very active wave climate with waves overtopping the >10 m-high platform several times a year (Anglin and MacIntosh, 2005).

The isolated boulders from the beaches nested between elevated coastal terraces near Punta Agujereada on Puerto Rico might have a multicausal origin as well. However, based on observations on boulder transport in the area during the 1918 tsunami (Reid and Taber, 1919), Moya and Mercado (2006) are most certainly correct in suggesting that tsunamis were involved.

The tsunamigenic origin of the boulder scatter and large coral heads transported inland (Fig. 8-I) on Anegada is also conclusive as it complies with state-of-the-art depositional models (Watt et al., 2012a) and is backed by inverse sediment transport modelling (Buckley et al., 2012), correlating fine deposits (Reinhardt et al., 2012) and documentary records (Atwater et al., 2012).

Some of the massive singular cliff-top boulders from the E sector – e.g., the one near Bottom Bay on Barbados (Schellmann and Radtke, 2004; Scheffers and Kelletat, 2006) – are consistent with patterns of both tsunami and storm deposition. Both processes need to be considered as the hazard imposed by both types of event is high in this region (Reading, 1990; Parsons and Geist, 2009). The contribution of a tsunami to the formation of the “block-and-ash flows” on St. Lucia (cf. Sigurdsson et al., 1980) as suggested by Scheffers et al. (2005) remains equivocal.

The pebble- to boulder-sized corals reported from Venezuela (Schubert, 1994) are difficult to evaluate as only limited information is given. Since they are definitely of marine origin, of Holocene age, and located high up in an area of low probability of hurricane landfall but significant local tsunami potential, the tsunami hypothesis seems reasonable.

Tsunami deposition of large boulders on Bonaire (Fig. 8-IV) seems likely and was suggested based on the large size, scattered distribution (Scheffers, 2002b; 2004, 2005; Watt et al., 2010), the application of initiation-of-motion criteria (Pignatelli et al., 2010; Engel and May, 2012), and the minor effects of recent high-category hurricanes passing the island (Scheffers and Scheffers, 2006). However, in view of the clear asymmetry of clast volume and size of individual boulders between the windward and leeward sides of the ABC islands and recent observations that extremely large boulders can be deposited in a scattered pattern during tropical cyclones (May et al., 2015b), a multicausal origin including the impact of strong, landfalling hurricanes cannot be excluded.

6.1.2.2. Ridges and ramparts/ridge complexes

Mostly polymodal ridges and ridge complexes (Morton et al., 2006, 2008a) or ramparts (Scheffers, 2002b, 2004, 2005; Scheffers et al., 2014) in varying elevations and distances from the coast seem to be the most common depositional landform along windward Caribbean coasts. Their height and width depends on elevation, shore-perpendicular topography, and source material. It is generally agreed that they mainly form during storms (Morton et al., 2008a), as observed in recent examples in the Caribbean (Scheffers, 2005; Spiske and Jaffe, 2009) and elsewhere (Table 2) (Richmond et al., 2011; Reyes et al., 2015). Their widespread occurrence on Grand Cayman (Rigby and Roberts, 1976; Hernandez-Avila et al., 1977; Jones and Hunter, 1992), Jamaica (Rowe et al., 2009; Miller et al., 2014), some of the eastern Bahaman islands (Kelletat et al., 2004), and the entire E sector (Aguilla, St. Martin, Guadeloupe, Barbados, St. Lucia, Grenada) (Schellmann and Radtke, 2004; Scheffers and Kelletat, 2006; Scheffers et al., 2005) is best explained by the high exposure to elevated wave action induced by strong, westward-moving hurricanes (Reading, 1990; Walsh and Reading, 1991), and indicates that any subaerial deposit of tsunamis in these areas is at high risk to become overprinted by the effects of recurring storm surge and waves. Therefore, after intense discussions on the polymodal ramparts of Bonaire, Curaçao, and Aruba over more than a decade (Scheffers, 2002b, 2004, 2005; Morton et al., 2006, 2008a; Watt et al., 2010), and the analysis of a set of >400 age estimates from Bonaire, which shows age-distance relationships but almost no significant overall age clusters, a stepwise evolution of the ramparts by multiple hurricanes is agreed upon, without, however, excluding contributions of one or very few major tsunamis (Scheffers et al., 2014).

For the recently published coastal “berm” from Yucatán, tsunami-induced formation was suggested based on the moderate geomorphic impact of recent storms such as Hurricane Gilbert in 1988 (Shaw and Benson, 2015). Nevertheless, the feature strongly resembles a polymodal ridge complex inconsistent with tsunami deposition (Morton et al., 2008a; Etienne et al., 2011). The dominating sand matrix is merely a function of sediment availability. This evaluation is furthermore supported by a relatively low probability of tsunami occurrence in the W sector (Parsons and Geist, 2009), and by either absence of wave-induced event deposits in adjacent coastal stratigraphic sequences (e.g., Macintyre et al., 2004; Monacci et al., 2009; Brown et al., 2014) or their reliable attribution to storm impact (McCloskey and Keller, 2009; McCloskey and Liu 2013a,b; Adomat and Gischler, 2015).

6.2. Correlation of tsunami deposits

(Supra-)regional correlation of sedimentary records of tsunamis can provide important information on magnitude and reach. In the Caribbean, such correlation is hampered by (i) a relatively low density of high-quality palaeotsunami data (see Chapter 5.1), (ii) the predominant occurrence of local to sub-regional tsunamis (see Chapter 3), and (iii) only few cases with consistent age control. In historical times, only the largest earthquake-induced events potentially affected larger parts of the Caribbean, as for instance the 1867 Virgin Island tsunami, for which historical accounts and models of run-up >0.5 m comprise the entire area between Puerto Rico and the Lesser Antilles island arc (N and E sectors) (O’Loughlin and Lander, 2003; Zahibo et al., 2003). Historical accounts of the 1755 Lisbon teletsunami are distributed between Cuba and Barbados (NGDC/WDS, 2016). However, the majority of tsunamis from submarine landslides or medium to lower-magnitude earthquakes within the Caribbean Basin probably affected just small areas. Thus, many deposits are likely to indicate only local and/or regional tsunamis. A sector-wide or even Caribbean-wide correlation of candidate tsunami deposits would, if at all, only work for major events, for which the SCDB scenario (Fig. 7) is a possible candidate.

One striking inter-island correlation of palaeotsunami deposits can be made in the N sector, where both the reliable account from Puerto Rico (Moya and Mercado, 2006) and the large coral heads transported inland from the N shore of Anegada (Fig. 8-I) (Weil Accardo et al., 2012; Atwater et al., 2013b, 2014) are radiocarbon-dated between 1200 and 1450 cal AD. Both records, if connected, point to the Puerto Rico Trench as a major tsunami hazard (Buckley et al., 2012; Atwater et al., 2013b). Furthermore, the N sector has several deposits convincingly associated with historical tsunamis (Moya and Mercado, 2006; Scheucher et al., 2011; Atwater et al., 2012) (Fig. 10).

Along the Venezuelan coast, possible tsunami deposits show rather poor age constraints. Those from lagoonal archives might be related to historical events (Weiss, 1979; Leal et al., 2014; Oropeza et al., 2015), for which the tsunami of 1530 seems to be a likely candidate. Whether other regional deposits of this age on Curaçao (Hornbach et al., 2008a) or Bonaire (Engel et al., 2010) can be linked to this regional event, which was directly observed only along the E Venezuelan coast (NGDC/WDS, 2016), remains speculative (Fig. 10).

On Bonaire, correlation of candidate tsunami deposits was possible at some sites and led to the tentative reconstruction of palaeotsunamis at c. 3600 BP, post-3300 BP (extreme-wave event [EWE] II), post-2000 BP, and 1300–500 BP (Engel et al., 2013). A set of U/Th data of coral rubble from Spelonk, all dating to shortly before 3300 BP (Scheffers et al., 2014) is probably related to EWE II, which might have led to the irreversible destruction of fringing coral reefs along central eastern Bonaire (Scheffers et al., 2006; Engel et al., 2013) (Fig. 10). Whether the closure of St. Michiel Lagoon on Curaçao (Klosowska, 2003) is related to either the 3600 BP or post-3300 BP event identified on Bonaire remains unclear.

→ Fig. 10 (Chronological correlation)

Some recent studies suggest significant repercussions of high-magnitude palaeotsunamis to Amerindian populations in the southern Caribbean by correlating them with archaeologically documented population setbacks (Scheffers et al., 2009; Hofman and Hoogland, 2015). As the recent re-analysis of chronological datasets and the modified interpretation of formation of the ridge complexes on Bonaire as outlined above challenge the inferences of strong palaeotsunamis at 4200 BP, 3100 BP, 1500 BP and 500 BP (Scheffers et al., 2009), such interrelations between tsunamis and prehistoric population dynamics remain a matter of debate.

6.3. Quantification of tsunami characteristics based on their deposits

The quantification of tsunami inundation parameters using sediment deposits is essential for coastal hazard assessment, in particular in the case of palaeotsunamis where no other source of information is available (Weiss and Bourgeois, 2012; Sugawara et al., 2014) (Fig. 4). Inundation distance can be inferred from the landward limit of a deposit, even though the relation between both parameters may vary significantly. Post-tsunami surveys revealed relationships between 50–60% (Sendai Plain, Tohoku-oki Tsunami 2011; Abe et al., 2012) and 90% (Kuril Islands, Kuril Island Tsunami 2006; MacInnes et al., 2009) mostly depending on sediment availability and composition, onshore topography and local preservation potential.

Inverse numerical models use characteristics of tsunami deposits in order to reconstruct parameters of tsunami inundation, such as flow velocity, wave height and inundation depth. A variety of models have been developed for both sand and boulder deposits (Sugawara et al., 2014; Jaffe et al., 2016), whereas their application to Caribbean datasets is clearly underdeveloped.

By applying a simple exponential relationship between flow velocity and the average b-axis of the five largest clasts adapted from flash flood hydraulics (Costa, 1983), an approach previously used for tsunami boulders from New South Wales by Young et al. (1996), Hearty (1997) inferred minimum flow speeds of 20 m s^{-1} for the giant Eleuthera boulders with b-axes of 5.5–11.5 m. Since this approach only considers intermediate axis length and does not take into account other factors influencing boulder transport such as the remaining axes or boulder shape, density, bottom roughness, inclination, pre-transport setting of the boulder (subaerial/subaqueous or joint-bounded), boulder source and the MIS 5e geomorphic setting, particle-particle collision or suspension load, the inferred values are questionable at best.

On Bonaire, initiation-of-motion criteria based on Nott (1997, 2003) were applied by several authors. By using uniform equations of Nott (1997), Scheffers (2002b) infers minimum tsunami wave heights of up to 46 and 33 m required to move the largest boulders under the assumption of boulder overturning and rotation perpendicular to the a-axis. Uncertainties still remain, even though three boulder axes, rock and fluid density, and coefficients of drag and lift are now considered. Spiske et al. (2008) studied the same boulder fields on Bonaire using the dataset of Scheffers (2002b) and enhanced initiation-of-motion criteria of Nott (2003). They considered a lower rock density of 1.8 g cm^{-3} and a submerged pre-transport setting of the boulders based on attached marine organisms and a relatively low degree of karstification. Reconstructed minimum tsunami heights are <3 m which is one reason for these authors to reject the tsunami hypothesis. Pignatelli et al. (2010) re-evaluated the same field dataset, applied modified equations of Nott (2003) as presented in Pignatelli et al. (2009), but considered that boulders were detached from the cliff edge and transported inland by a tsunami (joint-bounded pre-transport setting, JBB). Depending on different previously published reefrock densities ranging between 1.8–2.7 g/cm^3 (Scheffers, 2002b; Spiske et al., 2008), minimum tsunami heights ranging from 6.3–13.4 m were inferred (Pignatelli et al., 2010). After improvements of the initiation-of-motion criteria were published by Nandasena et al. (2011), Engel and May (2012) re-measured the largest boulders' individual densities and volumes using differential GPS and applied further modifications to the equations in order to account for realistic boulder volume. The JBB scenario was chosen based on observations of smaller boulders quarried from the cliff edge and transported inland during a recent storm. Minimum tsunami wave heights required to shift the largest boulder are 6.7 and 8.9 m, respectively (Engel and May, 2012). Based on a numerical approach of Pignatelli et al. (2009), the maximum tsunami inundation distance on top of the elevated carbonate platform of northeastern Bonaire (Fig. 8-IV) as indicated by the largest boulders was calculated to be in the range of 243 m (Engel and May, 2012) and 164–565 m (Pignatelli et al., 2010), respectively, depending on rock density. No direct relation could be made between quantification of marine inundation and risk, as the boulder fields are located far from residential areas and other valuable features such as important infrastructure .

In view of the broad range of reconstructed minimum wave heights on Bonaire resulting from simple inverse modelling approaches, it becomes clear that diverging approaches of boulder mapping and measurements of density in heterogeneous reefrock boulders strongly influence model outputs (e.g., Jaffe et al., 2016). Further uncertainties derive from an ambiguous pre-transport setting (e.g., Nott, 2003; Jaffe et al., 2016), oversimplification, such as a stable Froude number, which significantly varies for tsunamis approaching the coast (Sugawara et al., 2014), the dynamic relationship between flow velocity and wave height, and non-consideration of the duration of forces, as well as bottom roughness, slope angle (Weiss and Diplas, 2015) or the boulder's complex shape (Zainali and Weiss, 2015). However, when using carefully evaluated field data, initiation-of-motion criteria can provide a useful estimate on wave heights and flow velocities, even though it has to be considered, in terms of coastal hazard assessment, that they often underestimate real conditions, as observed in case studies after recent tsunamis (Paris et al., 2010).

A forward model of sediment transport combines the tsunami source and a hydrodynamic and sediment-transport model with the local bathymetry and topography on one or several spatial scales. The model is validated using sedimentary field data (Sugawara et al., 2014). One application from the Caribbean exists from Anegada (BVI). Buckley et al. (2012) identified a M 8.0 earthquake at the outer rise along the Puerto Rico Trench to have generated a tsunami reaching onshore flow velocities of up to 10 m/s, a height of >5 m at the shoreline and an inundation distance of >1000 m by applying a sediment-transport model, which considers fluid drag, inertia, buoyancy, and lift forces on boulders comprising both sliding and overturning transport modes. In the light of these promising results, the application of sediment-transport models and their validation with palaeotsunami deposits should be supported and encouraged in the Caribbean in order to serve coastal hazard assessment.

6.4. Implications for tsunami hazard assessment

Even though it is widely accepted that coastal hazard assessment may benefit from palaeotsunami investigations, a proper transfer with regard to the Caribbean has so far only been made in one case study from north Jamaica, where, however, the focus is on hurricanes (Rowe et al., 2009; Miller et al., 2014). Based on the assumption, that boulder ridges from Jamaica accumulate over time at the landward limit of potential damage induced by major extreme wave events, Miller et al. (2014) propose to use them as minimum setback distances for coastal development. These recommendations of up to 130 m-wide no-build zones starkly contrast with current regulations where setback distances lie between 6–30 m, depending on surface elevation and gradient (Miller et al., 2014).

Considering the spatial distribution of extreme-wave deposits for planning and land use is reasonable, in particular when characteristics of coastal flooding are reliably quantified through modelling of the sediment transport. However, at several places in the Caribbean these valuable indicators of hazard-prone areas are being excessively mined for construction purposes (Scheffers, 2002a,b; 2005) further leading to an increase of inundation distances (Morton et al., 2006). The dramatic consequences of carbonate sand and boulder mining in the Caribbean in combination with elevated wave energy, including coastal erosion and also the inevitable destruction of the archaeological record, have recently been outlined by Fitzpatrick (2012).

To sum up, a great potential for assessing tsunami hazard in the Caribbean has yet to be unlocked through interdisciplinary research comprising more detailed studies of extreme-wave deposits, estimation of long-term frequency-magnitude patterns based on the deposits' chronology, site-specific quantification of flooding characteristics in vulnerable areas, and their implementation in – already existing (von Hillebrandt-Andrade, 2013) – coastal hazard management and planning.

7. Conclusions

Many Holocene coastal stratigraphic records have been explored in the Caribbean. Only few of them report disturbance of background sedimentation and/or allochthonous deposits and relate these finds to extreme-wave events. A focus on such events and attempts to identify tsunami deposits as a contribution to local and regional coastal hazard assessment is rare, in particular when compared to other regions such as south Japan (Garrett et al., 2016) or the Indian Ocean (e.g., Jankaew et al., 2008; Alam et al., 2012; Brill et al., 2012), even though the Caribbean has a significant tsunami potential based on the historical record. Several fine-grained deposits consistent with tsunami facies models (Table 1) were reviewed. More data exist from subaerial coarse-clast deposits, even though the determination of the exact depositional process (tsunami, storm) and the timing often remains ambiguous. Therefore, high detail and common standards in stratigraphic documentation and analysis (e.g., Scheffers and Kelletat, 2003; Mamo et al., 2009) combined with the application of new innovative approaches (e.g., μCT; May et al., 2016) are needed in future studies from the Caribbean.

The widespread polymodal ridge complexes, in many places interpreted as tsunamigenic in previous publications (Table 5), seem to rather comply to stepwise accumulation mostly during strong hurricanes (Table 2) (Morton et al., 2008a; Scheffers et al., 2014) where they mark the terminal distance of coarse-clast transport and long-term limit of transport capacity by storm waves overtopping the elevated platforms (Khan et al., 2010; Miller et al., 2014). Tsunamis – depending on availability of source material and coastal topography – rather form laterally unsorted, widely distributed fields of cobbles and boulders (Watt et al., 2012a). Large singular boulders (up to >100 t) found on many elevated coastal platforms are consistent with both, storm and tsunami deposition, as demonstrated by both the recent Tohoku-oki Tsunami 2011 (Nandasena et al., 2013) and Typhoon Haiyan in the Philippines (May et al., 2015b). However, larger transport distances of tsunami boulders might still represent a useful criterion to distinguish between both processes (Goto et al., 2010; Etienne et al., 2011).

Source areas of fine-grained candidate tsunami deposits from the Caribbean seem to focus on the shallow subtidal (including the upper coral reef zone), but reveal minor incorporation of sediment from deeper waters (e.g., Engel et al., 2012) and terrestrial material in the upper part deposited by the backwash (e.g., Engel et al., 2010). While ridges and ridge complexes are mainly built of reefal debris, large boulders on top of elevated coastal platforms mainly derive from the cliff edge (e.g., Robinson et al., 2006; Khan et al., 2010; Engel and May, 2012). In some places, they preferentially cluster around terrace indentations (e.g., Jones and Hunter, 1992; Robinson et al., 2006; Watt et al., 2010).

The spatial correlation of prehistoric tsunami deposits of the same event on a regional scale is so far only marginally possible due to the low density of high-quality palaeotsunami data, only very few cases with consistent age constraints, and the predominant occurrence of local to sub-regional tsunamis on historical scales. If representing the same event, the potential medieval tsunami deposits identified on Anegada (Atwater et al., 2013b, 2014) and Puerto Rico (Moya and Mercado, 2006) are an exception as they might indicate a significant tsunami hazard emanating from earthquakes at the Puerto Rico Trench (Atwater et al., 2013b). The presented potential numerical scenarios of tsunamis generated at the SCBD (Fig. 7) as well as several giant mass wasting deposits at the foot of continental slopes (e.g., Deplus et al., 2001; Le Friant et al., 2009; Leslie and Mann, 2016) reveal the hazard of pan-Caribbean impacts and the possibility of supra-regional correlation of palaeotsunami deposits and geomorphic traces.

As extreme-wave deposits are unequivocally understudied in the Caribbean, there is an enormous potential for coastal hazard assessment to be developed. Quantitative information on maximum flow depth, inundation distance and flow velocities drawn from such deposits by applying improved numerical models of sediment transport is still very limited. Thus, further palaeotsunami studies using high-resolution methods of bedform and stratigraphical documentation and generating consistent chronological models with independent age control, combined with refined inverse and forward models of sediment transport and deposition, are required to reconstruct long-term patterns of magnitude and frequency of palaeotsunamis in the Caribbean – a prerequisite for reliably mapping hazard-prone areas. To date, proposed palaeotsunami deposits from the Caribbean probably represent only a fraction of actually occurred prehistoric tsunamis and, therefore, reflect major tsunami inundations inadequately.

Acknowledgements

This review was made possible through funds and time budgets associated with a Max Delbrück Prize for junior researchers, a measure of the future concept of the University of Cologne in the framework of the Excellence Initiative (DFG ZUK 81/1). It is furthermore based on experience made through previous research on Caribbean tsunamis funded by the Deutsche Forschungsgemeinschaft (BR 877/26-1). The manuscript benefitted from thoughtful pre-submission comments by D. Kelletat and associated discussions. We thank A. Scheffers, D. Kelletat, B. Atwater, B. Richmond, and G. Gelfenbaum for making photographs available. B. Atwater kindly provided insights into unpublished data. Language editing by K. Jacobson is acknowledged. The manuscript benefitted from helpful comments by two anonymous reviewers and the handling editor A. Strasser.

References

Abe, T., Goto, K., Sugawara, D., 2012. Relationship between the maximum extent of tsunami sand and the inundation limit of the 2011 Tohoku-oki tsunami on the Sendai Plain. Sedimentary Geology 282, 142–150.

Adger, W.N., Hughes, T.P., Folke, C., Carpenter, S.R., Rockström, J., 2005. Social-Ecological Resilience to Coastal Disasters. Science 309, 1036–1039.

Adomat, F., Gischler, E., 2015. Sedimentary Patterns and Evolution of Coastal Environments during the Holocene in Central Belize, Central America. Journal of Coastal Research 31, 802–826.

Adomat, F., Gischler, E., 2016. Assessing the suitability of Holocene environments along the central Belize coast, Central America, for the reconstruction of hurricane records. International Journal of Earth Sciences, doi: 10.1007/s00531-016-1319-y.

Alam, E., Dominey-Howes, D., Chagué-Goff, C., Goff, J., 2012. Tsunamis of the northeast Indian Ocean with a particular focus on the Bay of Bengal region—A synthesis and review. Earth-Science Reviews 114, 175–193.

Alfaro, E., Holz, M., 2014. Seismic geomorphological analysis of deepwater gravity-driven deposits on a slope system of the southern Colombian Caribbean margin. Marine and Petroleum Geology 57, 294–311.

Anglin, D., MacIntosh, K., 2005. Glass Window Bridge & Causeway Project, Bahamas. In: Allsop, N.W.H. (Ed.), Proceedings of the International Conference on Coastlines, Structures and Breakwaters 2005, organized on behalf of the Maritime Board of the Institution of Civil Engineers and held in London, on 20–22 April 2005. London, Thomas Telford Publishing, pp. 363–374.

Atwater, B.F., ten Brink, U.S., Buckley, M., Halley, R.S., Jaffe, B.E., López-Venegas, A.M., Reinhardt, E.G., Tuttle, M.P., Watt, S., Wei, Y., 2012. Geomorphic and stratigraphic evidence for an unusual tsunami or storm a few centuries ago at Anegada, British Virgin Islands. Natural Hazards 63, 51–84.

Atwater, B.F., Cisternas, M., Yulianto, E., Prendergast, A.L., Jankaew, K., Eipert, A.A., Fernando, W.I.S., Tejakusum, I., Schiappacasse, I., Sawai, Y., 2013a. The 1960 tsunami on beach-ridge plains near Maullín, Chile: Landward descent, renewed breaches, aggraded fans, multiple predecessors. Andean Geology 40, 393–418.

Atwater, B., ten Brink, U.S., Fuentes, Z., Halley, B.B., Spiske, M., Tuttle, M.P., Wei, Y., 2013b. Further evidence for a medieval tsunami from the Puerto Rico Trench. AGU Fall Meeting 2013, Abstract NH31A-1591.

Atwater, B.F., Fuentes, Z., Halley, R.B., ten Brink, U.S., Tuttle, M.P., 2014. Effects of 2010 Hurricane Earl amidst geologic evidence for greater overwash at Anegada, British Virgin Islands. Advances in Geosciences 38, 21–30.

Audemard, F.J., 2007. Revised seismic history of the Pilar fault, northeastern Venezuela, from the Cariaco 1997 earthquake and recent preliminary paleoseismic results. Journal of Seismology 11, 311–326.

Babu, N., Suresh Babu, D.S., Mohan Das, P.N., 2007. Impact of tsunami on texture and mineralogy of a major placer deposit in southwest coast of India. Environmental Geology 52, 71–80.

Bahlburg, H., Weiss, R., 2007. Sedimentology of the December 26, 2004, Sumatra tsunami deposits in eastern India (Tamil Nadu) and Kenya. International Journal of Earth Sciences 96, 1195–1209.

Bahlburg, H., Spiske, M., 2012. Sedimentology of tsunami inflow and backflow deposits: key differences revealed in a modern example. Sedimentology 59, 1063–1086.

Barbano, M.S., Pirrotta, C., Gerardi, F., 2010. Large boulders along the south-eastern Ionian coast of Sicily: Storm or tsunami deposits? Marine Geology 275, 140–154.

Barkan, R., ten Brink, U., 2010. Tsunami Simulations of the 1867 Virgin Island Earthquake: Constraints on Epicenter Location and Fault Parameters. Bulletin of the Seismological Society of America 100, 995–1009.

Barkan, R., ten Brink, U.S., Lin, J., 2009. Far field tsunami simulations of the 1755 Lisbon earthquake: Implications for tsunami hazard to the U.S. East Coast and the Caribbean Tsunami hazard along the U.S. Atlantic coast. Marine Geology 264, 109–122.

Barra, R., Cisternas, M., Suarez, C., Araneda, A., Piñones, O., Popp, P., 2004. PCBs and HCHs in a salt-marsh sediment record from South-Central Chile: use of tsunami signatures and ^{137}Cs fallout as temporal markers. Chemosphere 55, 965–972.

Benner, R., Browne, T., Brückner, H., Kelletat, D., Scheffers, A., 2010. Boulder Transport by Waves: Progress in Physical Modeling. Zeitschrift für Geomorphologie 54 (Suppl. 3), 127–146.

Bertran, P., Bonnissent, D., Imbert, D., Lozouet, P., Serrand, N., Stouvenot, C., 2004. Paléoclimat des Petit Antilles depuis 4000 ans BP: l'enregistrement de la lagune de Grand-Case à Saint-Martin. Comptes Rendues Geoscience 336, 1501–1510.

Bilham, R., 2010. Lessons from the Haiti earthquake. Nature 463, 878–879.

Biolchi, S., Furlani, S., Antonioli, F., Baldassini, N., Causon Deguara, J., Devoto, S., Di Stefano, A., Evans, J., Gambin, T., Gauci, R., Mastronuzzi, G., Monaco, C., Scicchitano, G., 2016. Boulder accumulations related to extreme wave events on the eastern coast of Malta. Natural Hazards and Earth System Sciences 16, 737–756.

Bishop, P., Sanderson, D., Hansom, J., Chaimanee, N., 2005. Age dating of tsunami deposits: lessons from the 26 December 2004 tsunami in Thailand. The Geographical Journal 171, 379–384.

Blume, H., 1962. Beiträge zur Klimatologie Westindiens. Erdkunde 16, 271–289.

Blumenstock, D.I., Forsberg, F.R., Johnson, C.G., 1961. The re-survey of typhoon effects on Jaluit atoll in the Marshall Islands. Nature 189, 618–620.

Bourgeois, J., Johnson, S.Y., 2001. Geologic evidence of earthquakes at the Snohomish delta, Washington, in the past 1200 yr. Geological Society of America Bulletin 113, 482–494.

Bourgeois, J., MacInnes, B., 2010. Tsunami boulder transport and other dramatic effects of the 15 November 2006 central Kuril Islands tsunami on the island of Matua. Zeitschrift für Geomorphologie 54 (Suppl. 3), 175–195.

Boyajian, G.E., Thayer, C.W., 1995. Clam Calamity: A Recent Supratidal Storm-Deposit as an Analog for Fossil Shell Beds. Palaios 10, 494–489.

Brill, D., Klasen, N., Jankaew, K., Brückner, H., Kelletat, D., Scheffers, A., Scheffers, S., 2012. Local inundation distances and regional tsunami recurrence in the Indian Ocean inferred from luminescence dating of sandy deposits in Thailand. Natural Hazards and Earth System Sciences 12, 2177–2192.

Brill, D., May, S.M., Engel, M., Reyes, M., Pint, A., Opitz, S., Dierick, M., Gonzalo, L.A., Esser, S., Brückner, H., 2016. Typhoon Haiyan's sedimentary record in coastal environments of the Philippines and its palaeotempestological implications. Natural Hazards and Earth System Sciences Discussions, doi: 10.5194/nhess-2016-224.

Brooks, G.R., Devine, B., Larson, R.A., Rood, B.P., 2007. Sedimentary development of Coral Bay, St. John, USVI: A shift from natural to anthropogenic influences. Caribbean Journal of Science 43, 226–243.

Brooks, G.R., Larson, R.A., Devine, B., Schwing, P.T., 2015. Annual to millennial record of sediment delivery to US Virgin Island coastal environments. The Holocene 25, 1015–1026.

Brown, A.L., Reinhardt, E.G., van Hengstum, P.J., Pilarczyk, J.E., 2014. A Coastal Yucatan Sinkhole Records Intense Hurricane Events. Journal of Coastal Research 30, 418–428.

Brückner, H., 2000. Küsten – sensible Geo- und Ökosysteme unter zunehmendem Stress. Petermanns Geographische Mitteilungen 143, 6–19.

Brunet, M., Le Friant, A., Boudon, G., Lafuerza, S., Talling, P., Hornbach, M., Ishizuka, O., Lebas, E., Guyard, H., IODP Expedition 340 Science Party, 2015. Composition, geometry, and emplacement dynamics of a large volcanic island landslide offshore Martinique: From volcano flank collapse to seafloor sediment failure? Geochemistry, Geophysics, Geosystems 17, 699–724,

Buckley, M.L., Wei, Y., Jaffe, B.E., Watt, S.G., 2012. Inverse modeling of velocities and inferred cause of overwash that emplaced inland fields of boulders at Anegada, British Virgin Islands. Natural Hazards 63, 133–149.

Burroughs, S.M., Tebbens, S.F., 2005. Power-law Scaling and Probabilistic Forecasting of Tsunami Runup Heights. Pure and Applied Geophysics 162, 331–342.

Byrne, D.B., Suarez, G., McCann, W.R., 1985. Muertos Trough subduction-microplate tectonics in the northern Caribbean? Nature 317, 420–421.

Caffrey, M.A., Horn, S.P., Orvis, K.H., Haberyan, K.A., 2015. Holocene environmental change at Laguna Saladilla, coastal north Hispaniola. Palaeogeography, Palaeoclimatology, Palaeoecology 436, 9–22.

Caron, V., 2011. Contrasted textural and taphonomic properties of high-energy wave deposits cemented in beachrocks (St. Bartholomew Island, French West Indies). Sedimentary Geology 237, 189–209.

Caron, V., 2012. Geomorphic and Sedimentologic Evidence of Extreme Wave Events Recorded by Beachrocks: A Case Study from the Island of St. Bartholomew (Lesser Antilles). Journal of Coastal Research 28, 811–828.

Caviedes, C., 1991. Five Hundred Years of Hurricanes in the Caribbean: Their Relationship with Global Climatic Variabilities. GeoJournal 23, 301 –310.

Chenoweth, M., Divine, D., 2008. A document-based 318-year record of tropical cyclones in the Lesser Antilles, 1690–2007. Geochemistry, Geophysics, Geosystems 9, Q08013.

Colón, S., Audemard, F.A., Beck, C., Avila, J., Padrón, C., De Batist, M., Paolini, M., Leal, A.F., Van Welden, A., 2015. The 1900 Mw 7.6 earthquake offshore north-central Venezuela: Is La Tortuga or San Sebastián the source fault? Marine and Petroleum Geology 67, 498–511.

Corral, A., Ossó, A., Llebot, J.E., 2010. Scaling of tropical-cyclone dissipation, Nature Physics 6, 693–696.

Costa, J.E., 1983. Paleohydraulic reconstruction of flash-flood peaks from boulder deposits in the Colorado Front Range. Geological Society of America Bulletin 94, 986–1004.

Costa, P.J.M., Andrade, C., Dawson, A.G., Mahaney, W.C., Freitas, M.C., Paris, R., Taborda, R., 2012. Microtextural characteristics of quartz grains transported and deposited by tsunamis and storms. Sedimentary Geology 275–276, 55–69.

Cox, R.T., Lumsden, D.N., Gough, K., Lloyd, R., Talnagi, J., 2008. Investigation of late Quaternary fault block uplift along the Motagua/Swan Islands fault system: Implications for seismic/tsunami hazard for the Bay of Honduras. Tectonophysics 457, 30–41.

Cox, R., Zentner, D.B., Kirchner, B.J., Cook, M.S., 2012. Boulder ridges on the Aran Islands (Ireland): Recent movements caused by storm waves, not tsunamis. Journal of Geology 120, 249–272.

Cox, R., Jahn, K.L., Watkins, O.G., 2016. Movement of boulders and megagravel by storm waves. Geophysical Research Abstracts 18, EGU2016-10535.

Cuven, S., Paris, R., Falvard, S., Miot-Noirault, E., Benbakkar, M., Schneider, J.-L., Billy, I., 2013. High-resolution analysis of a tsunami deposit: Case-study from the 1755 Lisbon tsunami in southwestern Spain. Marine Geology 337, 98–111.

Dall'Osso, F., Dominey-Howes, D., 2010. Public assessment of the usefulness of "draft" tsunami evacuation maps from Sydney, Australia – implications for the establishment of formal evacuation plans. Natural Hazards and Earth System Sciences 10, 1739–1750.

Dalman, M.R., Park, L.E., 2012. Tracking hurricane and climate change records in a Bahamian coastal lake: Clear Pond, San Salvador Island, Bahamas, in: Gamble, D.W., Kindler, P. (Eds.), Proceedings of the 15th Symposium on the Geology of the Bahamas and other Carbonate Regions. Gerace Research Center, San Salvador, pp. 15–32.

Davies, H.L., Davies, J.M., Perembo, R.C.B., Lus, W.Y., 2003. The Aitape 1998 Tsunami: Reconstructing the Event from Interviews and Field Mapping. Pure and Applied Geophysics 160, 1895–1922.

Dawson, S., 2007. Diatom biostratigraphy of tsunami deposits: examples from the 1998 Papua New Guinea tsunami. Sedimentary Geology 200, 328–335.

Denommee, K.C., Bentley, S.J., Droxler, A.W., 2014. Climatic controls on hurricane patterns: a 1200-y near-annual record from Lighthouse Reef, Belize. Scientific Reports 4, 3876.

Deplus, C., Le Friant, A., Boudon, C., Komorowski, J.-C., Villemant, B., Harford, C., Ségoufin, J., Cheminée, J.-L., 2001. Submarine evidence for large-scale debris avalanches in the Lesser Antilles Arc. Earth and Planetary Science Letters 192, 145–157.

De Buisonjé, P.H., 1974. Neogene and Quaternary geology of Aruba, Curaçao and Bonaire (Netherlands Antilles). PhD thesis, Rijksuniversiteit Utrecht, The Netherlands.

Dix, G.R., Patterson, R.T., Park, L.E., 1999. Marine saline ponds as sedimentary archives of late Holocene climate and sea-level variation along a carbonate platform margin: Lee Stocking Island, Bahamas. Palaeogeography, Palaeoclimatology, Palaeoecology 150, 223–246.

Donato, S.V., Reinhardt, E.G., Boyce, J.I., Rothaus, R., Vosmer, T., 2008. Identifying tsunami deposits using bivalve shell taphonomy. Geology 36, 199–202.

Donnelly, J.P., 2005. Evidence of past intense tropical cyclones from backbarrier salt pond sediments: a case study from Isla de Culebrita, Puerto Rico, USA. Journal of Coastal Research SI 42, 201–210.

Donnelly, J.P., Woodruff, J.D., 2007. Intense hurricane activity over the past 5,000 years controlled by El Niño and the West African monsoon. Nature 447, 465–468.

Donovan, S.K., 1994. Northern South America, in: Donovan, S.K., Jackson, T.A. (Eds.), Caribbean Geology – An Introduction. Kingston, UWIPA, pp. 229–248.

Douka, K., Hedges, R.E.M., Higham, T.F.G., 2010. Improved AMS ^{14}C Dating of Shell Carbonates Using High-Precision X-Ray Diffraction and a Novel Density Separation Protocol (CarDS). Radiocarbon 52, 735–751.

Draper, G., Jackson, T.A., Donovan, S.K., 1994. Geologic Provinces of the Caribbean Region, in: Donovan, S.K., Jackson, T.A. (Eds.), Caribbean Geology – An Introduction. Kingston, UWIPA, pp. 3–12.

Dura, T., Hemphill-Haley, E., Sawai, Y., Horton, B.P., 2016. The application of diatoms to reconstruct the history of subduction zone earthquakes and tsunamis. Earth-Science Reviews 152, 181–197.

Engel, M., Brückner, H., 2011. The identification of palaeo-tsunami deposits - a major challenge in coastal sedimentary research, in: Karius, V., Hadler, H., Deicke, M., von Eynatten, H., Brückner, H., Vött, A. (Eds.), Dynamische Küsten Grundlagen, Zusammenhänge und Auswirkungen im Spiegel angewandter Küstenforschung. Proceedings of the 28th Annual Meeting of the German Working Group on Geography of Oceans and Coasts, 22–25 Apr 2010, Hallig Hooge. Coastline Reports 17, 65–80.

Engel, M., May, S.M., 2012. Bonaire's boulder fields revisited: Evidence for Holocene tsunami impact on the Leeward Antilles. Quaternary Science Reviews 54, 126–141.

Engel, M., Bolten, A., Brückner, H., Daut, G., Kelletat, D., Schäbitz, F., Scheffers, A., Scheffers, S.R., Vött, A., Wille, M., Willershäuser, T., 2009. Reading the chapter of extreme wave events in nearshore geo-bio-archives of Bonaire (Netherlands Antilles) – initial results from Lagun and Boka Bartol. Marburger Geographische Schriften 145, 157–178.

Engel, M., Brückner, H., Wennrich, V., Scheffers, A., Kelletat, D., Vött, A., Schäbitz, F., Daut, G., Willershäuser, T., May, S.M., 2010. Coastal stratigraphies of eastern Bonaire (Netherlands Antilles): new insights into the palaeo-tsunami history of the southern Caribbean. Sedimentary Geology 231, 14–30.

Engel, M., Brückner, H., Messenzehl, K., Frenzel, P., May, S.M., Scheffers, A., Scheffers, S., Wennrich, V., Kelletat, D., 2012. Shoreline changes and high-energy wave impacts at the leeward coast of Bonaire (Netherlands Antilles). Earth, Planets and Space 64, 905–921.

Engel, M., Brückner, H., Fürstenberg, S., Frenzel, P., Konopczak, A.M., Scheffers, A., Kelletat, D., May, S.M., Schäbitz, F., Daut, G., 2013. A prehistoric tsunami induced long-lasting ecosystem changes on a semi-arid tropical island – the case of Boka Bartol (Bonaire, Leeward Antilles). Naturwissenschaften 100, 51–67.

Engel, M., Kindler, P., Godefroid, F., 2015. Interactive comment on "Ice melt, sea level rise and superstorms: evidence from paleoclimate data, climate modeling, and modern observations that 2 °C global warming is highly dangerous" by J. Hansen et al. Atmospheric Chemistry and Physics Discussions 15, C6270–C6281.

Etienne, S., 2012. Marine inundation hazards in French Polynesia: geomorphic impacts of Tropical Cyclone Oli in February 2010 , in: Terry, J.P., Goff, J. (Eds.), Natural Hazards in the Asia-Pacific Region: Recent Advances and Emerging Concepts. Geological Society, London, Special Publication 361, 21–39.

Etienne, S., Paris, R., 2010. Boulder accumulations related to storms on the Reykjanes Peninsula, Iceland. Geomorphology 114, 55–70.

Etienne, S., Terry, J.P., 2012. Coral blocks, gravel tongues and sand sheets: features of coastal accretion and sediment nourishment by Cyclone Tomas (March 2010) on Taveuni Island, Fiji. Geomorphology 175–176, 54–65.

Etienne, S., Buckley, M., Paris, R., Nandasena, A.K., Clark, K., Strotz, L., Chagué-Goff, C., Goff, J., Richmond, B., 2011. The use of boulders for characterizing past tsunamis: Lessons from the 2004 Indian Ocean and 2009 South Pacific tsunamis. Earth-Science Reviews 107, 76–90.

Fairbanks, R.G., 1989. A 17,000-year glacio-eustatic sea level record: influence of glacial melting rates on the Younger Dryas event and deep-ocean circulation. Nature 342, 637–642.

Feldens, P., Schwarzer, K.,, Sakuna, D., Szczuciński, W., Sompongchaiyakul, P., 2012. Sediment distribution on the inner continental shelf off Khao Lak (Thailand) after the 2004 Indian Ocean tsunami. Earth, Planets and Space 64, 875–887.

Feuillet, N., Beauducel, F., Tapponnier, P., 2011. Tectonic context of moderate to large historical earthquakes in the Lesser Antilles and mechanical coupling with volcanoes. Journal of Geophysical Research 116, B10308.

Fitzpatrick, S.M., 2012. On the shoals of giants: natural catastrophes and the overall destruction of the Caribbean's archaeological record. Journal of Coastal Conservation 16, 173–186.

Focke, J.W., 1978. Limestone cliff morphology on Curaçao (Netherlands Antilles), with special attention to the origin of notches and vermetid/coralline algal surf benches ("corniches", "trottoirs"). Zeitschrift für Geomorphologie 22, 329–349.

Fritz, H.M., Hillaire, J.V., Molière, E., Wei, Y., Mohammed, F., 2013. Twin Tsunamis Triggered by the 12 January 2010 Haiti Earthquake. Pure and Applied Geophysics 170, 1463–1474.

Fuentes, Z., Huérfano-Moreno, V., 2013. Earthquake potential of the Muertos Trough: onshore sleuthing for tsunami deposits. Geological Society of America, Abstracts with Programs 45(2), 63.

Gallegos, A., 1996. Descriptive physical oceanography of the Caribbean Sea, in: Maul, G.A. (Ed.), Small Islands: Marine Science and Sustainable Development. American Geophysical Union, Washington D.C., pp. 36–55.

Garrett, E., Fujiwara, O., Garrett, P., Heyvaert, V.M.A., Shishikura, M., Yokoyama, Y., Hubert-Ferrari, A., Brückner, H., Nakamura, A., De Batist, M., the QuakeRecNankai team, 2016. A systematic review of geological evidence for Holocene earthquakes and tsunamis along the Nankai-Suruga Trough, Japan. Earth-Science Reviews 159, 337–357.

Gelfenbaum, G., Jaffe, B., 2003. Erosion and Sedimentation from the 17 July, 1998 Papua New Guinea Tsunami. Pure and Applied Geophysics 160, 1969–1999.

Gischler, E., 2003. Holocene lagoonal development in the isolated carbonate platforms off Belize. Sedimentary Geology 159, 113–132.

Gischler, E., Shinn, E.A., Oschmann, W., Fiebig, J., Buster, N., 2008. A 1500-Year Holocene Caribbean Climate Archive from the Blue Hole, Lighthouse Reef, Belize. Journal of Coastal Research 24, 1496–1506.

Goff, J., Chagué-Goff, C., Nichol, S., Jaffe, B., Dominey-Howes, D., 2012. Progress in palaeotsunami research. Sedimentary Geology 243–244, 70–88.

Goldenberg, S.B., Shapiro, L.J., 1996. Physical mechanisms for the association of El Nińo and West African Rain-fall with Atlantic Major Hurricane Activity. Journal of Climate 9, 1169–1187.

González, C., Urrego, L.E., Martínez, J.I., Polanía, J., Yokoyama, Y., 2010. Mangrove dynamics in the southwestern Caribbean since the 'Little Ice Age': A history of human and natural disturbances. The Holocene 20, 849–861.

Gonzalez, L.A., Ruiz, H.M., Taggart, B.E., Budd, A.F., Monell, V., 1997. Geology of Isla de Mona, Puerto Rico, in: Vacher, H.L., Quinn, T. (Eds.), Geology and Hydrogeology of Carbonate Islands. Developments in Sedimentology 54, 327–358.

Goto, K., Chavanich, S.A., Imamura, F., Kunthasap, P., Matsui, T., Minoura, K., Sugawara, D., Yanagisawa, H., 2007. Distribution, origin and transport process of boulders deposited by the 2004 Indian Ocean tsunami at Pakarang Cape, Thailand. Sedimentary Geology 202, 821–837.

Goto, K., Kawana, T., Imamura, F., 2010. Historical and geological evidence of boulders deposited by tsunamis, southern Ryukyu Islands, Japan. Earth-Science Reviews 102, 77–99.

Goto, K., Miyagi, K., Kawana, T., Takahashi, J., Imamura, F., 2011. Emplacement and movement of boulders by known storm waves — Field evidence from the Okinawa Islands, Japan. Marine Geology 283, 66–78.

Goto, K., Sugawara, D., Ikema, S., Miyagi, T., 2012. Sedimentary processes associated with sand and boulder deposits formed by the 2011 Tohoku-oki tsunami at Sabusawa Island, Japan. Sedimentary Geology 282, 188–198.

Granja-Bruña, J.L., Carbó-Gorosabel, A., Llanes Estrada, P., Muños-Martín, A., ten Brink, U.S., Gómez Ballesteros, M., Druet, M., Pazos, A., 2014. Morphostructure at the junction between the Beata ridge and the Greater Antilles island arc (offshore Hispaniola southern slope). Tectonophysics 618, 138–163.

Grindlay, N.R., Hearne, M., Mann, P., 2005. High risk of tsunami in the Northern Caribbean. Eos 86, 121; 126.

Hansen, J., Sato, M., Hearty, P., Ruedy, R., Kelley, M., Masson-Delmotte, V., Russell, G., Tselioudis, G., Cao, J., Rignot, E., Velicogna, I., Tormey, B., Donovan, B., Kandiano, E., von Schuckmann, K., Kharecha, P., Legrande, A.N., Bauer, M., Lo, K.-W., 2016. Ice melt, sea level rise and superstorms: evidence from paleoclimate data, climate modeling, and modern observations that 2 °C global warming could be dangerous. Atmospheric Chemistry and Physics 16, 3761–3812.

Harbitz, C.B., Glimsdal, S., Bazin, S., Zamora, N., Løvholt, F., Bungum, H., Smebye, H., Gauer, P., Kjekstad, O., 2012. Tsunami hazard in the Caribbean: Regional exposure derived from credible worst case scenarios. Continental Shelf Research 38, 1–23.

Hall, A.M., Hansom, J.D., Williams, D.M., Jarvis, J., 2006. Distribution, geomorphology and lithofacies of cliff-top storm deposits: examples from the high-energy coasts of Scotland and Ireland. Marine Geology 232, 131–155.

Hasler, C.-A., Simpson, G., Kindler, P., 2010. Platform margin collapse simulation: the case of the North Eleuthera massive boulders. The 15th Symposium on the Geology of the Bahamas and other Carbonate Regions, Abstracts and Program, pp. 22–23.

Hawkes, A.D., Horton, B.P., 2012. Sedimentary record of storm deposits from Hurricane Ike, Galveston and San Luis Islands, Texas. Geomorphology 171, 180–189.

Hawkes, A.D., Bird, M., Cowie, S., Grundy-Warr, C., Horton, B.P., Hwai, A.T.S., Law, L., Macgregor, C., Nott, J., Ong, J.E., Rigg, J., Robinson, R., Tan-Mullins, M., Sa, T.T., Yasin, Z., Aik, L.W., 2007. Sediments deposited by the 2004 Indian Ocean Tsunami along the Malaysia–Thailand Peninsula. Marine Geology 242, 169–190.

Hayes, G.P., McNamara, D.E., Seidman, L., Roger, J., 2014. Quantifying potential earthquake and tsunami hazard in the Lesser Antilles subduction zone of the Caribbean region. Geophysical Journal International 196, 510–521.

Hearty, P.J., 1997. Boulder deposits from Large Waves during the Last Interglaciation on North Eleuthera Island, Bahamas. Quaternary Research 48, 326–338.

Hearty, P.J., Neumann, A.C., 2001. Rapid sea level and climate change at the close ofthe Last Interglaciation (MIS 5e): evidence from the Bahama Islands. Quaternary Science Reviews 20, 1881–1895.

Hearty, P.J., Neumann, A.C., Kaufman, D.S., 1998. Chevron Ridges and Runup Deposits in the Bahamas from Storms Late in Oxygen-Isotope Substage 5e. Quaternary Research 50, 309–322.

Hearty, P.J., Tormey, B.R., Neumann, A.C., 2002. Discussion of "Palaeoclimatic significance of co-occurring windand water-induced sedimentary structures in the last-interglacial coastal deposits from Bermuda and the Bahamas” (Kindler and Strasser, 2000, Sedimentary Geology, 131, 1–7). Sedimentary Geology 147, 429–435.

Hemphill-Haley, E., 1996. Diatoms as an aid in identifying late-Holocene tsunami deposits. The Holocene 6, 439–448.

Hendry, M.D., 1987. Tectonic and eustatic control on late Cenozoic sedimentation within an active plate boundary zone, west coast margin, Jamaica. Geological Society of America Bulletin 99, 718–728.

Hernandez-Avila, M.L., Roberts, H.H., Rouse, L.J., 1977. Hurricane-generated waves and coastal boulder rampart formation, in: D.L. Taylor (Ed.), Proceedings of Third International Coral Reef Symposium Vol. 2: Geology. Rosenstiel School of Marine and Atmospheric Science, Miami, pp. 71–78.

Hindson, R.A., Andrade, C., 1999. Sedimentation and hydrodynamic processes associated with the tsunami generated by the 1755 Lisbon earthquake. Quaternary International 56, 27–38.

Hippensteel, S.P., Eastin, M.D., Garcia, W.J., 2013. The geological legacy of Hurricane Irene: Implications for the fidelity of the paleo-storm record. GSA Today 23, 4–10.

Hobgood, J., 2005. Tropical cyclones, in: Oliver, J.E. (Ed.), Encyclopedia of World Climatology. Springer, Dordrecht, pp. 750–755.

Hofman, C.L., Hoogland, M.L.P., 2015. Beautiful tropical islands in the Caribbean Sea – Human responses to floods and droughts and the indigenous archaeological heritage of the Caribbean, in: Willems, W.J.H., van Schaik, H.P.J. (Eds.), Water & heritage – material, conceptual and spiritual connections. Sidestone Press, Leiden, pp. 99–120.

Hornbach, M.J., Mann, P., Wolf, S., King, W., Boon, R., 2008a. Assessing slope stability at Seroe Mansinga and Caracas Bay, Curaçao. Final report for APNA, Willemstad, Curaçao, 62 pp. URL: https://www.researchgate.net/publication/255664525_Assessing_Slope_Stability_at_Seroe_Mansinga_and_Caracas_Bay_Curacao, last access: 25 Feb 2016.

Hornbach, M.J., Mondziel, S.A., Grindlay, N.R., Frohlich, C., Mann, P., 2008b. Did a submarine slide trigger the 1918 Puerto Rico tsunami? Science of Tsunami Hazards 27(2), 22–31.

Hornbach, M., Mann, P., Taylor, F.W., Bowen, S.W., 2010. Estimating the Age of Near-Shore Carbonate Slides Using Coral Reefs and Erosional Markers: A Case Study from Curaçao, Netherlands Antilles. The Sedimentary Record 8, 4–10.

Horton, B.P., Rossi, V., Hawkes, A.D., 2009. The sedimentary record of the 2005 hurricane season from the Mississippi and Alabama coastlines. Quaternary International 195, 15–30.

Horton, B.P., Sawai, Y., Hawkes, A.D., Witter, R.C., 2011. Sedimentology and paleontology of a tsunami deposit accompanying the great Chilean earthquake of February 2010, Marine Micropaleontology 79, 132–138.

Hunt, J.E., Wynn, R.B., Talling, P.J., Masson, D.G., 2013. Multistage collapse of eight western Canary Island landslides in the last 1.5 Ma: Sedimentological and geochemical evidence from subunits in submarine flow deposits. Geochemistry, Geophysics, Geosystems 14, 2159–2181.

Hussain, S.M., Krishnamurthy, R., Gandhi, M.S., Ilayaraja, K., Ganesan, P., Mohan, S.P., 2006. Micropalaeontological investigations on tsunamigenic sediments of Andaman Islands. Current Science 91, 1655–1667.

Hussain, S.M., Mohan, S.P., Jonathan, M.P., 2010. Ostracoda as an aid in identifying 2004 tsunami sediments: a report from SE coast of India. Natural Hazards 55, 513–522.

Ishimura, D., Miyauchi, T., 2015. Historical and paleo-tsunami deposits during the last 4000 years and their correlations with historical tsunami events in Koyadori on the Sanriku Coast, northeastern Japan. Progress in Earth and Planetary Science 2, 16.

Jackson, L.P., 2013. Caribbean Sea Level Change: observational analysis from millennial to decadal timescales. PhD thesis, University of Leeds, URL: http://etheses.whiterose.ac.uk/id/eprint/5779 (last access: 06 June 2016).

Jaffe, B., Gelfenbaum, G., Rubin, D., Peters, R., Anima, R., Swensson, M., Olcese, D., Bernales, L., Gomez, J., Riega, P., 2003. Tsunami deposits: identification and interpretation of tsunami deposits from the June 23, 2001 Perú tsunami. Proceedings of the International Conference on Coastal Sediments 2003. CD-ROM Published by World Scientific Publishing Corp and East Meets West Productions, Corpus Christi, TX, USA, 13 pp.

Jaffe, B.E., Buckley, M.L., Richmond, B.M., Morton, R.A., Moya, J.C., Gelfenbaum, G., Watt, S.G., 2008. Evidence of Tsunami in a Coastal Pond in NW Puerto Rico. Eos Transactions AGU 89(53), Fall Meeting Supplement, Abstract OS53A-1291.

Jaffe, B., Goto, K., Sugawara, D., Gelfenbaum, G., La Selle, S.P., 2016. Uncertainty in Tsunami Sediment Transport Modeling. Journal of Disaster Research 11, 647–661.

Jagodziński, R., Sternal, B., Szczuciński, W., Chagué-Goff, C., Sugawara, D., 2012. Heavy minerals in the 2011 Tohoku-oki tsunami deposits—insights into sediment sources and hydrodynamics. Sedimentary Geology 282, 57–64.

Jankaew, K., Atwater, B.F., Sawai, Y., Choowong, M., Charoentitirat, T., Martin, M.E., Prendergast, A., 2008. Medieval forewarning of the 2004 Indian Ocean tsunami in Thailand. Nature 455, 1228–1231.

Jessen, C.A., Pedersen, J.B.T., Bartholdy, J., Seidenkrantz, M.-S., Kuijpers, A., 2008. A late Holocene palaeoenvironmental record from Altona Bay, St. Croix, US Virgin Islands. Geografisk Tidsskrift – Danish Journal of Geography 108(2), 59–70.

Jones, B., Hunter, I.G., 1992. Very large boulders on the coast of Grand Cayman: the effects of giant waves on rocky coastlines. Journal of Coastal Research 8, 763–774.

Kain, C.L., Wassmer, P., Goff, J., Chagué-Goff, C., Gomez, C., Hart, D.E., Fierro, D., Jacobsen, G.E., Zawadzki, A., 2016. Determining flow patterns and emplacement dynamics from tsunami deposits with no visible sedimentary structure. Earth Surface Processes and Landforms, doi: 10.1002/esp.4020.

Kelletat, D., Scheffers, A., Scheffers, S., 2004. Holocene tsunami deposits on the Bahaman Islands of Long Island and Eleuthera. Zeitschrift für Geomorphologie 48, 519–540.

Kelletat, D., Scheffers, S.R., Scheffers. A., 2007. Field Signatures of the SE-Asian Mega-Tsunami along the West Coast of Thailand Compared to Holocene Paleo-Tsunami from the Atlantic Region. Pure and Applied Geophysics 164, 413–431.

Kennedy, A.B., Mori, N., Zhang, Y., Yasuda, T., Chen, S.-E., Tajima, Y., Pecor, W., Toride, K., 2015. Observations and Modeling of Coastal Boulder Transport and Loading During Super Typhoon Haiyan. Coastal Engineering Journal 58, 1640004.

Khan, S., Robinson, E., Rowe, D.-A., Coutou, R., 2010. Size and mass of shoreline boulders moved and emplaced by recent hurricanes, Jamaica. Zeitschrift für Geomorphologie 54 (Suppl. 3), 281–299.

Kilfeather, A.A., Blackford, J.J., van der Meer, J.J.M., 2007. Micromorphological Analysis of Coastal Sediments from Willapa Bay, Washington, USA: A Technique for Analysing Inferred Tsunami Deposits. Pure and Applied Geophysics 164, 509–525.

Kindler, P., Strasser, A., 2000. Palaeoclimatic significance of co-occurring wind- and water-induced sedimentary structures in the last-interglacial coastal deposits from Bermuda and the Bahamas. Sedimentary Geology 131, 1–7.

Kindler, P., Strasser, A., 2002. Palaeoclimatic significance of co-occurring wind- and water-induced sedimentary structures in last-interglacial coastal deposits from Bermuda and the Bahamas: response to Hearty et al.'s comment. Sedimentary Geology 147, 437–443.

Kindler, P., Mylroie, J.E., Curran, H.A., Carew, J.L., Gamble, D.W., Rothfus, T.A., Savarese, M., Sealey, N.E., 2010. Geology of Central Eleuthera, Bahamas: A Field Trip Guide. 15th Symposium on the Geology of the Bahamas and Other Carbonate Regions. Gerace Research Centre, San Salvador, Bahamas.

Klosowska, B.B., 2003. Late Holocene embayment and salina record of Curaçao (Dutch Antilles): Criteria to monitor environmental change and biodiversity. PhD thesis, Vrije Universiteit Amsterdam, The Netherlands.

Knutson, T.R., McBride, J.L., Chan, J., Emanuel, K., Holland, G., Landsea, C., Held, I., Kossin, J.P., Srivastava, A.K., Sugi, M., 2010. Tropical cyclones and climate change. Nature Geoscience 3, 157–163.

Komatsubara, J., Fujiwara, O., 2007. Overview of Holocene tsunami deposits along the Nankai, Suruga, and Sagami Troughs, southwest Japan. Pure and Applied Geophysics 164, 493–507.

Kortekaas, S., Dawson, A., 2007. Distinguishing tsunami and storm deposits: an example from Martinhal, SW Portugal. Sedimentary Geology 200, 208–221.

Korup O., Clague, J.J., 2009. Natural hazards, extreme events, and mountain topography. Quaternary Science Reviews 28, 977–990.

Lambeck, K., 2002. Sea level change from mid Holocene to recent time: An Australian example with global implications, in: Mitrovica, J.X., Vermeersen, B.L.A. (Eds.), Ice sheets, sea level and the dynamic Earth. American Geophysical Union, Washington, pp. 33–50.

Lario, J., Luque, L., Goy, J.L., Spencer, C., Cabero, A., Bardají, T., Borja, F., Dabrio, C.J., Civis, J., González-Delgado, J.A., Borja, C., Alonso-Azcárate, J., 2010. Tsunami vs. storm surge deposits: a review of the sedimentological and geomorphological records of extreme wave events (EWE) during the Holocene in the Gulf of Cadiz, Spain. Zeitschrift für Geomorphologie 54 (Suppl. 3), 301–316.

Lario, J., Zazo, C., Goy, J.L., 2016. Tectonic and morphosedimentary features of the 2010 Chile earthquake and tsunami in the Arauco Gulf and Mataquito River (Central Chile). Geomorphology 267, 16–24.

Larsen, R.A., Brooks, G.R., Devine, B., Schwing, P.T., Holmes, C.W., Jilbert, T., Reichart, G.-J., 2015. Elemental signature of terrigenous sediment runoff as recorded in coastal salt ponds: US Virgin Islands. Applied Geochemistry 63, 573–585.

Lau, A.Y.A., Etienne, S., Terry, J.P., Switzer, A.D., Lee, Y.S., 2014. A preliminary study of the distribution, sizes and orientation of large reef-top coral boulders deposited by extreme waves at Makemo Atoll, French Polynesia. Journal of Coastal Research, SI 70, 272–277.

Le Friant, A., Heinrich, P., Boudon, G., 2008. Field survey and numerical simulation of the 21 November 2004 tsunami at Les Saintes (Lesser Antilles). Geophysical Research Letters 35, L12308.

Le Friant, A., Boudon, G., Arnulf, A., Robertson, R.E.A., 2009. Debris avalanche deposits offshore St. Vincent (West Indies): Impact of flank-collapse events on the morphological evolution of the island. Journal of Volcanology and Geothermal Research 179, 1–10.

Leal, K., Scremin, L., Audemard, F., Carillo, E., 2014. Paleotsunamis en el registro geológico de Cumaná, estado Sucre, Venezuela oriental. Boletín de Geología 36(2), 45–70.

Lebas, E., Le Friant, A., Boudon, G., Watt, S.F.L., Talling, P.J., Feuillet, N., Deplus, C., Berndt, C., Vardy, M.E., 2011. Multiple widespread landslides during the long-term evolution of a volcanic island: Insights from high-resolution seismic data, Montserrat, Lesser Antilles. Geochemistry, Geophysics, Geosystems 12, Q05006.

Leslie, S., Mann, P., 2016. Giant submarine landslides on the Colombian margin and tsunami risk in the Caribbean Sea. Earth and Planetary Science Letters 449, 382–394..

López-Venegas, A.M., ten Brink, U.S., Geist, E.L., 2008. Submarine landslide as the source for the October 11, 1918 Mona Passage tsunami: Observations and modeling. Marine Geology 254, 35–46.

MacInnes, B.T., Bourgeois, J., Pinegina, T.K., Kravchunovskaya, E.A., 2009. Tsunami geomorphology: erosion and deposition from the 15 November 2006 Kuril Island tsunami. Geology 37, 995–998.

Macintyre, I.G., Littler, M.M., Littler, D.S., 1995. Holocene history of Tobacco Range, Belize, Central America. Atoll Research Bulletin 430.

Macintyre, I.A., Glynn, P.W., Steneck, R.S., 2001. A classic Caribbean algal ridge, Holandés Cays, Panamá: an algal coated storm deposit. Coral Reefs 20, 95–105.

Macintyre, I.G., Toscano, M.A., Lighty, R.G., Bond, G.B., 2004. Holocene history of the mangrove islands of twin Cays, Belize, Central America. Atoll Research Bulletin 510.

Malaizé, B., Bertran, P., Carbonel, P., Bonnissent, D., Charlier, K., Galop, D., Imbert, D., Serrand, N., Stouvenot, C., Pujol, C. 2011. Hurricanes and climate in the Caribbean during the past 3700 years BP. The Holocene 21, 911–924.

Mamo, B., Strotz, L., Dominey-Howes, D., 2009. Tsunami sediments and their foraminiferal assemblages. Earth-Science Reviews 96, 263–278.

Mann, P., Calais, E., Ruegg, J.-C., DeMets, C., Jansma, P.E., Mattioli, G.S., 2002. Oblique collision in the northeastern Caribbean from GPS measurements and geological observations. Tectonics 21, 1057.

Maragos, J.E., Baines, G.B.K., Beveridge, P.J., 1973. Tropical Cyclone Bebe creates a new land formation on Funafuti Atoll. Science 181, 1161–1164.

Martin Arcos, M.E., MacInnes, B.T., Arreaga, P., Rivera-Hernandez, F., Weiss, R., Lynett, P., 2013. An amalgamated meter-thick sedimentary package enabled by the 2011 Tohoku tsunami in El Garrapatero, Galapagos Islands. Quaternary Research 80, 9–19.

Matsumoto, D., Naruse, H., Fujino, S., Surphawajruksakul, A., Jarupongsakul, T., Sakakura, N., Murayama, M., 2008. Truncated flame structures within a deposit of the Indian Ocean Tsunami: evidence of synsedimentary deformation. Sedimentology 55, 1559–1570.

Mattheus, C.R., Fowler, J.K., 2015. Paleotempestite distribution across an isolated carbonate platform, San Salvador Island, Bahamas. Journal of Coastal Research 31, 842–858.

May, S.M., Brill, D., Engel, M., Scheffers, A., Pint, A., Opitz, S., Wennrich, V., Squire, P., Kelletat, D., Brückner, H., 2015a. Traces of historical tropical cyclones and tsunamis in the Ashburton Delta (north-west Australia). Sedimentology 62, 1546–1572.

May, S.M., Engel, M., Brill, D., Cuadra, C., Lagmay, A.M.F., Santiago, J., Suarez, K., Reyes, M., Brückner, H., 2015b. Block and boulder transport in Eastern Samar (Philippines) during Supertyphoon Haiyan. Earth Surface Dynamics 3, 543–558.

May, S.M., Falvard, S., Norpoth, M., Pint, A., Brill, D., Engel, M., Scheffers, A., Dierick, M., Paris, R., Squire, P., Brückner, H., 2016. A mid-Holocene candidate tsunami deposit from the NW Cape (Western Australia). Sedimentary Geology 332, 40–50.

McAdoo, B.G., Samuelu Ah-Leong, J., Bell, L., Ifopo, P., Ward, J., Lovell, E., Skelton, P., 2011. Coral reefs as buffers during the 2009 South Pacific tsunami, Upolu Island, Samoa. Earth-Science Reviews 107, 147–155.

McCloskey, T.A., Keller, G., 2009. 5000 year sedimentary record of hurricane strikes on the central coast of Belize. Quaternary International 195, 53–68.

McCloskey, T.A., Liu, K.-b., 2012. A sedimentary based history of hurricane strikes on the southern Caribbean coast of Nicaragua. Quaternary Research 78, 454–464.

McCloskey, T.A., Liu, K.-b., 2013a. A 7000 year record of paleohurricane activity from a coastal wetland in Belize. The Holocene 23, 278–291.

McCloskey, T.A., Liu, K.-b., 2013b. Sedimentary History of Mangrove Cays in Turneffe Islands, Belize: Evidence for Sudden Environmental Reversals. Journal of Coastal Research 29, 971–983.

McGregor, D.F.M., Potter, R.B., 1997. Environmental change and sustainability in the Caribbean: Terrestrial perspectives. Beiträge zur Geographischen Regionalforschung in Lateinamerika 10, 1–15.

McKee, K.L., Cahoon, D.R., Feller, I.C., 2007. Caribbean mangroves adjust to rising sea level through biotic controls on change in soil elevation. Global Ecology and Biogeography 16, 545–556.

Meschede, M., Frisch, W., 1998. A plate-tectonic model for the Mesozoic and Early Cenozoic history of the Caribbean plate. Tectonophysics 296, 269–291.

Miller, S., Rowe, D.-A., Brown, L., Mandal, A., 2014. Wave-emplaced boulders: implications for development of “prime real estate” seafront, North Coast Jamaica. Bulletin of Engineering Geology and the Environment 73, 109–122.

Milne, G.A., Peros, M., 2013. Data–model comparison of Holocene sea-level change in the circum-Caribbean region. Global and Planetary Change 107, 119–131.

Minoura, K., Nakaya, S., 1991. Traces of tsunami preserved in inter-tidal lacustrine and marsh deposits: Some examples from northeast Japan. Journal of Geology 99, 265–287.

Minoura, K., Nakaya, S., Uchida, M., 1994. Tsunami deposits in a lacustrine sequence of the Sanriku coast, northeast Japan. Sedimentary Geology 89, 25–31.

Monacci, N.M., Meier-Grünhagen, U., Finney, B.P., Behling, H., Wooller, M.J., 2009. Mangrove ecosystem changes during the Holocene at Spanish Lookout Cay, Belize. Palaeogeogrpahy, Palaeoclimatology, Palaeoecology 280, 37–46.

Moore, A., McAdoo, B.G., Ruffman, A., 2007. Landward fining from multiple sources in a sand sheet deposited by the 1929 Grand Banks tsunami, Newfoundland. Sedimentary Geology 200, 336–346.

Moore, A., Goff, J., McAdoo, B.G., Fritz, H.M., Gusman, A., Kalligeris, N., Kalsum, K., Susanto, A., Suteja, D., Synolakis, C.E., 2011. Sedimentary deposits from the 17 July 2006 Western Java Tsunami, Indonesia: use of grain size analyses to assess tsunami flow depth, speed, and traction carpet characteristics. Pure and Applied Geophysics 168, 1951–1961.

Morton R.A., 2010. First-order controls of extreme-storm impacts on the Mississippi–Alabama barrier-island chain. Journal of Coastal Research 26, 635–648.

Morton, R.A., Richmond, B.M., Jaffe, B.E., Gelfenbaum, G., 2006. Reconnaissance investigation of Caribbean extreme wave deposits – preliminary observations, interpretations, and research directions. USGS Open-File Report 2006-1293.

Morton, R.A., Gelfenbaum, G., Jaffe, B.E, 2007. Physical criteria for distinguishing sandy tsunami and storm deposits using modern examples. Sedimentary Geology 200, 184–207.

Morton, R.A., Richmond, B.M., Jaffe, B.E., Gelfenbaum, G., 2008a. Coarse-clast ridge complexes of the Caribbean: A preliminary basis for distinguishing tsunami and storm-wave origins. Journal of Sedimentary Research 78, 624–637.

Morton R.A., Goff J.R., Nichol, S.L., 2008b. Hydrodynamic implications of textural trends in sand deposits of the 2004 tsunami in Sri Lanka. Sedimentary Geology 207, 56–64.

Moscardelli, L., Hornbach, M., Wood, L., 2010. Tsunamigenic risks associated with mass transport complexes in offshore Trinidad and Venezuela, in: Mosher, D.C., Shipp, R.C., Moscardelli, L., Chaytor, J.D., Baxter, C.D.P., Lee, H.J., Urgeles, R. (Eds.), Submarine Mass Movements and Their Consequences. Springer, Dordrecht, pp. 733–744.

Moya, J.C., Mercado, A., 2006. Geomorphologic and stratigraphic investigations on historic and pre-historic tsunami in northwestern Puerto Rico: implications for long term coastal evolution, in: Mercado-Irizarry, A., Liu, P. (Eds.), Caribbean tsunami hazard. World Scientific, Singapore, pp. 149–177.

Mylroie, J.E., 2008. Late Quaternary sea-level position: evidence from Bahamian carbonate deposition and dissolution cycles. Quaternary International 183, 61–75.

Nanayama, F., Shigeno, K., Satake, K., Shimokawa, K., Koitabashi, S., Miyasaka, S., Ishii, M., 2000. Sedimentary differences between the 1993 Hokkaido nansei-oki tsunami and the 1959 Miyakojima typhoon at Taisei, southwestern Hokkaido, northern Japan. Sedimentary Geology 135, 255–264.

Nandasena, N.A.K., Paris, R., Tanaka, N., 2011. Reassessment of hydrodynamic equations: Minimum flow velocity to initiate boulder transport by high energy events (storms, tsunamis). Marine Geology 281, 70–84.

Nandasena, N.A.K., Tanaka, N., Sasaki, Y., Osada, M., 2013. Boulder transport by the 2011 Great East Japan tsunami: Comprehensive field observations and whither model predictions? Marine Geology 346, 292–309.

Naruse, H., Fujino, S., Suphawajruksakul, A., Jarupongsakul, T., 2010. Features and formation processes of multiple deposition layers from the 2004 Indian Ocean Tsunami at Ban Nam Kem, southern Thailand. Island Arc 19, 399–411.

NGDC/WDS (National Geophysical Data Center/World Data Service), 2016. Global Historical Tsunami Database. National Geophysical Data Center, NOAA, doi:10.7289/V5PN93H7.

Nichol, S.L., Kench, P.S., 2008. Sedimentology and preservation potential of carbonate sand sheets deposited by the December 2004 Indian Ocean tsunami: South Baa Atoll, Maldives. Sedimentology 55, 1173–1187.

Nishimura, Y., Miyaji, N., 1995. Tsunami Deposits from the 1993 Southwest Hokkaido Earthquake and the 1640 Hokkaido Komagatake Eruption, Northern Japan. Pure and Applied Geophysics 144, 719–733.

Nott, J., 1997. Extremely high-energy wave deposits inside the Great Barrier Reef, Australia: determining the cause-tsunami or tropical cyclone. Marine Geology 141, 193 –207.

Nott, J., 2003. Waves, coastal boulder deposits and the importance of the pre-transport setting. Earth and Planetary Science Letters 210, 269–276.

Oetjen, J., Engel, M., Effkemann, C., May, S.M., Pudasaini, S.P., Wöffler, T., Aizinger, V., Schüttrumpf, H., Brückner, H., 2015. Numerical modelling of tsunami scenarios for the island of Bonaire (Leeward Antilles). Programme and abstract book, 4th International Tsunami Field Symposium, 23–27 March 2015, Kata Beach, Phuket, Thailand, pp. 81–85.

O'Loughlin, K.F., Lander, J.F., 2003. Caribbean Tsunamis – A 500-Year History from 1498–1998. Kluwer, Dordrecht.

Okada, Y., 1985. Surface deformation due to shear and tensile faults in a half-space. Bulletin of the Seismological Society of America 75, 1135–1154.

Oropeza, J., Audemard, F.A., Beck, C., Vallée, M., 2015. New potential sedimentary evidences of paleotsunamis on coastal lagoons of Chacopata, State of Sucre, Venezuela. In: Blumetti, A.M., Cinti, F., De Martini, P., Galadini, F., Guerrieri, L., Michetti, A.M., Pantosti, D., Vittori, E. (Eds.), 6th International INQUA Meeting on Paleoseismology, Active Tectonics and Archaeoseismology, 19–24 April 2015, Pescina, Fucino Basin, Italy. Miscellanea INGV 27, 343–345.

Palmer, S., Burn, M., 2012. A Late-Holocene record of marine washover events from a coastal lagoon in Jamaica, West Indies. Quaternary International 279–280, 365–366.

Pantosti, D., Barbano, M.S., Smedile, A., De Martini, P.M., Tigano, G., 2008. Geological evidence of paleotsunamis at Torre degli Inglesi (northeast Sicily). Geophysical Research Letters 35, L05311.

Pararas-Carayannis, G., 2004. Volcanic tsunami generating source mechanisms in the eastern Caribbean region. Science of Tsunami Hazards 22, 74–114.

Paris, R., 2015. Source mechanisms of volcanic tsunamis. Philosophical Transactions of the Royal Society A 373, 20140380.

Paris, R., Lavigne, F., Wassmer, P., Sartohadi, J., 2007. Coastal sedimentation associated with the December 26, 2004 tsunami in Lhok Nga, west Banda Aceh (Sumatra, Indonesia). Marine Geology 238, 93–106.

Paris, R., Wassmer, P., Sartohadi, J., Lavigne, F., Barthomeuf, B., Desgages, E., Grancher, D., Baumert, P., Vautier, F., Brunstein, D., Gomez, C., 2009. Tsunamis as geomorphic crises: Lessons from the December 26, 2004 tsunami in Lhok Nga, West Banda Aceh (Sumatra, Indonesia). Geomorphology 104, 59–72.

Paris, R., Fournier, J., Poizot, E., Etienne, S., Morin, J., Lavigne, F., Wassmer, P., 2010. Boulder and fine sediment transport and deposition by the 2004 tsunami in Lhok Nga (western Banda Aceh, Sumatra, Indonesia): A coupled offshore–onshore model. Marine Geology 268, 43–54.

Paris, R., Wassmer, P., Lavigne, F., Belousov, A., Belousova, M., Iskandarsyah, Y., Benbakkar, M., Ontowirjo, B., Mazzoni, N., 2014. Coupling eruption and tsunami records: the Krakatau 1883 case study, Indonesia. Bulletin of Volcanology 76, 814.

Park, L.E., 2012. Comparing two long-term hurricane frequency and intensity records from San Salvador Island, Bahamas. Journal of Coastal Research 28, 891– 902.

Park, L.E., Siewers, F., Metzger, T., Sipahioglu, S., 2009. After the hurricane hits: Recovery and response to large storm events in a saline lake, San Salvador Island, Bahamas. Quaternary International 195, 98–105.

Parsons, M.L., 1998. Salt Marsh Sedimentary Record of the Landfall of Hurricane Andrew on the Louisiana Coast: Diatoms and Other Paleoindicators. Journal of Coastal Research 14, 939–950.

Parsons, T., Geist, E.L., 2009. Tsunami probability in the Caribbean region. Pure and Applied Geophysics 165, 2089–2116.

Peros, M.C., Reinhardt, E.G., Davis, A.M., 2007a. A 6000-year record of ecological and hydrological changes from Laguna de la Leche, north coastal Cuba. Quaternary Research 67, 69–82.

Peros, M.C., Reinhardt, E.G., Schwarcz, H.P., Davis, A.M., 2007b. High-resolution paleosalinity reconstruction from Laguna de la Leche, north coastal Cuba, using Sr, O, and C isotopes. Palaeogeography, Palaeoclimatology, Palaeoecology 245, 535–550.

Peters, R., Jaffe, B., 2010. Identification of Tsunami Deposits in the Geologic Record: Developing Criteria Using Recent Tsunami Deposits. USGS Open-File Report 2010-1239.

Phantuwongraj, S., Choowong, M., 2012. Tsunami versus storm deposits from Thailand. Natural Hazards 63, 31–50.

Pignatelli, C., Sansò, P., Mastronuzzi, G., 2009. Evaluation of tsunami flooding using geomorphologic evidence. Marine Geology 260, 6–18.

Pignatelli, C., Scheffers, A., Scheffers, S., Mastronuzzi, G., 2010. Assessment of extreme wave flooding from geomorphologic evidence in Bonaire (Netherlands Antilles). Zeitschrift für Geomorphologie 54 (Suppl. 3), 219–245.

Pilarczyk, J.E., Reinhardt, E.G., 2012. *Homotrema rubrum* (Lamarck) taphonomy as an overwash indicator in Marine Ponds on Anegada, British Virgin Islands. Natural Hazards 63, 85–100.

Pilarczyk, J.E., Horton, B.P., Soria, J.L.A., Switzer, A.D. Siringan, F., Fritz, H.M., Khan, N.S., Ildefonso, S., Doctor, A.A., Garcia, M.L., 2016. Micropaleontology of the 2013 Typhoon Haiyan overwash sediments from the Leyte Gulf, Philippines. Sedimentary Geology 339, 104–114.

Pindell, J.L., Kennan, K., 2009. Tectonic evolution of the Gulf of Mexico, Caribbean and northern South America in the mantle reference frame: an update, in: James, K.H., Lorente, M.A., Pindell, J.L.

(Eds.), The origin and evolution of the Caribbean Plate. Geological Society, London, Special Publication 328, 1–55.

Putra, P.S., Nishimura, Y., Yulianto, E., 2013. Sedimentary Features of Tsunami Deposits in Carbonate-Dominated Beach Environments: A Case Study from the 25 October 2010 Mentawai Tsunami. Pure and Applied Geophysics 170, 1583–1600.

Radtke, U., Schellmann, G., Scheffers, A., Kelletat, D., Kromer, B., Kasper, H.U., 2003. Electron spin resonance and radiocarbon dating of coral deposited by Holocene tsunami events on Curaçao, Bonaire and Aruba (Netherlands Antilles). Quaternary Science Reviews 22, 1309–1315.

Rahiman, T.I.H., Pettinga, J.R., Watts, P., 2007. The source mechanism and numerical modelling of the 1953 Suva tsunami, Fiji. Marine Geology 237, 55–70.

Rajendran, C.P., Rajendran, K., Srinivasalu, S., Andrade, V., Aravazhi, P., Sanwal, J., 2011. Geoarchaeological Evidence of a Chola-Period Tsunami from an Ancient Port at Kaveripattinam on the Southeastern Coast of India. Geoarchaeology 26, 867–887.

Ramalho, R.S., Winckler, G., Madeira, J., Helffrich, G.R, Hipólito, A., Quartau, R., Adena, K., Schaefer, J.M., 2015. Hazard potential of volcanic flank collapses raised by new megatsunami evidence. Science Advances 1(9), e1500456.

Ramcharan, E.K., 2004. Mid-to-late Holocene sea level influence on coastal wetland development in Trinidad. Quaternary International 120, 145–151.

Ramcharan, E.K., McAndrews, J.H., 2006. Holocene development of coastal wetland at Maracas Bay, Trinidad, West Indies. Journal of Coastal Research 22, 581–586.

Rappaport, E.N., Fernandez-Partagas, J., 1997. The deadliest Atlantic tropical cyclones, 1492-1996. NOAA Technical Memorandum NWS NHC 47, URL: http://www.nhc.noaa.gov/pastdeadly.shtml?, last access 20 Nov 2015.

Razzhigaeva, N.G., Ganzei, L.A., Grebennikova, T.A., Ivanova, E.D., Kaistrenko, V.M., 2006. Sedimentation Particularities during the Tsunami of December 26, 2004, in Northern Indonesia: Simelue Island and the Medan Coast of Sumatra Island. Oceanology 46, 875–890.

Reading, A.J., 1990. Caribbean tropical storm activity over the past four centuries. International Journal of Climatology 10, 365–376.

Reid, H.F., Taber, S., 1919. The Porto Rico earthquakes of October-November 1918. Bulletin of the Seismological Society of America 9, 95–127.

Reinhardt, E.G., Goodman, B.E., Boyce, J.I., Lopez, G., van Hengstum, P., Rink, W., Mart, Y., Raban, A., 2006. The tsunami of 13 December A.D. 115 and the destruction of Herod the Great's harbor at Caesarea Maritima, Israel. Geology 34, 1061–1064.

Reinhardt, E.G., Pilarczyk, J., Brown, A., 2012. Probable tsunami origin for a Shell and Sand Sheet from marine ponds on Anegada, British Virgin Islands. Natural Hazards 63, 101–117.

Reyes, M., Engel, M., May, S.M., Brill, D., Brückner, H., 2015. Life and death after Super Typhoon Haiyan. Coral Reefs 34, 419.

Richmond, B.M., Watt, S., Buckley, M., Jaffe, B.E., Gelfenbaum, G., Morton, R.A., 2011. Recent storm and tsunami coarse-clast deposit characteristics, southeast Hawai'i. Marine Geology 283, 79–89.

Richmond, B. Szczuciński, W., Chagué-Goff, C., Goto, K., Sugawara, D., Witter, R., Tappin, D.R., Jaffe, B., Fujino, S., Nishimura, Y., Goff, J., 2012. Erosion, deposition and landscape change on the Sendai coastal plain, Japan, resulting from the March 11, 2011 Tohoku-oki tsunami. Sedimentary Geology 282, 27–39.

Rigby, J.K., Roberts, H.H., 1976. Geology, reefs and marine communities of Grand Cayman Island, B.W.I. Brigham Young University, Geology Studies, Special Publication 4, 1–95.

Rixhon, G., May, S.M., Engel, M., Mechernich, S., Keulertz, R., Schröder-Ritzau, A., Fohlmeister, J., Frank, N., Dunai, T., Brückner, H., 2016. Multiple dating approach (^{14}C, U/Th and ^{36}Cl) of tsunami-transported reef-top megaclasts on Bonaire (Leeward Antilles) – potential and current limitations. Geophysical Research Abstracts 18, EGU2016-6633.

Robinson, E., Rowe, D.-A.C., Khan, S.A., 2006. Wave-emplaced boulders on Jamaica's rocky shorelines. Zeitschrift für Geomorphologie, Suppl. Vol. 146, 39–57.

Rowe, D.-A., Khan, S., Robinson, E., 2009. Hurricanes or tsunami? Comparative analysis of extensive boulder arrays along the southwest and north coasts of Jamaica: Lessons for coastal management, in: McGregor, D., Dodman, D., Barker, D. (Eds.), Global change and Caribbean vulnerability. University of the West Indies Press, Kingston, pp. 49-73.

Samankassou, E., Viret, G., Kindler, P., 2008. Tsunami evidence during marine oxygen-isotope substage 5e on Eleuthera Island, Bahamas. The 14th Symposium on the Geology of the Bahamas and other Carbonate Regions, Abstracts and Program, pp. 21–22.

Sato, T., Nakamura, N., Goto, K., Kumagai, Y., Nagahama, H., Minoura, K., 2014. Paleomagnetism reveals the emplacement age of tsunamigenic coral boulders on Ishigaki Island, Japan. Geology 42, 603–606.

Sawai, Y., Jankaew, K., Martin, M.E., Prendergast, A., Choowong, M., Charoentitirat, T., 2009. Diatom assemblages in tsunami deposits associated with the 2004 Indian Ocean tsunami at Phra Thong Island, Thailand. Marine Micropaleontology 73, 70–79.

Sawai, Y., Namegaya, Y., Okamura, Y., Satake, K., Shishikura, M., 2012. Challenges of anticipating the 2011 Tohoku earthquake and tsunami using coastal geology. Geophysical Research Letters 39, L21309.

Scheffers, A.M., 2002a. Paleotsunami evidences from boulder deposits on Aruba, Curaçao and Bonaire. Science of Tsunami Hazards 20, 26–37.

Scheffers, A., 2002b. Paleotsunami in the Caribbean: field evidences and datings from Aruba, Curaçao and Bonaire. Essener Geographische Arbeiten 33.

Scheffers, A., 2004. Tsunami imprints on the Leeward Netherlands Antilles (Aruba, Curaçao, Bonaire) and their relation to other coastal problems. Quaternary International 120, 163–172.

Scheffers, A., 2005. Coastal response to extreme wave events – hurricanes and tsunamis on Bonaire. Essener Geographische Arbeiten 37.

Scheffers, A., 2006a. Ripple marks in coarse tsunami deposits. Zeitschrift für Geomorphologie, Suppl. Vol. 146, 221–233.

Scheffers, A., 2006b. Sedimentary impacts of Holocene tsunami events from the intra-American seas and southern Europe. Zeitschrift für Geomorphologie, Suppl. Vol. 146, 7–37.

Scheffers, A., Kelletat, D., 2003. Sedimentologic and geomorphologic tsunami imprints worldwide – a review. Earth-Science Reviews 63, 83–92.

Scheffers, A., Kelletat, D., 2006. New evidence and datings of Holocene paleo-tsunami events in the Caribbean (Barbados, St. Martin and Anguilla), in: Mercado-Irizarry, A., Liu, P. (Eds.), Caribbean tsunami hazard. World Scientific, Singapore, pp. 178–202.

Scheffers, A., Scheffers, S., 2006. Documentation of Hurricane Ivan on the coastline of Bonaire. Journal of Coastal Research 22, 1437–1450.

Scheffers, A., Scheffers, S., Kelletat, D., 2005. Paleo-tsunami relics on the southern and central Antillean Island Arc. Journal of Coastal Research 21, 263–273.

Scheffers, S., Scheffers, A., Radtke, U., Kelletat, D., Staben, K., Bak, R., 2006. Tsunamis trigger long-lasting phase-shift in a coral reef ecosystem. Zeitschrift für Geomorphologie, Suppl. Vol. 146, 59–79.

Scheffers, S.R., Haviser, J., Browne, T., Scheffers, A., 2009a. Tsunamis, hurricanes, the demise of coral reefs and shifts in prehistoric human populations in the Caribbean. Quaternary International 195, 69–87.

Scheffers, A.M., Engel, M., Scheffers, S.R., May, S.M., Hänßler, E., Löhr, K., Joannes-Boyau, R., Kelletat, D.H., Brückner, H., Vött, A., Schellmann, G., Schäbitz, F., Radtke, U., Sommer, B., 2014. Coastal landforms and event histories in a tropical carbonate environment, in: Martini, I.P. (Ed.), Coastal

Environments: from the Arctic to the Tropics. Geological Society of London, Special Publication 388, 503–531.

Schellmann, G., Radtke, U., 2004. The Marine Quaternary of Barbados. Kölner Geographische Arbeiten 81.

Schellmann, G., Radtke, U., Brückner, H., 2011. Electron Spin Resonance Dating (ESR), in: Hopley, D. (Ed.), Encyclopedia of Modern Coral Reefs – Structure, Form and Process. Springer, Dordrecht, pp. 368–372.

Scheucher, L.E.A., Vortisch, W., 2011. Field survey and hydrodynamics of storm-deposited boulders in the Southwestern Dominican Republic: Playa Azul, Provincia De Barahona, in: Bornemann, A., Brachert, T.C., Ehrmann, W. (Eds.), SEDIMENT 2011 – Sediments: Archives of the Earth System, Leipzig, June 23–26, 2011, Abstracts, pp. 88–89.

Scheucher, L.E.A., Piller, W.E., Vortisch, W., 2011. Foraminiferal analysis of tsunami deposits: two examples from the northeastern and southwestern coast of the Dominican Republic, in: Bornemann, A., Brachert, T.C., Ehrmann, W. (Eds.), SEDIMENT 2011 – Sediments: Archives of the Earth System, Leipzig, June 23–26, 2011, Abstracts, pp. 86–87.

Schubert, C., 1994. Tsunamis in Venezuela: Some Observations on their Occurrence. Journal of Coastal Research SI 12, 189–195.

Schubert, C., Valastro, S., 1976. Quaternary geology of La Orchila Island, central Venezuelan offshore, Caribbean Sea. Geological Society of America Bulletin 87, 1131–1142.

Sedgwick, P.E., Davis, R.A., 2003. Stratigraphy of washover deposits in Florida: implications for recognition in the stratigraphic record. Marine Geology 200, 31–48.

Shaw, C.E., Benson, L., 2015. Possible Tsunami Deposits on the Caribbean Coast of the Yucatán Peninsula. Journal of Coastal Research 31, 1306–1316.

Shaw, J., You, Y., Mohrig, D., Kocurek, G., 2015. Tracking hurricane-generated storm surge with washover fan stratigraphy. Geology 43, 127–130.

Smith, M.S., Shepherd, J.B., 1995. Potential Cauchy-Poisson Waves Generated by Submarine Eruptions of Kick 'em Jenny Volcano. Natural Hazards 11, 75–94.

Sigurdsson, H., Sparks, R.S.J., Carey, S.N., Huang, T.C., 1980. Volcanogenic Sedimentation in the Lesser Antilles Arc. Journal of Geology 88, 523–540.

Sohbati, R., Murray, A.S., Chapot, M.S., Jain, M., Pederson, J., 2012. Optically stimulated luminescence (OSL) as a chronometer for surface exposure dating. Journal of Geophysical Research 117, B09202.

Spiske, M., 2016. Coral-rubble ridges as dynamic coastal features – short-term reworking and weathering processes. Advances in Geosciences 38, 55–61.

Spiske, M., Jaffe, B.E., 2009. Sedimentology and hydrodynamic implications of a coarse-grained hurricane sequence in a carbonate reef setting. Geology 37, 839–842.

Spiske, M., Halley, R.B., 2014. A coral-rubble ridge as evidence for hurricane overwash, Anegada (British Virgin Islands). Advances in Geosciences 38, 9–20.

Spiske, M., Böröcz, Z., Bahlburg, H., 2008. The role of porosity in discriminating between tsunami and hurricane emplacement of boulders – A case study from the Lesser Antilles, southern Caribbean. Earth and Planetary Science Letters 268, 384–396.

Spiske, M., Piepenbreier, J., Benavente, C., Bahlburg, H., 2013. Preservation potential of tsunami deposits on arid siliciclastic coasts. Earth-Science Reviews 126, 58–73.

Srinivasalu, S., Thangadurai, N., Jonathan, M.P., Armstrong-Altrin, J.S., Ayyamperumal, T., Ram-Mohan, V., 2008. Evaluation of trace-metal enrichments from the 26 December 2004 tsunami sediments along the Southeast coast of India. Environmental Geology 53, 1711–1721.

Stein, J., Stein, S., 2013. Rebuilding Tohoku: A joint geophysical and economic framework for hazard mitigation. GSA Today 22, 42–44.

Stewart, S.R., 2004. Tropical Cyclone Report Hurricane Ivan 2–24 September 2004. NOAA National Hurricane Center, URL: http://www.nhc.noaa.gov/data/tcr/AL092004_Ivan.pdf , last access 16 Sep 2016.

Sugawara, D., Minoura, K., Imamura, F., 2008. Tsunamis and tsunami sedimentology, in: Shiki, T., Tsuji, Y., Yamazaki, T., Minoura, K. (Eds.), Tsunamiites – Features and Implications. Elsevier, Amsterdam, Oxford, pp. 9–49.

Sugawara, D., Goto, K., Jaffe, B.E., 2014. Numerical models of tsunami sediment transport – Current understanding and future directions. Marine Geology 352, 295–320.

Switzer, A.D., Jones, B.G., 2008. Setup, Deposition, and Sedimentary Characteristics of Two Storm Overwash Deposits, Abrahams Bosom Beach, Southeastern Australia. Journal of Coastal Research 24 (1A), 189–200.

Switzer, A.D., Srinivasalu, S., Thangadurai, N., Ram Mohan, V., 2012. Bedding structures in Indian tsunami deposits that provide clues to the dynamics of tsunami inundation, in: Terry, J.P., Goff, J. (Eds.), Natural Hazards in the Asia-Pacific Region: Recent Advances and Emerging Concepts. Geological Society, London, Special Publication 361, 61–77.

Switzer, A.D., Yu, F., Gouramanis, C., Soria, L.A.J., Pham, D.T., 2014. An integrated approach to assessing coastal hazards at multi-century timescales. Journal of Coastal Research SI 70, 723–728.

Szczuciński, W., 2012. The post-depositional changes of the onshore 2004 tsunami deposits on the Andaman Sea coast of Thailand. Natural Hazards 60, 115–133.

Szczuciński, W., Niedzielski, P., Kozak, L., Frankowski, M., Zioła, A., Lorenc, S., 2007. Effects of rainy season on mobilization of contaminants from tsunami deposits left in a coastal zone of Thailand by the 26 December 2004 tsunami. Environmental Geology 53, 253–264.

Szczuciński, W., Kokociński, M., Rzeszewski, M., Chagué-Goff, C., Cachão, M., Goto, K., Sugawara, D., 2012. Sediment sources and sedimentation processes of 2011 Tohoku-oki tsunami deposits on the Sendai Plain, Japan — Insights from diatoms, nannoliths and grain size distribution. Sedimentary Geology 282, 40–56.

Szczuciński, W., Pawłowska, J., Lejzerowicz, F., Nishimura, Y., Kokociński, M., Majewski, W., Nakamura, Y., Pawlowski, J., 2016. Ancient sedimentary DNA reveals past tsunami deposits. Marine Geology 381, 29–33.

Taggart, B.E., Lundberg, J., Carew, J.L., Mylroie, J.E., 1993. Holocene reef-rock boulders on Isla de Mona, Puerto Rico transported by a hurricane or seismic sea wave. Geological Society of America Abstracts with Programs, 25(6), A-61.

Tamura, T., Sawai, Y., Ikehara, K., Nakashima, R., Hara, J., Kanai, Y., 2015. Shallow-marine deposits associated with the 2011 Tohoku-oki tsunami in Sendai Bay, Japan. Journal of Quaternary Science 30, 293–297.

Tanguy, J.-C., 1994. The 1902–1905 eruptions of Montagne Pelée, Martinique: anatomy and retrospection. Journal of Volcanology and Geothermal Research 60, 87–107.

ten Brink, U., Twichell, D., Geist, E., Chaytor, J., Locat, J., Lee, H., Buczkowski, B., Barkan, R., Solow, A., Andrews, B., Parsons, T., Lynett, P., Lin, J., Sansoucy, M., 2008. Evaluation of Tsunami Sources with the Potential to Impact the U.S. Atlantic and Gulf Coasts – An Updated Report to the Nuclear Regulatory Commission. U.S. Geological Survey Administrative Report.

ten Brink, U.S., Marshak, S., Granja Bruña, J.-L., 2009. Bivergent thrust wedges surrounding oceanic island arcs: Insight from observations and sandbox models of the northeastern Caribbean plate. Geological Society of America Bulletin 121, 1522–1536.

Terry, J.P., Lau, A.Y.A., Etienne, S., 2013. Reef-Platform Coral Boulders – Evidence for High-Energy Marine Inundation Events on Tropical Coastlines. Springer, Singapore.

Tomblin, J., 1981. Earthquakes, volcanoes and hurricanes: A review of natural hazards and vulnerability in the West Indies. Ambio 10, 340–344.

Toscano, M.A., Macintyre, I.A., 2003. Corrected western Atlantic sea-level curve for the last 11,000 years based on calibrated ^{14}C dates from *Acropora palmata* framework and intertidal mangrove peat. Coral Reefs 22, 257–270.

Tuttle, M.P., Ruffman, A., Anderson, T., Jeter, H., 2004. Distinguishing Tsunami from Storm Deposits in Eastern North America: The 1929 Grand Banks Tsunami versus the 1991 Halloween Storm. Seismological Research Letters 75, 117–131.

Uchida, J.-I., Fujiwara, O., Hasegawa, S., Kamataki, T., 2010. Sources and depositional processes of tsunami deposits: Analysis using foraminiferal tests and hydrodynamic verification. Island Arc 19, 427–442.

UNEP, 2004. Regional Profile – Wider Caribbean Region. URL: http://www.unep.org/regionalseas/programmes/unpro/caribbean/ (last access 25 Nov 2015).

UNESCO, 2012. Exercise CARIBE WAVE/LANTEX 13 – A Caribbean Tsunami Warning Exercise, 20 March 2013. Volume 1, Participant Handbook. Intergovernmental Oceanographic Commission Technical Series 101.

Urquhart, G.R., 2009. Paleoecological record of hurricane disturbance and forest regeneration in Nicaragua. Quaternary International 195, 88–97.

Viret, G., 2008. Mégablocs au nord d'Eleuthera (Bahamas): preuve de vagues extrêmes au sous-stade isotopique 5e ou restes érosionnels? MSc thesis, University of Geneva.

von Hillebrandt-Andrade, C., 2013. Minimizing Caribbean Tsunami Risk. Science 341, 966–968.

Walsh, R., Reading, A., 1991. Historical changes in tropical cyclone frequency within the Caribbean since 1500. Würzburger Geographische Arbeiten 80, 199–240.

Wang, P., Horwitz, M.H., 2007. Erosional and depositional characteristics of regional overwash deposits caused by multiple hurricanes. Sedimentology 54, 545–564.

Wang, D.W., Mitchell, D.A., Teague, W.J., Jarosz, E., Hulbert, M.S., 2005. Extreme waves under Hurricane Ivan. Science 309, 896.

Ward, S.N., Day, S., 2001. Cumbre Vieja Volcano – potential collapse and tsunami at La Palma, Canary Islands. Geophysical Research Letters 28, 3397–4000.

Wassmer, P., Schneider, J.-L., Fonfrège, A.-V., Lavigne, F., Paris, R., Gomez, C., 2010. Use of anisotropy of magnetic susceptibility (AMS) in the study of tsunami deposits: Application to the 2004 deposits on the eastern coast of Banda Aceh, North Sumatra, Indonesia. Marine Geology 275, 255–272.

Watt, S.G., Jaffe, B.E., Morton, R.A., Richmond, B.M., Gelfenbaum, G., 2010. Description of extreme-wave deposits on the northern coast of Bonaire, Netherlands Antilles. USGS Open-File Report 2010-1180.

Watt, S., Buckley, M., Jaffe, B.E., 2012a. Inland fields of dispersed cobbles and boulders as evidence for a tsunami on Anegada, British Virgin Islands. Natural Hazards 63, 119–131.

Watt, S.F.L, Talling, P.J., Vardy, M.E., Heller, V., Hühnerbach, V., Urlaub, M., Sarkar, S., Masson, D.G., Henstock, T.J., Minshull, T.A., Paulatto, M., Le Friant, A., Lebas, E., Berndt, C., Crutchley, G.J., Karstens, J., Stinton, A.J., Maeno, F., 2012b. Combinations of volcanic-flank and seafloor-sediment failure offshore Montserrat, and their implications for tsunami generation. Earth and Planetary Science Letters, 319–320, 228–240.

Weil Accardo, J., Feuillet, N., Robert, H., Atwater, B., ten Brink, U.S., Deschamps, P., Tuttle, M.P., Wei, Y., Fuentes, Z., 2012. Age of overwash and rate of relative sea-level rise inferred from detrital heads and microatolls of medieval corals at Anegada, British Virgin Islands. AGU Fall Meeting 2012, Abstract T41A-2562.

Weiss, M.P., 1979. A saline lagoon on Cayo Sal, Western Venezuela. Atoll Research Bulletin 232, 1–33.

Weiss, R., 2012. The mystery of boulders moved by tsunamis and storms. Marine Geology 295–298, 28–33.

Weiss, R., Bourgeois, J., 2012. Understanding Sediments – Reducing Tsunami Risk. Science 336, 1117–1118.

Weiss, R., Diplas, P., 2015. Untangling boulder dislodgement in storms and tsunamis: Is it possible with simple theories? Geochemistry, Geophysics, Geosystems 16, 890–898.

Williams, H.F.L., 2009. Stratigraphy, sedimentology and microfossil content of Hurricane Rita storm surge deposits in Southwest Louisiana, Journal of Coastal Research 25, 1041–1051.

Williams, H.F.L., 2011. Shell bed tempestites in the Chenier Plain of Louisiana: late Holocene example and modern analogue. Journal of Quaternary Science 26, 199–206.

Williams, H.F.L., Flanagan, W.M., 2009. Contribution of Hurricane Rita storm surge to long-term sedimentation in Louisiana coastal woodlands and marshes. Journal of Coastal Research SI 56, 1671–1675.

Woodroffe, C.D., 1981. Mangrove swamp stratigraphy and Holocene transgression, Grand Cayman Islands, West Indies. Marine Geology 41, 271–294.

Woodruff, J.D., Donnelly, J.D., Mohrig, D., Geyer, W.R., 2008. Reconstructing relative flooding intensities responsible for hurricane induced deposits from Laguna Playa Grande, Vieques, Puerto Rico. Geology 36, 391–394.

Yamada, M., Fujino, S., Goto, K., 2014. Deposition of sediments of diverse sizes by the 2011 Tohoku-oki tsunami at Miyako City, Japan. Marine Geology 358, 67–78.

Yawsangratt, S., Szczuciński, W., Chaimanee, N., Chatprasert, S., Majewski, W., Lorenc, S., 2012. Evidence of probable paleotsunami deposits on Kho Khao Island, Phang Nga Province, Thailand. Natural Hazards 63, 151–163.

Young, R.W., Bryant, E.A., Price, D.M., 1996. Catastrophic wave (tsunami?) transport of boulders in southern New South Wales, Australia. Zeitschrift für Geomorphologie 40, 191–207.

Zahibo, N., Pelinovsky, E., 2001. Evaluation of tsunami risk in the Lesser Antilles. Natural Hazards and Earth System Sciences 1, 221–231.

Zahibo, N., Pelinovsky, E., Yalciner, A., Kurkin, A., Koselkov, A., Zaitsev, A., 2003. The 1867 Virgin Island tsunami: observations and modeling. Oceanologica Acta 26, 609–621.

Zahibo, N., Pelinovsky, E., Okal, E., Yalçiner, A., Kharif, C., Talipova, T., Kozelkov, A., 2005. The earthquake and tsunami of November 21, 2004 at Les Saintes, Guadeloupe, Lesser Antilles. Science of Tsunami Hazards 23, 25–39.

Zainali, A., Weiss, R., 2015. Boulder dislodgement and transport by solitary waves: Insights from three-dimensional numerical simulations. Geophysical Research Letters 42, 4490–4497.

Zonneveld, J.I.S., de Buisonjé, P.H., Herweijer, J.P., 1977. Geomorphology and denudation processes, in: Anonymous (Ed.), Guide to the field excursions on Curaçao, Bonaire and Aruba, Netherlands Antilles. 8th Caribbean Geological Conference on Curaçao, 9–24 July 1977. GUA Paper of Geology 10, 56–68.

Table 1: Characteristics of sand-dominated tsunami and storm deposits as inferred from recent and selected historical and palaeo-events. Furthermore, their potential in the separation between tsunami and storm deposits is evaluated. IOT = Indian Ocean Tsunami; PNG = Papua New Guinea; [A] Jagodziński et al. (2012); [B] Richmond et al. (2012); [C] Szczuciński et al. (2012) – all Tohoku-oki Tsunami 2011, Sendai plain, Japan; [D] Gelfenbaum and Jaffe (2003) – Aitape Tsunami 1998, Papua New Guinea (PNG); [E] Babu et al. (2007) – IOT 2004, southwest India; [F] Uchida et al. (2010) – specific review; [G] Jaffe et al. (2003) – Peru Tsunami 2001, south Peru; [H] Bahlburg and Weiss (2007) – IOT 2004, southeast India; [I] Hawkes et al. (2007); [J] Naruse et al. (2010) – both IOT 2004, Andaman coast, Thailand; [K] Nichol and Kench (2008) – IOT 2004, Maldives; [L] Szczuciński (2012) – IOT 2004, Andaman coast, Thailand; [M] Lario et al. (2016) – Chile Tsunami 2010, central Chile; [N] Switzer et al. (2012) – IOT 2004, southeast India; [O] Morton et al. (2007) – Aitape Tsunami 1998, PNG; [P] Phantuwongraj and Choowong (2012) – IOT 2004, Andaman coast, Thailand; [Q] Moore et al. (2011) – West Java Tsunami 2006, Java, Indonesia; [R] Kain et al. (2016) – tsunamis of 1868 and 1960, Okains Bay, New Zealand; [S] Spiske et al. (2013) – Peru Tsunami 2001, south Peru; [T] Goff et al. (2012) – specific review; [U] Martin Arcos et al. (2013) – Tohoku-oki Tsunami 2011, Galapagos; [V] Sawai et al. (2009) – IOT 2004, Andaman coast, Thailand; [W] Brill et al. (2012) – IOT 2004, Andaman coast, Thailand; [X] Cuven et al. (2013) – Lisbon Tsunami 1755, southwest Spain; [Y] Horton et al. (2011) – Chile Tsunami 2010, south-central Chile; [Z] Paris et al. (2014) – Krakatoa Tsunami 1883, Java and Sumatra, Indonesia; [AA] Nishimura and Miyaji (1995) – Hokkaido-nansei-oki Tsunami 1993, Oshima Peninsula, Japan; [AB] Pantosti et al. (2008) – historical tsunamis of AD 17 and AD 1783(?), northeast Sicily, Italy; [AC] Rajendran et al. (2011) – palaeotsunami, southeast India; [AD] Kilfeather et al. (2007) – Orphan Tsunami 1700(?), Washington State, USA; [AE] Bahlburg and Weiss (2007) – IOT 2004, Kenya; [AF] Matsumoto et al. (2008) – IOT 2004, Andaman coast, Thailand; [AG] Minoura et al, (1994); [AH] Ishimura and Miyauchi, 2015 – both historical tsunamis, Sanriku coast, Japan; [AI] Bahlburg and Spiske (2012) – Chile Tsunami 2010, Isla Mocha, Chile; [AJ] Nanayama et al. (2000) – Hokkaido-nansei-oki Tsunami 1993, Oshima Peninsula, Japan; [AK] Paris et al. (2010) – IOT 2004, northwest Sumatra, Indonesia; [AL] Donato et al. (2008) – Makran Tsunami 1945, Sur lagoon, Oman; [AM] Reinhardt et al. (2006) – historical tsunami AD 115, Caesarea, Israel; [AN] Mamo et al. (2009) – specific review; [AO] Davies et al. (2003) – Aitape Tsunami 1998, PNG; [AP] Putra et al. (2013) – Mentawai Tsunami 2010, southern Mentawais, Indonesia; [AQ] Hindson and Andrade (1999) – Lisbon Tsunami 1755, south Portugal; [AR] Hussain et al. (2006) – IOT 2004, Andaman and Nicobar Islands; [AS] Kortekaas and Dawson (2007) – Lisbon Tsunami 17555, southwest Portugal; [AT] Yawsangratt et al. (2012) – IOT 2004, Andaman coast, Thailand; [AU] Szczuciński et al. (2016) – palaeotsunami, Hokkaido, Japan; [AV] Hussain et al. (2010) – IOT 2004, southeast India; [AW] Hemphill-Haley (1996) – Orphan Tsunami 1700(?), Washington State, USA; [AX] Dawson (2007) – Aitape Tsunami 1998, PNG; [AY] Dura et al. (2016) – specific review; [AZ]

Tuttle et al. (2004) – Grand Banks Tsunami 1929, Burin Peninsula, Canada; [BA] Engel et al. (2009) – palaeotsunami, Bonaire, Leeward Antilles; [BB] Szczuciński et al. (2007) – IOT 2004, Andaman coast, Thailand; [BC] Srinivasalu et al. (2008) – IOT 2004, southeast India; [BD] Costa et al. (2012) – Lisbon Tsunami 1755, south Portugal; [BE] Costa et al. (2012) – IOT 2004, northwest Sumatra, Indonesia; [BF] Peters and Jaffe (2010) – specific review; [BG] Paris et al. (2007) – IOT 2004, northwest Sumatra, Indonesia; [BH] Abe et al. (2012) – Tohoku-oki Tsunami 2011, Sendai plain, Japan; [BI] MacInnes et al. (2009) – Kuril Island Tsunami 2006, Kuril Islands, Russia; [BJ] Morton et al. (2008b) – IOT 2004, Sri Lanka; [BK] Moore et al. (2007) – Grand Banks Tsunami 1929, Newfoundland, Canada; [BL] Atwater et al. (2013a) – Chile Tsunami 1960, Maullín, Chile; [BM] Nanayama et al. (2000) – Miyakojima Typhoon 1959, southwest Hokkaido, Japan; [BN] Switzer and Jones (2008) – storms in 2001, southeast Australia; [BO] Williams (2009) – Hurricane Rita 2005, southwest Louisiana, USA; [BP] Parsons (1998) – Hurricane Andrew 1992, Louisiana, USA; [BQ] Morton et al. (2007) – Hurricane Carla 1961, Gulf of Mexico/Hurricane Isabel 2003, western Atlantic Ocean; [BR] Wang and Horwitz (2007) – several hurricanes 2004/2005, Florida, USA; [BS] Brill et al. (2016) – Typhoon Haiyan 2013, Visayas, Philippines; [BT] Horton et al. (2009) – Hurricanes Katrina and Rita 2005, Mississippi, Alabama, USA; [BU] Williams (2011) – Hurricane Ike 2008, southwest Louisiana, USA; [BV] Tuttle et al. (2004) – Halloween Storm 1991, Massachusetts, USA; [BW] Sedgwick and Davis (2003) – recent storms, Florida; [BX] Phantuwongraj and Choowong (2012) – recent storms, Gulf of Thailand; [BY] Shaw et al. (2015) – Hurricane Ike 2008, Texas, USA; [BZ] Boyajian and Thayer (1995) – winter storm 1992, New Jersey, USA; [CA] Hawkes and Horton (2012) – Hurricane Ike 2008, Texas, USA; [CB] Pilarczyk et al. (2016) – Typhoon Haiyan 2013, Visayas, Philippines; [CC] Hippensteel et al. (2013) – Hurricane Irene 2011, North Carolina, USA; [CD] Kortekaas and Dawson (2007) – post-1755 storm, southwest Portugal; [CE] Williams and Flanagan (2009) – Hurricane Rita 2005, southwest Louisiana, USA; [CF] Morton (2010) – recent hurricanes, Mississippi, Alabama, USA; [CG] Wassmer et al. (2010) – IOT 2004, northwest Sumatra, Indonesia; [CH] May et al. (2016) – palaeotsunami, Cape Range peninsula, Western Australia.

Sedimentary feature	**Tsunami deposits**	**Storm deposits**	**Indicative potential**	**Remarks**
Sediment source	• Mostly beach, dunes [A–C] • A minor terrestrial component, in particular in the finer, mud-dominated fraction [A] • Significant part (>60%) may come from offshore [D,E], including deeper shelf and bathyal zone [F]	• Mainly shoreface, beach and dune [BM–BO] • Minor part from shallow embayments, if present [BP]	Medium–high	• Tsunami deposits tend to have a wider range of source areas; a bathyal or deeper component has not been reported from storm deposits

Lower contact	• Generally sharp and erosional as a function of bottom shear stress (flow velocity, depth, bedload) [B,G–J] • In some cases sharp but non-erosional [K] • Sharp contact may vanish within years after deposition [L] • In rare cases, sharp contact may be absent even in fresh deposits [M]	• Generally sharp [BO,BQ–BS] • Erosional contact in few cases [BR,BT]; more common in the proximal part [BO] or in case of coarse shell beds [BU]	Low	• An erosive lower contact seems to be more common in tsunami deposits
Lower contact of subunits	• Mostly sharp, in some cases even erosional [N]	• Sharp and in some cases even erosional, if present [BO]	Not indicative	-
Bedding structures	• Entire deposit may be normally graded [D] • Multiple normally graded subunits related to the number of tsunami waves [I,O,P] • Lower part of subunits may be inversely graded (traction carpet), but has lower preservation potential due to immediate erosion [J,P,Q] • Bedding is very complex; number of subunits and pattern of grading varies significantly along a shore-perpendicular transect [J,N] • Deposit may also show no grading at all [K,R] • Basal cross-bedding may occur close to the shore [H] • Fining upward may change to coarsening upward in subaerial deposits within years due to removal of the fine fraction in the uppermost part [K,S]	• In lower part mostly planar lamination [BQ,BS], in some cases trough cross bedding observed [BO] • Climbing ripples may occur in basal part [BO] • Foreset bedding (subaqueous deposition) very common in the thicker, proximal deposit [BM–BO,BV], but may also occur in the more distal part [BW,BX] • Foreset bedding c. 30°, planar bedding <4° [BW] • Foreset bedding is confined to a thickness of >20 cm, thinner deposits show (sub-)planar bedding [BX] • Topset may be clearly developed [BY] • Often (sub-)planar lamination in case of subaerial deposition, separated into several normally or ungraded laminasets [BN,BQ,BX] • Inverse grading may also occur [BO] • Preservation of bedding structures may vary as a function of elevation, bioturbation, sea-level change and frequency of storms [BW]	Medium to high if well preserved	• Foreset bedding in combination with bottom and topsets indicative of storm overwash • Low number of graded beds with basal traction carpet indicative of tsunami deposition • Anisotropy of magnetic susceptibility [CG] or µCT [BS, CH] offer great potential to study such features on a very small scale, even if they are not macroscopically visible
Grain size distribution	• Function of highly variable hydrodynamic conditions, sediment source, local topography and distance to shoreline [T] • Mostly coarser than the background sediments [P,S] • Mostly bi- to multimodal [S], but may also be unimodal in sand [B] • May be modified within years due to winnowing of finer fraction [S,U]	• Mostly unimodal [BO], but can be bimodal as function of the sediment source [BS] • Mostly coarser than the background sediments [BT]	Low–medium	• Storm deposits tend to show unimodal, tsunami deposits bi- or multimodal distributions, but site-specific deviations from this pattern need to be considered

Sorting	• Mostly poor to moderate sorting; generally poorer sorted than vertically confining deposits [E,P]	• Mostly well sorted [BO,BS,BX], but may vary within a deposit from poor to very well [BQ]	Low–medium	• Storm surge deposits tend to be better sorted than tsunami deposits due to more restricted source areas; site-specific deviations from this pattern need to be considered
Internal mud laminae	• Sand deposit has a mud cap where mud is comprised in the sediment source [D,G] • Thin mud drapes may be present within sandy subunits representing suspension load of the waning stage between waves [G,J] • Mud layers may contain a range of different light objects, such as plant remains [V]	• Internal mud laminae not reported [BQ] • Mud cap on top may exist [BO]	Medium	• A low number of internal mud laminae may be indicative of tsunami deposition
Intraclasts	• Deposit may contain rip-up clasts of underlying cohesive substrate [B,P,W,X] • Intraclasts may comprise pebbles [B,Y], pumice [Z], etc. • Intraclasts may comprise recent anthropogenic materials [B,AA] or ancient artifacts, such as bones, teeth , glass, pottery etc.; deposit may even be clast supported [AB,AC] • Rip-up clasts may occur on a microscopic scale [AD]	• Rip-up clasts usually absent [BQ], but have been reported in very rare cases [BU,BX] • All sorts of objects may occur as intraclasts (asphalt, tree logs, plastic litter, wood, pebbles, cobbles, boulders, glass bottles, etc.) [BM,BR,BV,BX]	Medium	• Rip-up clasts of underlying cohesive substrate are much more common in tsunami deposits
Heavy minerals	• Heavy mineral laminae often present in the lower part of subunits depending on the sediment source [E,AE]	• May be present in foreset and planar lamination, depending on sediment source [BQ–BS] • Higher concentration at base of normally graded laminasets [BN]	Low	• Highly site-dependent: Can be useful in combination with a thorough characterization of source environments
Truncated flame structures/ loading structures	• Truncated flame structures in the upper, finer part of a subunit may occur due to synchronous erosion and deformation induced by an overlying, coarser subunit [AF] • Basal loading structures may occur in water-saturated sedimentary settings [AG,AH]	• Not reported	Medium	• Even though load structures are only rarely reported from tsunami deposits they are highly indicative as they seem to be absent in storm deposits
Backflow-induced structures	• Not necessarily present; function of onshore inclination and topography [AI] • Strong component of terrestrial deposits [AJ] • Seaward cross-bedding or parallel lamination on top of the deposit [N,P] • Seaward ripple formation may occur on top of the deposit [AK] • Seaward imbrication of flat intraclasts may occur [AJ] • Backflow structures may have poor preservation potential [P]	• Backflow structures mostly absent [BM,BS] • Some small-scale cut-and-fill structures (channels) may be present in upper part of the deposit [BV]	Low–medium	• Backflow cut-and-fill showing seaward cross-bedding is much more common in tsunami deposits whereas bidirectional flow can also occur after storm inundation as a function of onshore topography
Mollusc shells	• Deposit may contain mollusc shells of a wide range of habitats in low [B] to high [AL] concentrations, largely depending on sediment source	• Source dependent [BQ] • Shell laminae more common in the proximal deposit [BO]	Low–medium	• Highly site-dependent, but a high number of articulated shells, angular breaks and stress fractures

	• High percentage of articulated bivalve shells [AL] if sediment source comprises bivalve shell habitat • Shell fragments may predominantly show angular breaks and stress fractures [AL] • Size of shell fragments may show overall normal grading [B,X] • Larger shells mostly convex-up and loosely packed [AM] • In coral reef settings, onshore deposits may contain larger coral fragments and other bioclasts [K,AK]	• Entire (graded) shell beds occur in widths of <50 m in the backbarrier where the concentration of skeletal remains is high in the foreshore [BU,BZ] • Shells are mostly disarticulated [BU], even though a dominance of articulated shells has also been observed [BZ] • Fine shell hash at the top of normally graded laminasets [BN]		may rather be indicative of a tsunami deposit
Foraminifera	• In general: Deposit may show allochthonous marine assemblage, mostly dominated by shallow marine/shelf taxa, changes in test numbers, size, or adult/juvenile ratio compared to background sedimentation, taphonomic changes [AN] • May include taxa from outer shelf to upper bathyal depths [AO,AP] • Many tests broken or abraded [AQ,AR, AS] • Dominance of inner-shelf and brackish/freshwater taxa, respectively, may indicate uprush and backflow component of a deposit [I] • Calcareous forams mostly larger in size than in vertically confining deposits [I] • Poor preservation potential: tests may dissolve quickly within years after deposition in tropical humid environments [AT] • Ancient DNA may help to trace weathered foraminifers in the deposit [AU]	• Allochthonous intertidal and subtidal, benthic (nearshore) and planktonic (offshore) taxa [CA,CB] • Presence strongly depending on sediment source [BN,BS,CB] • More diverse assemblages than vertically confining deposits [CB] • Calcareous forams mostly larger in size than in vertically confining deposits [CB] • Test size decreases inland [CB] • Preservation potential of tests may be low due to dissolution [CC]; more robust taxa preferentially preserved [BN] • Many tests broken [CD]	Medium	• Even though assemblages of storm and tsunami deposits can be very similar, the presence of those from deeper waters below the storm wave base may be used as indicator for tsunami deposition
Ostracods	• Onshore deposit may contain allochthonous marine assemblage [AQ,AR] • Preservation of valves may vary between rather well [AQ] and poor [AV] • Low carapace/valve ratios may indicate high-energy inflow of tsunami [AV]	• Not yet investigated in detail	-	-
Diatoms	• Deposit may contain diatoms from a range of different habitats from freshwater and brackish to fully marine depending on the sediment source [C,V,AW] • Larger beach and shallow subtidal taxa may dominate in the bedload component of a deposit (lower part), while lighter marine and/or planktonic taxa may dominate the suspension load of the upper part [V]	• Deposit may contain diatoms from a range of different habitats from freshwater to salt marsh and shallow marine, including planktonic taxa [BP]	Low	• Too few information on diatoms from recent storm deposits available

	• Taphonomy of valves may range from >75% broken [AX] to mostly well preserved [V,AW] • Concentration of diatoms in the deposit varies, depends on sediment source: mostly low where beach and dune sands dominate, higher where material from terrestrial soils or marshes is incorporated [AY]			
Pollen	• Dramatic changes of pollen assemblage in the deposit, e.g. from a wooded bog to saltmarsh community [AZ] or through a sudden decline of mangroves [BA]	• Not yet investigated in detail	-	-
Geochemical signature	• Increased concentrations in dissolved salts (Na, Ca, Mg, Cl, S) compared to vertically confining deposits [BB,BC] • Salts are quickly removed where the deposit is exposed to high rates of rainfall [BB] • Deposit may be enriched with trace metals where the sediment source is anthropogenically contaminated [BB,BC]	• Not yet investigated in detail	Low	Peaks in dissolved salts may indicate marine flooding but provide no evidence for the depositional process ; however, increases in terrestrial ions (e.g. Fe, K) may be used to trace the backwash component of a tsunami deposit
Microtexture on quartz grains	• Percussion marks highly abundant where sediment concentration in tsunami flow is high [BD] • Fresh surfaces dominant where sediment concentration is lower [BE]	• Fresh surfaces dominating, low number of percussion marks [CE]	Low	Very dependent on local sediment sources and sediment concentration during storm or tsunami inundation, too few empirical studies
Thickness	• Mostly less than 30 cm, localized up to 150 cm, depending on sediment availability, hydrodynamic conditions and onshore topography [BF] • Usually thickest part up to several tens of metres landward behind a zone of erosion, then landward thinning [BG]	• Mostly thick and narrow, >30 cm up to >1 m, thinning landward [BO,BQ,BV] • Thickest in topographic lows [BO,CA]	Low	Highly variable and a function of local topography, sediment availability and magnitude of the flooding
Landward extent	• Strongly depending on size of the tsunami, sediment availability, and local topography [BF] • Sand sheet deposition may occur up to several km inland on a low-angle coastal plain [B,BG] • Relation between landward extent of the deposit and inundation may vary between 50–60% [BH] and 90% [BI] • May be locally discontinuous [Q,BJ] • In most cases landward fining trend [C,G,BK] • May breach barriers and build fans [BL]	• Washover fan or sand sheet thins and fines inland [BO,CE] • Landward thinning often abrupt [BO] • Storm overwash often builds (coalesced) fans behind barrier breaches [BS,CF]	Medium	Tsunami deposits seem to have a relative greater inland extent and tend to occupy higher elevations than storm deposits

Table 2: Characteristics of coarse-clast tsunami and storm deposits as inferred from recent and selected historical and palaeo-events. Furthermore, their potential in the separation between tsunami and storm deposits is evaluated. IOT = Indian Ocean Tsunami; BVI = British Virgin Islands;

[A] Richmond et al. (2011) – tsunamis of 1868 and 1975, Hawai'i; [B] Yamada et al. (2014) – Tohoku-oki Tsunami 2011, Sanriku coast, Japan; [C] Rahiman et al. (2007) – Suva Tsunami 1953, Fiji; [D] Terry et al. (2013) – specific review; [E] Goto et al. (2007) – IOT 2004, Andaman coast, Thailand; [F] Kelletat et al. (2007) – IOT 2004, Andaman coast, Thailand; [G] Paris et al. (2009) – IOT 2004, northwest Sumatra, Indonesia; [H] McAdoo et al. (2011) – South Pacific Tsunami 2009, Samoa; [I] Buckley et al. (2012) – historical tsunami, Anegada, BVI; [J] Nandasena et al. (2013) – Tohoku-oki Tsunami 2011, Sanriku coast, Japan; [K] Goto et al. (2012) – Tohoku-oki Tsunami 2011, Sabusawa Island, Japan; [L] Bourgeois and MacInnes (2010) – Central Kuril Island Tsunami 2006, Matua Island, Kuril Islands; [M] Goto et al. (2010) – Meiwa Tsunami 1771, Ishigaki Island, Japan; [N] Paris et al. (2014) – Krakatoa Tsunami 1883, west Java, Indonesia; [O] Etienne et al. (2011) – specific review; [P] Bahlburg and Spiske (2012) – Chile Tsunami 2010, Isla Mocha, Chile; [Q] Razzhigaeva et al. (2006) – IOT 2004, Simeulue Island, Indonesia; [R] Scheffers (2002b, 2004) – palaeotsunamis, Bonaire, Leeward Antilles; [S] Scheffers and Kelletat (2003) – specific review; [T] Scheffers and Scheffers (2006) – Hurricane Ivan 2004, Bonaire, Leeward Antilles; [U] Khan et al. (2010) – Hurricane Dean 2007, Jamaica; [V] Goto et al. (2011) – recent typhoons, Okinawa Islands, Japan; [W] Cox et al. (2012) – recent winter storms, Aran Islands, Ireland; [X] May et al. (2015b) – Typhoon Haiyan 2013, Eastern Samar, Philippines; [Y] Maragos et al. (1973) – Tropical cyclone Bebe 1972, Funafuti Atoll, Tuvalu; [Z] Hernandez-Avila et al. (1977) – (sub-)recent hurricanes, Grand Cayman; [AA] Spiske and Jaffe (2009) – Hurricane Lenny 1999, Bonaire, Leeward Antilles; [AB] Etienne and Terry (2012) – Tropical cyclone Tomas 2010, Fiji; [AC] Etienne (2012) – Tropical cyclone Oli, French Polynesia; [AD] Spiske and Halley (2014) – historical hurricanes, Anegada, BVI; [AE] Kennedy et al. (2015) – Typhoon Haiyan 2013, Eastern Samar, Philippines; [AF] Brill et al. (2016) – Typhoon Haiyan 2013, central Visayas, Philippines; [AG] Miller et al. (2014) – historical hurricanes, Jamaica; [AH] Cox et al. (2016) – winter storms 2013–2014, Aran Islands, Ireland; [AI] Etienne and Paris (2010) – subrecent storms, Reykjanes Peninsula, Iceland; [AJ] Morton et al. (2008a) – past hurricanes, Caribbean; [AK] Blumenstock et al. (1961) – Typhoon Ophelia 1958, Marshall Islands; [AL] Richmond et al. (2011) – historical storms, Hawai'i; [AM] Scheffers et al. (2014) – past hurricanes, Bonaire, Leeward Antilles; [AN] Scheffers (2002b) – past hurricanes, Bonaire, Leeward Antilles; [AO] Spiske (2016) – Hurricane Earl 2010, Anegada, BVI.

Sedimentary/ geomorphic feature	**Tsunami deposits**	**Storm deposits**	**Indicative potential**	**Remarks**
Sediment source	• Subaerial cliff edges [A,B] • Reef crest or slope [C,D] • Living or dead coral colonies or large coral slabs in shallow water [E–G]	• Subaerial cliff edges or cliff top [T–X] • Reef crest or slope [D,V] • Living or dead coral colonies or large coral slabs in shallow water [T,Y–AA] • Exhumed beachrock outcrops [AB]	Low	• Boulder sources very similar for transport during tsunamis and storms

	• Exhumed beachrock outcrops [G,H] • Onshore rock outcrops [I,J] • Intertidal or onshore artificial structures: seawalls, rip-rap boulders, roads, concrete structures, etc. [B,G,K] • Most boulders rest in subtidal [L] to supratidal [B] position prior to transport	• Artificial structures such as rip rap boulders [AC] • Most coarse clasts rest in subtidal [T,AA,AD–AF], intertidal [V] or supratidal [X,AE] position prior to transport as stepwise transport inland is very common [AG]		
Singular mega-boulders	• Very large isolated boulders or fine blocks up to several hundred tons [B,J,M,N] • Distributed in intertidal or supratidal position, up to 750 m inland where onshore topography is low [B,M] • Presence is a function of availability and tsunami magnitude [O]	• Very large isolated boulders or fine blocks up to several hundred tons in intertidal [V,W] or cliff-top [X,AH] position • Only short transport distance for largest boulders >100 t recorded [U,W,AH] • Presence is a function of availability, storm magnitude, and other processes associated with the storm, such as infragravity waves [W] or vertical jets at cliffs [AH]	Low-medium	• Boulder size or weight alone is not suitable to distinguish between tsunami and storm • The transport distance of very large tsunami boulders seem to be greater; they are distributed further inland
Boulder fields	• Fields of scattered boulders very common [A,E,G] • In most cases no shore-perpendicular fining trend [A,E,G,P] • Abrupt landward fining only at the landward limit of boulder distribution [B] • General landward fining may occur where return flow plays a major role [K] • Boulders may show imbrication [G]	• Fields of boulders occur, for instance, on intertidal reef flats [V], but their inland extent is rather small [AE] • Exponential landward fining is common (V,AE,AI]	Medium	• Landward fining in a boulder distribution seems to be indicative of repeated storm impact in case non-linear wave phenomena such as infragravity waves do not play a role
Linear constructional landforms (ramparts, ridges)	• Not observed in tsunamis [A,D,K,O] • Coarse-clast ridges may form right after the tsunami as an immediate response to the erosive event [G] • Small rampart observed after the IOT 2004 was attributed to low-amplitude sea-level variations at the final stage of the tsunami [Q] • In some cases, ramparts have been associated with palaeotsunamis [R,S]	• Highly depending on availability of sediments, clast size, and wave run-up [AJ] • Upper intertidal ridges or ramparts (broader ridge-complexes) of coral rubble close to the coast or along the edge of a shallow reef flat [T,Y,Z,AB,AF,AK,AL] • Small, narrow ridges, cliff-top ridges [W,AL] and ramparts [AM] in elevations up to 40 m [W] • Ridges more narrow, steeper, better sorted, unimodal, from gravel to boulder size, low sand content, up to several metres high [T,AM], may be segmented or cuspate in higher position [AL] • Ramparts (ridge complexes) very wide (up to 200 m), steep seaward side, low inclination inland (wedge-shaped), poorly sorted (sand to boulder), multimodal, layered [Y,AJ,AM,AN]	High	• Large shore-parallel constructional landforms are highly indicative of long-term formation dominated by recurring storms

		• Smaller, narrow ridges close to sea level may be built during one single storm [T,AF], but are prone to reworking by subsequent events [AK,AO] • Coarse-clast ridges may form washover lobes at their landward side [AA,AK] • Clast imbrication may indicate flow direction [AA,AJ] • Ridges/ramparts may extend for several kilometres parallel to the shore [X,Z,AM]		

Table 1: Earthquake and fault parameters used for simulating pan-Caribbean tsunamis originating at the Muertos Thrust Belt (MTB) and the South Caribbean Deformed Belt (SCBD).

Parameter	**Muertos Thrust Belt (MTB) scenario**	**South Caribbean Deformed Belt (SCBD) scenario**
M	7.99 (7.8 given in ten Brink et al., 2009)	8.8 (8.5 given in ten Brink et al., 2008; UNESCO, 2012)
Fault length	188 km (170 km given in ten Brink et al., 2009)	550 km (ten Brink et al., 2008)
Strike	92.1–143.3°	74.5° (ten Brink et al., 2008)
Width	61 km (45 km given in ten Brink et al., 2009)	100 km (UNESCO, 2012)
Depth	24 km (NGDC/WDS, 2016)	10 km (UNESCO, 2012)
Dip	10° (Byrne et al., 1985; ten Brink et al., 2009)	17° (ten Brink et al., 2008; UNESCO, 2012)
Slip	3.0 m (ten Brink et al., 2009)	7.8 m

Table 4: Sediment-based reconstructions of palaeoenvironments and coastal processes reviewed for evidence of extreme-wave events. All sites are indicated in Fig. 3. For all sites, the 30-yr probability of tsunami run-up >0.5 m (Parsons and Geist, 2009), the calculated amplitude of the Virgin Island Tsunami of 1867 (Zahibo et al., 2003), tsunami height in the SCDB scenario (Fig. 7), and the decadal number of hurricanes (Reading, 1990) is shown. The depositional process is coded as follows: 0 = No disturbance in the stratigraphy/no coarse-clast record evident; 1 = Disturbance/deposition attributed to storm; tsunami impact is excluded; 2 = Disturbance/deposition documented and storm is favoured over tsunami, but the latter is not entirely excluded; 3 = Disturbance/deposition is ascribed to either hurricane or tsunami; 4 = Disturbance/deposition is documented and tsunami is favoured over hurricane, but the latter is not entirely excluded; 5 = Disturbance/deposition is documented, ascribed to tsunami, and hurricane is excluded.

No.	Author(s)	Goal of the study	Location	Time covered by sediment archive (years BP)	Type of sediment archive	Evidence for extreme wave events	Age of the candidate tsunami deposit	30-year prob. of tsunami run-up > 0.5 m	Amplitude 1867 tsunami (m)	Tsunami height SCDB scenario (m)	Decadal number of hurricanes	Interpetation in the original source (see order of literature sources)
1	McCloskey and Keller (2009), McCloskey and Liu 2013a)	Reconstruction of palaeotempests	Gales Poin, Mullins River, Commerce Bight (Belize)	5000–0; 7000–0	C/D:Swamp, lagoon	Hurricanes inferred, since absence of historical accounts on tsunamis and low tsunami potential of the area	-	0 (Belize City)	n/d	n/d	5–9	1
2	Adomat and Gischler (2015, 2016)	Reconstructing Holocene coastal environments and palaeo-hurricanes	Manatee Lagoon, Colson Point Lagoon, Commerce Bight Lagoon, Sapodilla Lagoon, Mullins River Beach (Central Belize)	c. 8000–0	C/D: Coastal lagoons, mangrove swamp	Multiple hurricane overwash and sediment deposition is inferred at all sites, tsunamis seem unlikely due to the low tsunami potential of the area	-	0 (Belize City)	n/d	n/d	5–9	1; 2
3	Macintyre et al., (1995, 2004); McKee et al. (2007)	Reconstructing rates of peat formation and mangrove complexes	Tobacco, Range; Twin Cays (Belize)	c. 7000–0	C: Mangrove island	No indication for extreme-wave events; sand lenses interpreted as shoreline migration	-	0 (Belize City)	n/d	n/d	5–9	0
4	Gischler (2003); Gischler et al. (2008); McCloskey and Liu (2013b); Denommee et al. (2014)	Reconstructing lagoonal development and climate variations	Turneffe Islands, Glovers Reef, Lighthouse Reef (Belize)	8500–0	A/C: Mangrove island, shallow reef, subaquatic sinkhole	Shell beds interpreted as reworking by storms and/or bioturbation, e.g. approx. 4500 BP ago; pattern of mixed layer of peat clasts in a carbonate matrix pure carbonate deposits bracketed by mangrove peat are ascribed to seismic activity or hurricanes	-	0 (Belize City)	n/d	n/d	5–9	1;1;1;1/2
5	Monacci et al.	Reconstructing	Spanish Lookout	8000–0	C: Mangrove	Continuous peat record,	-	0 (Belize	n/d	n/d	5–9	0

	(2009)	mangrove dynamics	Cay (Belize)		island	no disturbance detected		City)				
6	Brown et al. (2014)	Evaluating the potential of karst sinkholes for archiving historical huricanes	Laguna Chumkopó (Yucatán, Mexico)	c. 7100–6700 and the last 50 years	A: 80 m deep karst sinkhole	Moderate to strong hurricanes are represented by thin graded sequences of resuspended material; no tsunamis discussed	-	5–10	n/d	0.21	10–14	0
7	Woodroffe (1981)	Spatio-temporal reconstruction of marine transgression	North Sound (Grand Cayman)	more than 2100–0	C: Mangrove swamp	No extreme-wave impact inferred	-	10.79	n/d	0.25	10–14	0
8	Peros et al. (2007a,b)	Reconstructing palaeoenvironmental change	Laguna de la Leche (Cuba)	c. 8000–0	E: Coastal lake	Storm impact inferred based on changes in C and O isotope ratios	-	c. 0	n/d	n/d	10–14	0
9	Hendry (1987)	Determining tectonic and eustatic influence on sedimentation	The Great Morass (northwest Jamaica)	Holocene	C/D/F: Lagoon, beach, wetland	No extreme-wave impact inferred	-	c. 5	n/d	0.33	5–9	0
10	Palmer and Burn (2012)	Identifying marine washover events	Manatee Bay (Jamaica)	"Millennial scale"	D: Enclosed lagoon	Several overwash strata, overwash fan in the east	-	c. 22	n/d	1.02	5–9	3
11	Hearty et al. (1998; 2002); Kindler and Strasser (2000; 2002)	Landward-pointing v-shaped chevron ridges, partly subaerial	northwestern Bahamas	MIS 5e	A: Shallow shelf	Ridges with thick, tabular beds with fenestrae at high elevations indicate extreme storm-wave action (Hearty et al., 1998); Kindler and Strasser (2000) suggest an aeolian origin, fenestrae are attributed to rain	End of MIS 5e	c. 0–5	n/d	0.18	10–14	1;0
12	Dix et al. (1999)	Reconstructing palaeoenvironmental change	Lee Stocking Island (Bahamas)	1500–0	E: Shallow ponds	Possible storm surge overwash inferred from *ex-situ* marine deposits	-	c. 0	n/d	n/d	10–14	1
13	Park (2012); Park et al. (2009); Dalman and Park (2012); Mattheus and Fowler (2015)	Evaluating ecological response to hurricane impacts	San Salvador Island (Bahamas)	up to >3500–0	E: Shallow pond	Salt Pond: Tsunami overwash possible, but considered to be unlikely, due to lack of modern tsunami deposition and presence of correlating freshening (rainwater input); 19 events marked by peaks in sand (Park et al., 2009); Clear Pond and others: Sandy overwash deposits identified in the sediment cores are interpreted as hurricane-induced (Dalman and Park, 2012; Mattheus and Fowler, 2015)	-	c. 3–5	n/d	n/d	10–14	0;2;1;1
14	Caffrey et al. (2015)	Reconstructing environmental change	Laguna Saladilla	c. 8000–0	E: Freshwater lake (c. 5 km from the coast)	Strom surge incursions inferred from peak occurrences in marine diatoms	-	c. 0–5	n/d	0.15	5–9	1
15	Fuentes and Huérfano-	Searching for tsunami deposits	Bahia de Ocoa (Dominican	?	D: Shallow lagoons	Several overwash deposits of coarse sand detected in	-	5–7	0.2–0.5 (Barahona,	2.29 (Peninsula	5–9	3

	Moreno (2013)		Republic)			cores			southwestern Dominican Republic)	de Pedernales)		
16	Scheucher et al. (2011)	Detecting tsunami deposits and foraminiferal characterization	Puerto Viejo (southwestern Dominican Republic)	300–0?	Beach (?)	Sand layer is ascribed to a historical tsunami	18 October 1751 tsunami	5–7	0.2–0.5 (Barahona, southwestern Dominican Republic)	2.29 (Peninsula de Pedernales)	5–9	5
17	Scheucher et al. (2011)	Detecting tsunami deposits and foraminiferal characterization	Playa Cosón (northeastern Dominican Republic)	?	Beach (?)	Sand layer is ascribed to the 8 August 1946 tsunami	08 August 1946 tsunami	c. 10	n/d	0.30	10–14	5
18	Morton et al. (2006); Moya and Mercado (2006); Jaffe et al. (2008)	Reconstructing pre-historical tsunamis	Aguadilla–Rincón (northwestern Puerto Rico)	> 2500–0	C/F: swamps	1–2 thin, possibly tsunamigenic sand layers in various depths at different locations, no age estimates; overwash deposits correlated with historical and prehistorical tsunamis	(post-) 2770-2350 BP, (post-) 680-540 BP, 11 Oct 1918	c. 10–20	Run-up 11 October 1918 tsunami: 3–6 m	1.04	10–14	5
19	Morton et al. (2006)	Evaluating coastal hazards using sedimentary records	Punta Cucharas, south Puerto Rico	?	C: wetlands	a grey sand-and-shell layer with a thickness of only 2 cm was found 1 m below a tidal flat. Depositional processes remain uncertain	?	c. 15	3.3–5.1 (Guayama, Puerto Rico)	2.03	10–14	3
20	Donnelly and Woodruff (2007); Woodruff et al. (2008)	Reconstructing fluctuations in hurricane frequency	Southwestern Vieques (Puerto Rico)	5000–0	D/E: Coastal lagoon	Periodic hurricane overwash inferred; tsunamis excluded	-	c. 15	3.0–3.5 m tsunami wave amplitude (southeast coast of Vieques), 3 main waves within 30 min.	0.62 (eastern Puerto Rico)	10–14	1
21	Donnelly (2005)	Reconstructing severe tropical cyclones	Isla de Culebrita (Puerto Rico)	2200–0	D/E: Back-barrier salt pond	Massive sand layer interpreted as 1867 hurricane-born; 1867 tsunami also possible	-	c. 15	6.1 m at adjacent Culebra	0.62 (eastern Puerto Rico)	10–14	2
22	Brooks et al. (2007, 2015); Larsen et al. (2015)	Identifiying human influence on sedimentation	St. Thomas, St. Croix, St. John (USVI)	>5000–0	Different coastal environments, Marginal marine embayment	Multiple marine overwash inferred from >100 sediment cores	-	13.85 % (Road Town, BVI)	3.2–7.5 (Cruz Bay, St. John)	0.45 (Anegada)	10–14	1;1;2
23	Atwater et al. (2012); Pilarczyk and Reinhardt (2012); Reinhardt et al. (2012)	Identifying marine overwash	Central and western Anegada (BVI)	c. 400–0	D/E: Coastal ponds	Tsunami or storm overwash inferred; taphonomic characteristics and spatial extent of a shell-rich sand sheet indicate tsunami deposition	1650–1800 AD	c. 10–15	2.3–5.2 (Road Town, Tortola)	0.45	10–14	3;3;4
24	Jessen et al.	Reconstructing	Altona Bay (St.	c. 4500–0	D: Lagoon	One event inferred, post-	-	c. 10–15	3.0–3.9	n/d	10–14	1

	(2008)	palaeoenvironments	Croix, USVI)			1960 AD hurricane						
25	Bertran et al. (2004); Malaizé et al. (2011)	Determining variability of hurricanes	Grand-Case (St. Martin)	c. 4000–0	D/E: Coastal pond	Up to 21 event layers; sand layers ascribed to hurricanes, but authors "cannot exclude that some sand layers correspond to tsunamis"	-	c. 3–5	Run-up 1867 tsunami: c. 1.5	0.52 (St. Kitts and Nevis)	10–14	2
26	Caron (2011, 2012)	Evaluating the preservation potential of extreme wave deposits by beachrock	St. Bartholomew	?	Beachrock	Considered as unlikely to be tsunamigenic	-	<10	n/d	0.52 (St. Kitts and Nevis)	10–14	2
27	Morton et al. (2006)	Evaluating coastal hazards using sedimentary records	Northwestern Basse-Terre (Guadeloupe)	?	C: Coastal plains and wetlands	no marine overwash identified	-	c. 10–12	0.6–1.6 (Basse-Terre)	0.88	10–14	0
28	Ramcharan (2004); Ramcharan and MacAndrews (2006)	Reconstructing Holocene wetland development	Maracas Bay (Trinidad)	7000–0	C: Swamps	No marine sedimentary impact	-	0 (Port-of-Spain)	0.5–1.2 (Port-of-Spain)	0.45	5–9	0
29	Oropeza et al. (2015)	Identification of palaeotsunami deposits	Bocaripo, Chacopata, and Morro de Chacopata lagoons (Sucre, northeast Venezuela)	?	D: Lagoon	Preliminary findings: 30 cm-thick alternating sequence of reddish sand and beige sandy silt (Bocaripo); mollusk-rich layer (36 cm-thick) might correspond to tsunami impact (Chacopata); discontinuous, 3 cm-thick sand layers with landward-directed ripples may indicate tsunami incursion (Morro de Chacopata)	after 960 ± 30 BC?	6.27 (Cumaná)	0.3–1.0	0.28 –0.49	5–9	5
30	Leal et al. (2014)	Identification of palaeotsunami deposits	Los Patos Lagoon near Cumaná (northeast Venezuela)	5000-? (age inversions)	D/E: Coastal lagoon	Tsunami deposits identified in the upper part of the sediment core, age remains unknown	historical?	6.27 (Cumaná)	0.3–1.0	0.30	5–9	5
31	Weiss (1979)	Sedimentological and geomorphological characterization	Cayo Sal (Venezuela)	3800–0	D: Enclosed lagoon	Hurricane or tsunami is suggested to have disturbed sedimentation of Cayo Sal	770–500 BP	c. 3–5	0.6–0.8 (Puerto Cabello)	0.94	2–4	3
32	Engel et al. (2010, 2012, 2013)	Evaluating the impact of extreme wave events on Holocene coastal ecosystems	Bonaire	8000–0	C/D/F: Enclosed lagoons, floodplains	Potential tsunamis inferred	3600 or later, 3300 or later, 2000 BP or later, plus one younger event	c. 7 (Willemstad, Curaçao)	0.1–0.8	up to 1.30	2–4	4
33	Klosowska (2003)	Reconstructing coastal palaeoenvironments	Lagoon St. Michiel (Curaçao)	5000–0	D: Saline lagoon	Rapid closure of lagoon at around 3500 BP might be related to tsunami impact	At around 3500 BP	c. 5–10	n/d	0.93	2–4	3

34	Hornbach et al. (2008a)	Reconstructing storm and tsunami events	Spaanse Waters, Lagoen Jan Thiel, Fuik Bay (Curaçao)	c. 1000–0	A: Sheltered coastal embayments	Surface *Halimeda* sand attributed to recent storms; “chaotic mixed” layer interpreted as tsunamigenic	460–310 cal BP	7.04 (Willemstad, Curaçao)	Negligible	1.57	2–4	4
35	González et al. (2010)	Reconstructing mangrove dynamics	Bahia Honda (San Andres, Colombia)	c. 3000–0 (hiatus from c. 2500–500/400)	C: Mangrove embayment	Major erosive disturbance event: 1605 hurricane?	-	c. 3	Negligible	n/d	2–4	1
36	Urquhart (2009); McCloskey and Liu (2012)	Evaluating mangrove response to hurricane impacts	Bluefields (southeast Nicaragua)	8000–0; 5000–0	E: Lagoon, 17 km from the coast; coastal marsh	Single major tsunami or hurricane (Urquhart, 2009); Clastic layers are interpreted as hurricane-induced due to low tsunami potential of the region (McCloskey and Liu, 2012)	(post-)3340 +/-40 BP (Urquhart, 2009)	0	0–0.2 (Puerto Cabezas)	0.47	2–4	2;1

Table 5: Coastal coarse-clast deposits reviewed for evidence of extreme-wave events. All sites are indicated in Fig. 3. For all sites, the 30-yr probability of tsunami run-up >0.5 m (Parsons and Geist, 2009), the calculated amplitude of the Virgin Island tsunami of 1867 (Zahibo et al., 2003), tsunami height in the SCDB scenario (Fig. 7), and the decadal number of hurricanes (Reading, 1990) is shown. The depositional process is coded as follows: 0 = No disturbance in the stratigraphy/no coarse-clast record evident; 1 = Disturbance/deposition attributed to storm; tsunami impact is excluded; 2 = Disturbance/deposition documented and storm is favoured over tsunami, but the latter is not entirely excluded; 3 = Disturbance/deposition is ascribed to either hurricane or tsunami; 4 = Disturbance/deposition is documented and tsunami is favoured over hurricane, but the latter is not entirely excluded; 5 = Disturbance/deposition is documented, ascribed to tsunami, and hurricane is excluded.

No.	Author(s)	Goal of the study	Location	Time covered by sediment archive (years BP)	Type of sediment archive	Evidence for extreme wave events	Age of the candidate tsunami deposit	30-year prob. of tsunami run-up > 0.5 m	Amplitude 1867 tsunami (m)	Tsunami height SCDB scenario (m)	Decadal number of hurricanes	Interpretation in the original source (see order of literature sources)
37	Shaw and Benson (2015)	Investigation of an anomalous sand and coarse-clast berm	Tankah to Puerto del Carmen (Yucatán, Mexico)	c. 1500–0	A: Coastal berm (sand and rubble)	Elevated coastal berm out of reach for hurricane waves, lack of distinct internal bedding, covered by boulders, landward extent of up to 400 m	c. 1500 BP		5–10	0.21	10–14	4
38	Jones and Hunter (1992); Robinson et al. (2006); Rowe et al.. (2009)	Study effect of extreme-wave condition on rocky coasts	Great Pedro Point/Blowholes (Grand Cayman)	Mid- to late Holocene; historical	B: Elevated carbonate platform (+7–12 m a.s.l.)	Large boulders of up to 40 t attributed to deposition during hurricanes or tsunamis; Robinson et al. (2006) favour storms	Two boulders moved around 1625–1688 AD or later	10.79	n/d	0.25	10–14	3;2
39	Rigby and Roberts, 1976); Hernandez-Avila et al. (1977); Jones and Hunter (1992)	Calculate storm-wave force required to induce breakup of corals as source material of ramparts; Study effect of extreme-wave condition on rocky coasts	Spots Bay, Breakers, Old Isaacs (Grand Cayman)	Mid- to late Holocene;	A/B: Elevated carbonate platform up to 4.5 m a.s.l.	Ramparts of coral pebbles and boulders were accumulated mainly during hurricanes of 1931 and 1932	-	10.79	n/d	0.25	10–14	1
40	Robinson et al. (2006); Morton et al. (2008a); Rowe et al. (2009); Khan et al. (2010); Miller et al. (2014)	Identification of geological evidence of tsunamis in service of coastal hazard assessment	Several sites on Jamaica	Mid- to late Holocene	B: Elevated carbonate platform	Large boulders mostly shifted by hurricanes; for some boulders tsunamis are not excluded; boulders of up to 80 t were moved during Hurricane Dean in 2007; two particular boulders moved during the 20th century	20th century?	Up to c. 22	n/d	up to 2.01	5–9	3

41	Hearty (1997); Hearty et al. (2002); Mylroie (2008); Samankassou et al. (2008); Viret (2008); Hasler et al. (2010); Kindler et al. (2010); Hansen et al. (2016)	Reconstruction of transport mechanism and time of deposition of large coastal boulders	Glass Window, northern Eleuthera (Bahamas)	MIS 5e	B: Elevated arbonate platform (10–20 m a.s.l.); Intertidal platform; emerged fossil beach (3 m a.s.l.); washover basin (6–8 m a.s.l.)	Large boulders and blocks of up to 2000 t attributed to tsunamis or storms exceeding the magnitude of the largest storms known in history (Hearty, 1997, 2002); evidence for wave emplacement was challenged by Mylroie (2008) associating the boulders with tower karst features; Samankassou et al. (2008), Hasler et al. (2010) and Kindler et al. (2010) interpret them as tsunami-emplaced boulders based on assumptions of lower transport capacity of storm waves and speculate on a landslide tsunami either on the Canary Islands or the adjacent platform margin; Hansen et al. (2016) link the boulders with superstorms unprecedented in the historical era	End of MIS 5e?	<2	n/d	0.18	10–14	3;0;0;4;4;4;3;1 (see details in column "Evidence for extreme wave events")
42	Kelletat et al. (2004)	Mapping of coarse-clast tsunami deposits	Eleuthera (Bahamas)	Mid- to late Holocene	B: Elevated carbonate platform (5–15 m a.s.l.)	Boulders of up to 200 t, partly imbricated, and bimodal deposits indicate tsunami wave heights of up to 20 m	3000 and 500 BP (based on uncal. ^{14}C data)	<2	n/d	0.18	10–14	5
43	Kelletat et al. (2004)	Mapping of coarse-clast tsunami deposits	Long Island (Bahamas)	Mid- to late Holocene	A/B: (Elevated) carbonate platform, Upper supratidal up to 15 m a.s.l.	Large boulders of up to 50 t, boulder and pebble fields and boulder ridges (bimodal)	3000, 1600(?), and 500 BP (based on uncal. ^{14}C data)	<2	n/d	0.27	10–14	5
44	Scheucher and Vortisch (2011)	Reconstructing extreme-wave events from coastal deposits	Playa Azul (Dominican Republic)	Mid- to late Holocene	A: Elevated carbonate platform	Boulders up to 7 t form a ridge parallel to the shoreline, 1–1.5 m a.s.l., interpreted as the result of storms	-	5–7	0.2–0.5 (Barahona, southwestern Dominican Republic)	2.29 (Peninsula de Pedernales)	5–9	1
45	Moya and Mercado (2006)	Reconstructing pre-historical tsunamis	Aguadilla–Rincón (northwest Puerto Rico)	Mid- to late Holocene	A /B/F: cliffs, beach and back of the dunes	onshore transport of coral colonies (up to 1.5 m) and large boulders is ascribed to prehistoric tsunami impact	11 Oct 1918 tsunami	c. 15–20	Local run-up 11 October 1918 tsunami: 3–6	0.95	10–14	5
46	Taggart et al. (1993); Gonzalez et al. (1997); Morton et al.	Reconstructing transport processes of coastal boulders;	Isla de Mona (Puerto Rico)	Mid- to late Holocene	A/B: Intertidal to elevated carbonate	Coarse-clast ridge complex (sand, cobbles and fine boulders) erosion and deposition is rather	After 4176 years ago	c. 5	<0.9	0.95 (northwest Puerto Rico)	10–14	3;3;2

	(2008a)	Evaluating coastal hazards using sedimentary records			platform (up to several metres a.s.l.)	associated with hurricane-induced waves by Morton et al. (2008a)						
47	Buckley et al. (2012); Watt et al. (2012a); Weil Accardo et al. (2012); Atwater et al. (2013b, 2014)	Identifying and dating marine overwash; Documentation of a cobble and boulder field and reconstruction of depositional process	Southeast of Windlass Bight, north shore of Anegada (BVI)	Mid- to late Holocene	F: Coastal flats behind beach ridges	Cobbles and fine boulders probably deposited by tsunami overwash based on spatial distribution, main axes orientation, numerical simulation and correlating finer deposits (Atwater et al. (2012)	AD 1200–1450; AD 1650–1800 AD	c. 10–15	2.3-5.2 (Road Town, Tortola)	0.45	10–14	4
48	Spiske and Halley (2014)	Reconstruct the depositional process of a ridge of coral rubble	Soldier Wash, north shore of Anegada (BVI)	A few tens of years (minimum age)	A: Limestone platform, 0.4–0.5 m high	Clast-supported structure, imbrications and the exclusively well-rounded material of the boulder ridge indicate build up during hurricane overwash	-	c. 10–15	2.3–5.2 (Road Town, Tortola)	0.45	10–14	1
49	Scheffers (2006b); Scheffers and Kelletat (2006)	Documentation of coarse-clast tsunami deposits	Anguilla and Scrub Island	Mid- to late Holocene	B: Elevated limestone platforms	boulders of up to 100 t, bimodal tsunami deposits at the east coast, tsunami boulder ridges, elongated bars of coral debris; boulder ridge at the southern coast	>1000 BP; <610 BP (based on uncal. ^{14}C data)	c. <2	n/d	0.52 (St. Kitts and Nevis)	5–9	5
50	Scheffers (2006); Scheffers and Kelletat (2006)	Documentation of coarse-clast tsunami deposits	St. Martin	Mid- to late Holocene	A/B: Elevated limestone platforms	very few boulders up to 10 t, "tsunami boulder spit" on an offshore volcanic island; a coral rubble ridge described as tsunamigenic at the east coast was dated to 500 BP	500 BP (based on uncal. ^{14}C data)	c. <5	n/d	0.52 (St. Kitts and Nevis)	5–9	5
51	Scheffers et al. (2005); Morton et al. (2006, 200a8)	Evaluating coastal hazards using sedimentary records	Guadeloupe	Mid- to late Holocene	A/B: Intertidal to cliff-top position (up to several metres a.s.l.)	Boulders of up to 30 t along the east coast and bimodal deposits indicate tsunami impact (Scheffers et al., 2005); since these deposits are within the range of hurricane-induced inundation and their morphology, Morton et al. (2006, 2008a) infer storm-dominated deposition	2700–2500 BP or slightly later (based on uncal. ^{14}C data)	11.79 (Basse-Terre)	0.6–1.6 (Basse-Terre)	0.88	10–14	5;2
52	Scheffers et al. (2005)	Documentation of coarse-clast tsunami deposits	St. Lucia	Mid-Pleistocene	Volcano flank xposure of pyroclastic deposits, 15–50 m a.s.l.	Mixture of fines to boulder incorporated into volcanic tephra represents mid-Pleistocene tsunami deposit	Mid-Pleistocene	5.52	n/d	0.95	5–9	5
53	Schellmann and Radtke (2004); Scheffers and Kelletat (2006)	Summarizing the inventory of marine Quaternary deposits;	Barbados	Mid- to late Holocene	B: Elevated limestone platforms	Some polymodal ramparts/ridge complexes at the northeast coast associated with deposition during hurricanes	4500 and 1400 BP (based on uncal. ^{14}C data)	n/d	n/d	0.58	5–9	2;5

		Documentation of coarse-clast tsunami deposits				(Schellmann and Radtke, 2004); Isolated boulders up to 170 t up to 15 m a.s.l. and other boulder ridge features indicate at least two strong tsunamis (Scheffers and Kelletat, 2006)						
54	Scheffers et al. (2005)	Documentation of coarse-clast tsunami deposits	Grenada	Pleistocene to Holocene	A/B: Supratidal of rocky shore	Cobbles and fine boulders in sand matrix, 0–3 m a.s.l., and semi-circular boulder ridge indicate tsunami deposition	Pleistocene and late Holocene	2.48	1.1–2.8	0.37	5–9	5
55	Schubert (1994)	Presenting geological evidence for a prehistoric tsunami	Puerto Colombia (Venezuela)	Mid- to late Holocene	B: Erosional terrace (cliff-top)	Coral pebbles to boulders with an average age of 1300 years distributed at an elevation of 10–20 m a.s.l.	c. 1300(?) years ago	<2	0.6–0.8 (Puerto Cabello)	0.52	2–4	4
56	Scheffers (2002a,b, 2004, 2005); Scheffers et al. (2006, 2014); Radtke et al. (2003); Morton et al. (2006, 2008a); Spiske et al. (2008); Pignatelli et al. (2010); Watt et al. (2010); Engel and May (2012)	Evaluating the depositional process for different types of coarse-clast deposits	Bonaire	Mid- to late Holocene	A/B: Intertidal to elevated carbonate platform	Largest blocks considered to be "consistent with tsunami deposits" (Watt et al., 2010, p. 60) by all authors, apart from Spiske et al. (2008); Scheffers (2002a,b, 2004, 2005) and Scheffers et al. (2006, 2009) ascribe the vast bimodal ramparts along the windward coast to tsunami deposition which has been criticized by Morton et al. (2006, 2008a); A scattered clast field north of Boka Olivia is associated with tsunami deposition by Scheffers (2002a,b, 2004, 2005), Morton et al. (2006) and Watt et al. (2010)	4300, 3900, 3300, 1200, and 500 BP (based on ESR and uncal. ^{14}C data; Scheffers, 2005)	c. 7 (Willemstad, Curaçao)	0.1–0.8	up to 1.30	5–9	see details in column "Evidence for extreme wave events"
57	Scheffers (2002,a,b, 2004); Radtke et al. (2003)	Evaluating the depositional process for different types of coarse-clast deposits	Curaçao	Mid- to late Holocene	A/B: Intertidal to elevated carbonate platform	Boulder fields and ridge complexes are attributed to tsunami impact	3500, 1500, and 500 BP (based on cal. ^{14}C data; Scheffers, 2002b)	c. 7 (Willemstad, Curaçao)	0.1–0.8 (Bonaire)	Up to 2.90	2–4	5
58	Scheffers (2002,a,b, 2004); Radtke et al. (2003)	Evaluating the depositional process for different types of coarse-clast deposits	Aruba	Mid- to late Holocene	A/B: Intertidal to elevated carbonate platform	Boulder fields and ridge complexes are attributed to tsunami impact	3500, 1500, and 500 BP (based on cal. ^{14}C data; Scheffers,	c. 7 (Willemstad, Curaçao)	0.1–0.8 (Bonaire)	Up to 3.26	2–4	5

							2002b)					
59	Macintyre et al. (2001)	Reconstructing formation of an intertidal ridge	Holandés Cays, Panama	Late Holocene	A: Coral reef (intertidal)	A cemented ridge on the reef flat with coralline algae cover was interpreted as storm-built around 2000–2800 ago	-	17.56 (Colón)	0–0.2 (Colón)	0.66	0–1	1

Fig. 1: Overview map of the Caribbean region based on the GEBCO One Minute Grid, version 2.0 (http://www.gebco.net) with overlays of the tectonic pattern (Pindell and Kennan, 2009) and vectors of plate movement (Meschede and Frisch, 1998). Black squares show observations of tsunami run-up since 1498. White rims indicate that multiple historical tsunamis were recorded (NGDC/WDS, 2016). BVI = British Virgin Islands; B = Bonaire; C = Curaçao; A = Aruba.

Fig. 2: a) Frequency-size distribution for reported heights of tsunamis vs. number per year. Each event is only represented once by its highest value. Triangles = maximum observational and instrumental accounts of wave height, flow depth or run-up height, documented for each tsunami in the Caribbean AD 1498–2015 (NGDC/WDS, 2016). Circles = maximum observational and instrumental accounts of wave height, flow depth or run-up height, documented for each tsunami worldwide AD 1498–2015 (NGDC/WDS, 2016). b) Heights of tsunamis vs. total number per year. Squares = Global dataset of only high-precision tide-gauge measurements and maximum flow depth or water height derived from post-tsunami measurements (NGDC/WDS, 2016).

Fig. 3: Overview of the Caribbean basin separated into five sectors (dashed lines). Greyscale quadrants indicate decadal frequencies of tropical cyclones based on tracks charted by the US Weather Bureau between 1871–1987 (Reading, 1990). Circles show the modelled probabilities of tsunami occurrence (run-up >0.5 m) within a period of 30 years (Parsons and Geist, 2009). Numbers refer to reviewed sites in Tables 2 and 3. Blue frames = fine sedimentary records; red frames = coarse-clast records. The width of the frames refers to the depositional process (storm or tsunami) inferred by the original author(s) (0 [thinnest frame] = No disturbance in the stratigraphy; 1 = Disturbance/deposition attributed to storm; tsunami impact is excluded; 2 = Disturbance/deposition documented and storm is favoured over tsunami, but the latter is not entirely excluded; 3 = Disturbance/deposition is ascribed to either hurricane or tsunami; 4 = Disturbance/deposition is documented and tsunami is favoured over hurricane, but the latter is not entirely excluded; 5 = Disturbance/deposition is documented, ascribed to tsunami, and hurricane is excluded; see also Tables 4 and 5).

Fig. 4: The role of palaeotsunami research in a tsunami hazard management process and schematic depiction and classification of sedimentary archives relevant to the Caribbean (see also Fig. 5). Steps 1–4 modified after Dall'Osso and Dominey-Howes (2010), details of Step 4 partly after Stein and Stein (2013).

Fig. 5: Potential sedimentary archives of tsunami- or storm-induced deposits or landforms in the Caribbean (see categories in Fig. 4) as exemplified in the Lac Bai area of southeast Bonaire (Fig. 1) (Satellite image: Digital Globe, 4 August 2013; oblique aerial insert image courtesy of D. Kelletat).

Fig. 6: Tsunami scenario from a rupture along the western Muertos Thrust Belt (MTB) and maximum heights along circum-Caribbean coasts. For earthquake parameters see Table 3.

Fig. 7: Tsunami scenario from a rupture along the South Caribbean Deformed Belt (SCDB) and maximum heights along circum-Caribbean coasts. For earthquake parameters see Table 3.

Fig. 8: Examples of candidate tsunami deposits from Anegada (Sites 23/47, Fig. 3) and Bonaire (Site 31/55, Fig. 3) (compare with archive categories A–F in Fig. 4). I) Large coral head (*Diploria* sp.) possibly transported onto an inland salt flat on Anegada by a tsunami. Periodic flooding of the salt flat during high-category hurricanes is indicated by a cover of dried microbial mat (photo courtesy of B. Atwater). Calibrated ^{14}C ages measured on this and other large corals transported inland lie in the range of AD 1200–1450 (Atwater et al. 2014, online supplement) II) Cerith-dominated mollusc assemblage of the sand-and-shell sheet on Anegada, sieved through 4 mm mesh (photo courtesy of B. Atwater). The deposit was dated to AD 1650–1800 and could represent either a historical tsunami (e.g., 1690 or 1755) or an extremely violent, unknown storm (Atwater et al., 2012). III) Tsunami deposit from Boka Bartol on Bonaire (6.86–6.67 m below surface) ^{14}C-dated to 3300–3000 cal BP (EWE II). It shows several criteria associated with tsunami deposition and had significant long-term impacts on the local hydroecology by transforming a narrow, mangrove-fringed open embayment into a hypersaline closed lagoon (Engel et al., 2013). IV) Extensive boulder field near Spelonk (e.g., Scheffers, 2002b, 2005; Spiske et al., 2008; Engel and May, 2012) on top of an elevated palaeo-reef terrace. Large singular boulders are possibly dislodged by tsunamis.

Fig. 9: Examples of storm-induced deposits and landforms from Bonaire (Site 55, Fig. 3) (compare with archive categories A–F in Fig. 4). I) Narrow intertidal ridge of coral rubble formed or at least significantly modified during Hurricane Ivan, northwestern Bonaire (cf. Scheffers and Scheffers, 2006). II) Sequence of coral rubble ridges on the low supratidal platform of Klein Bonaire (photograph courtesy of D. Kelletat) formed mostly by storms over several millennia (Scheffers et al., 2014). III) Supratidal coral rubble ridge near Salina Tern, northwestern Bonaire, with internal stratification and palaeosol horizons also indicating a multi-phase formation during storms (Engel et al., 2012). IV) Broad rampart/ridge complex of the Washikemba area. Stratification and textural sorting in a similar ridge complex near Boka Onima (photo insert courtesy of U.S. Geological Survey, modified) indicates a multi-phase formation (cf. Morton et al., 2008a). V) Cross profiles show the geomorphic differences between the broad windward ramparts (red) and the more narrow leeward ridges on Bonaire (Scheffers et al., 2014), which are predominantly a function of the width of the supratidal platform and approaching direction of major storms.

Fig. 10: Compilation of dated candidate tsunami deposits of Holocene age. Sites are indicated in Fig. 3 and details and citations of records are given in Tables 4 and 5. Abbreviations for sites on Bonaire: SPE = Spelonk; KLB = Klein Bonaire; SAT = Saliña Tam; NUK = Nukove. For different areas

on Bonaire age-frequency plots of corrected ESR- and ^{14}C-dated coral rubble from coastal landforms accumulated by extreme events are displayed. For age-frequency plots bin size is 300 years; the y-axis shows the number of age datings inside each bin (for details see Scheffers et al., 2014).

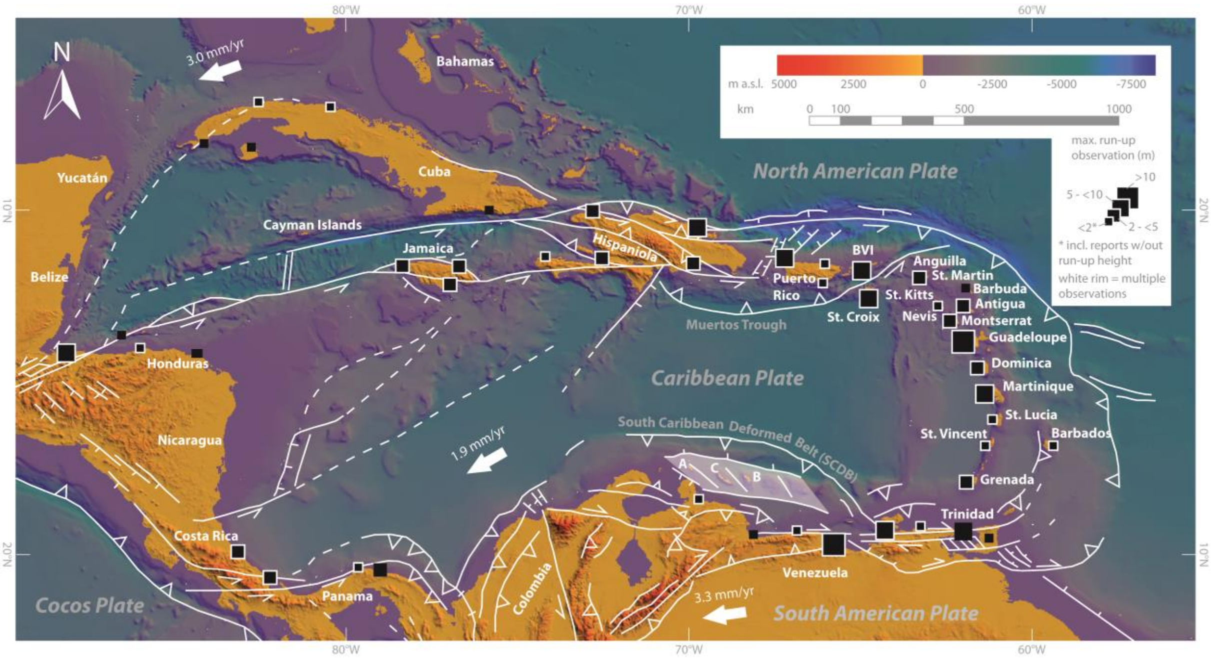
80°W
70°W
60°W
N
3.0 mm/yr
Bahamas
m a.s.l. 5000 2500 0 -2500 -5000 -7500
km 0 100 500 1000
max. run-up observation (m)
>10
5 - <10
2 - <5
<2*
* incl. reports w/out run-up height
white rim = multiple observations
Yucatán
Cuba
North American Plate
Cayman Islands
Jamaica
Hispaniola
Belize
Puerto Rico
BVI
Anguilla
St. Martin
Barbuda
St. Kitts
Antigua
St. Croix
Nevis
Montserrat
Guadeloupe
Muertos Trough
Honduras
Dominica
Caribbean Plate
Martinique
St. Lucia
Nicaragua
South Caribbean Deformed Belt (SCDB)
St. Vincent
Barbados
1.9 mm/yr
A
C
B
Grenada
Trinidad
Costa Rica
Venezuela
Panama
Colombia
3.3 mm/yr
Cocos Plate
South American Plate

Fig. 1

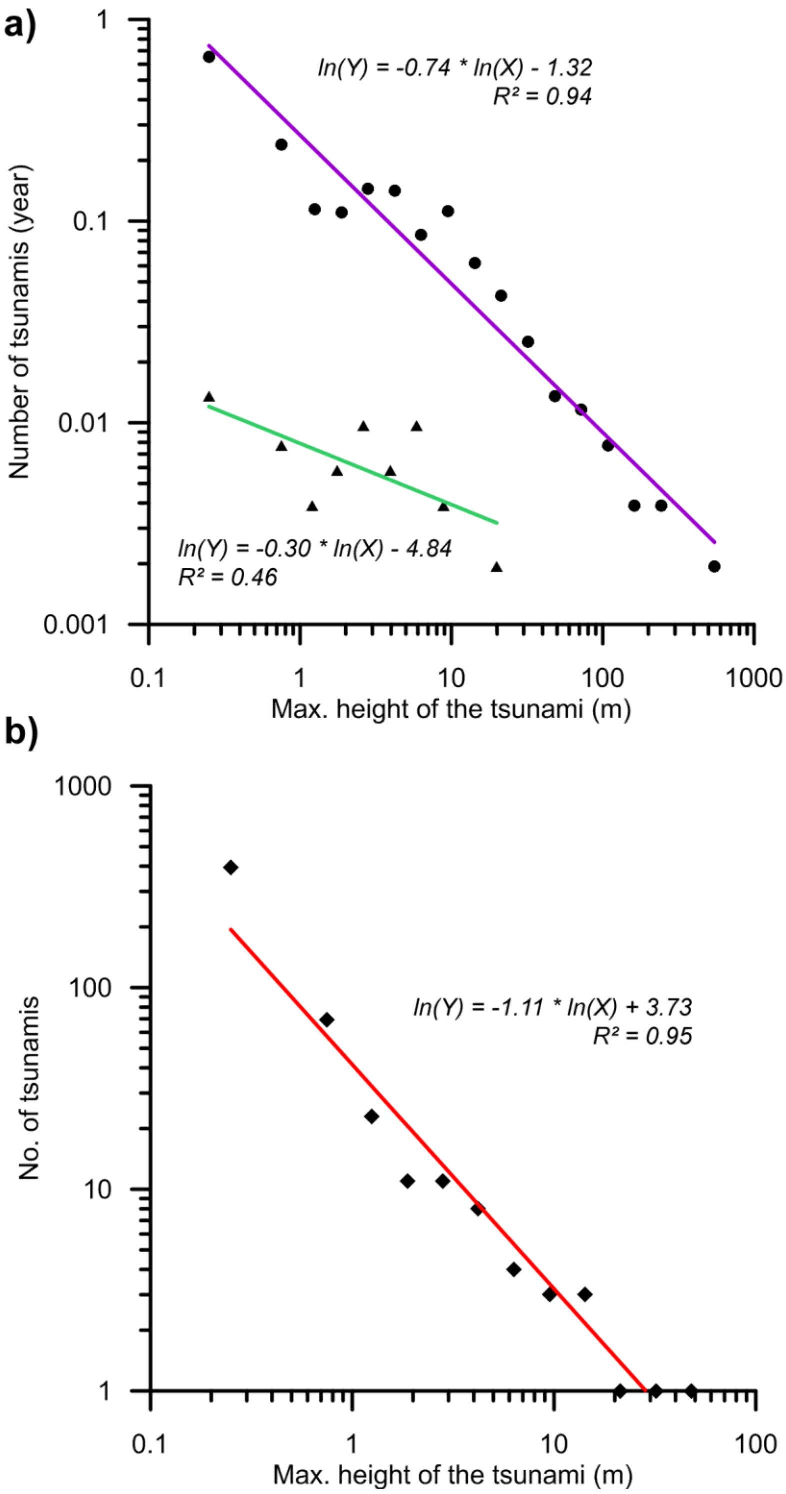
a)
1
0.1
0.01
0.001
Number of tsunamis (year)
ln(Y) = -0.74 * ln(X) - 1.32
R² = 0.94
ln(Y) = -0.30 * ln(X) - 4.84
R² = 0.46
0.1
1
10
100
1000
Max. height of the tsunami (m)
b)
1000
100
10
1
No. of tsunamis
ln(Y) = -1.11 * ln(X) + 3.73
R² = 0.95
0.1
1
10
100
Max. height of the tsunami (m)

Fig. 2

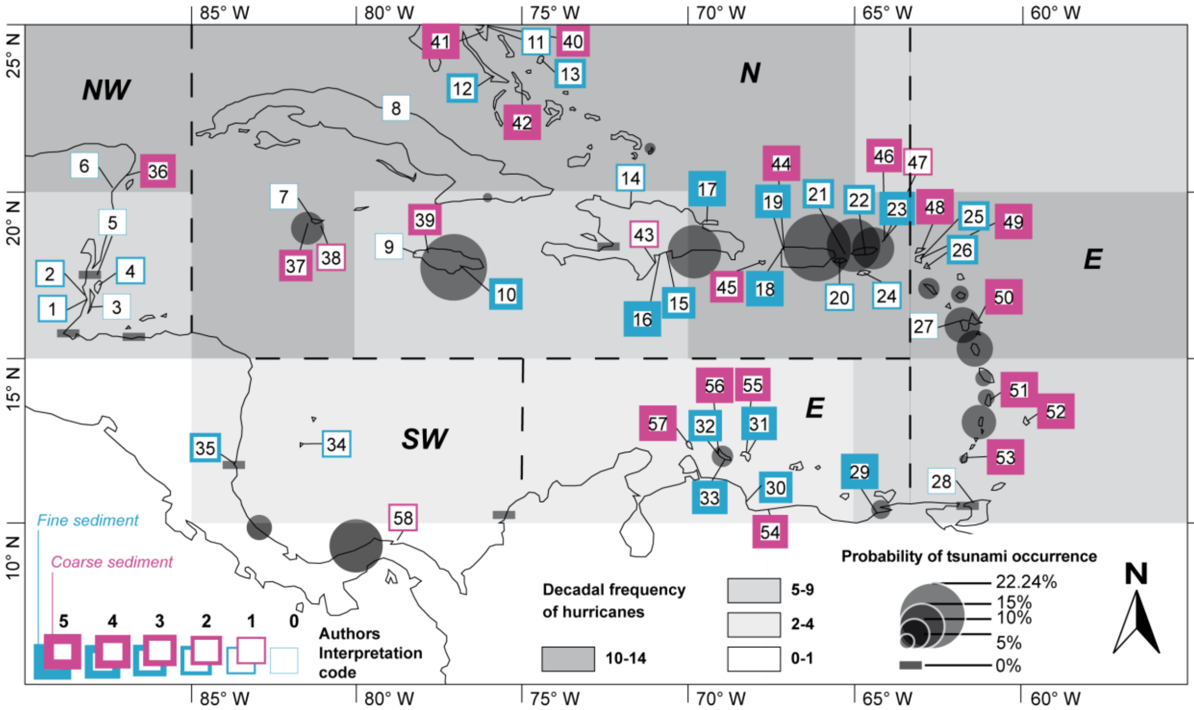
85° W
80° W
75° W
70° W
65° W
60° W
25° N
20° N
15° N
10° N
NW
N
E
SW
E
Fine sediment
Coarse sediment
5
4
3
2
1
0
Authors Interpretation code
Decadal frequency of hurricanes
10-14
5-9
2-4
0-1
Probability of tsunami occurrence
22.24%
15%
10%
5%
0%
N

Fig. 3

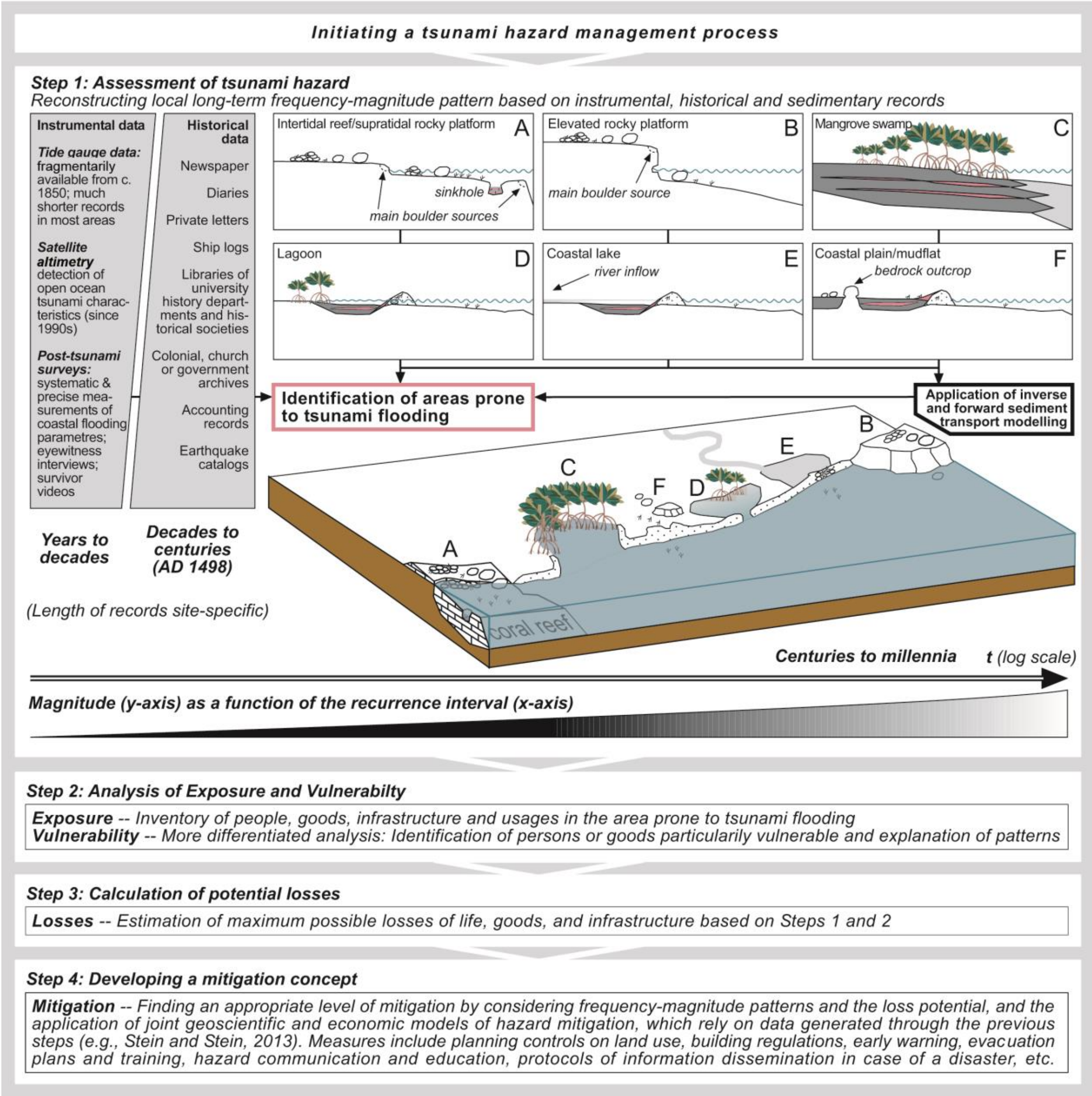
Initiating a tsunami hazard management process
Step 1: Assessment of tsunami hazard
Reconstructing local long-term frequency-magnitude pattern based on instrumental, historical and sedimentary records
Instrumental data
Tide gauge data: fragmentarily available from c. 1850; much shorter records in most areas
Satellite altimetry detection of open ocean tsunami characteristics (since 1990s)
Post-tsunami surveys: systematic & precise measurements of coastal flooding parametres; eyewitness interviews; survivor videos
Historical data
Newspaper
Diaries
Private letters
Ship logs
Libraries of university history departments and historical societies
Colonial, church or government archives
Accounting records
Earthquake catalogs
Years to decades
Decades to centuries (AD 1498)
(Length of records site-specific)
Intertidal reef/supratidal rocky platform A
sinkhole
main boulder sources
Elevated rocky platform B
main boulder source
Mangrove swamp C
Lagoon D
Coastal lake E
river inflow
Coastal plain/mudflat F
bedrock outcrop
Identification of areas prone to tsunami flooding
Application of inverse and forward sediment transport modelling
coral reef
Centuries to millennia
t (log scale)
Magnitude (y-axis) as a function of the recurrence interval (x-axis)
Step 2: Analysis of Exposure and Vulnerabilty
Exposure -- Inventory of people, goods, infrastructure and usages in the area prone to tsunami flooding
Vulnerability -- More differentiated analysis: Identification of persons or goods particularily vulnerable and explanation of patterns
Step 3: Calculation of potential losses
Losses -- Estimation of maximum possible losses of life, goods, and infrastructure based on Steps 1 and 2
Step 4: Developing a mitigation concept
Mitigation -- Finding an appropriate level of mitigation by considering frequency-magnitude patterns and the loss potential, and the application of joint geoscientific and economic models of hazard mitigation, which rely on data generated through the previous steps (e.g., Stein and Stein, 2013). Measures include planning controls on land use, building regulations, early warning, evacuation plans and training, hazard communication and education, protocols of information dissemination in case of a disaster, etc.

Fig. 4

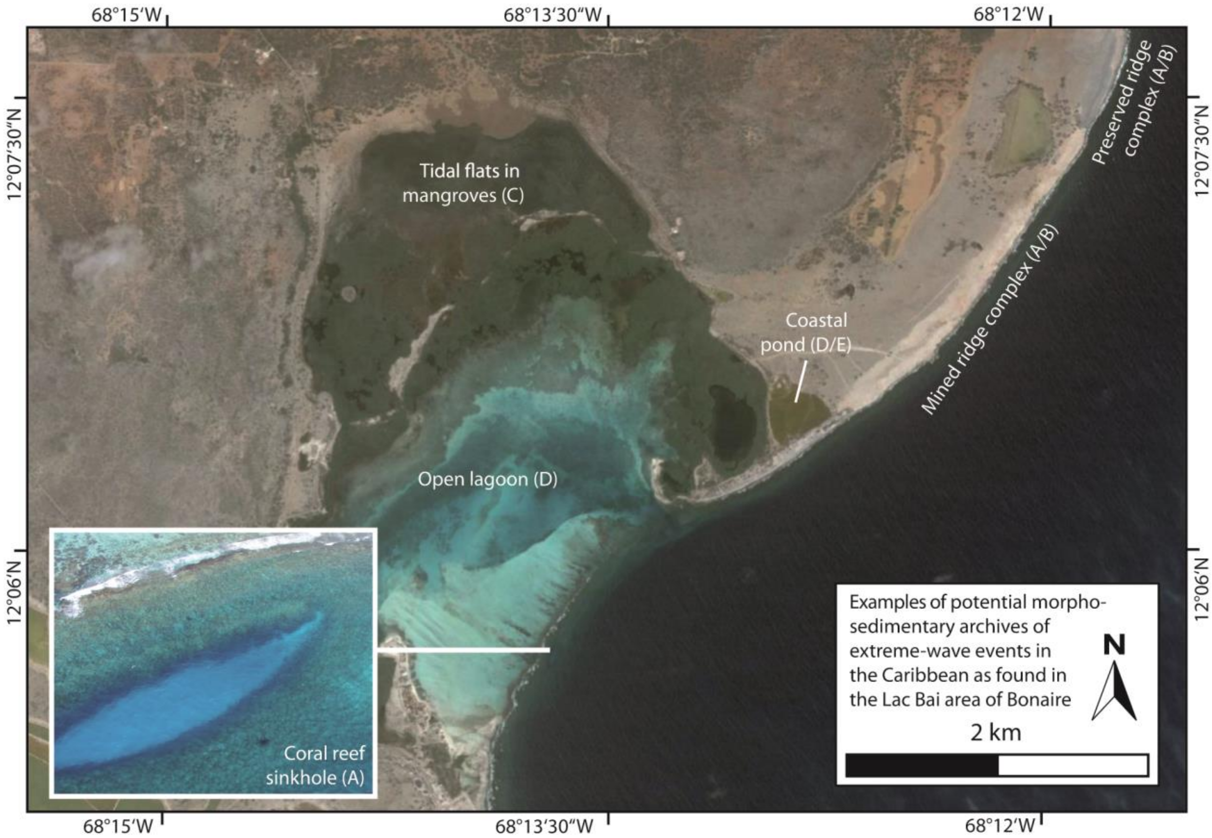

2199

2200 Fig. 5

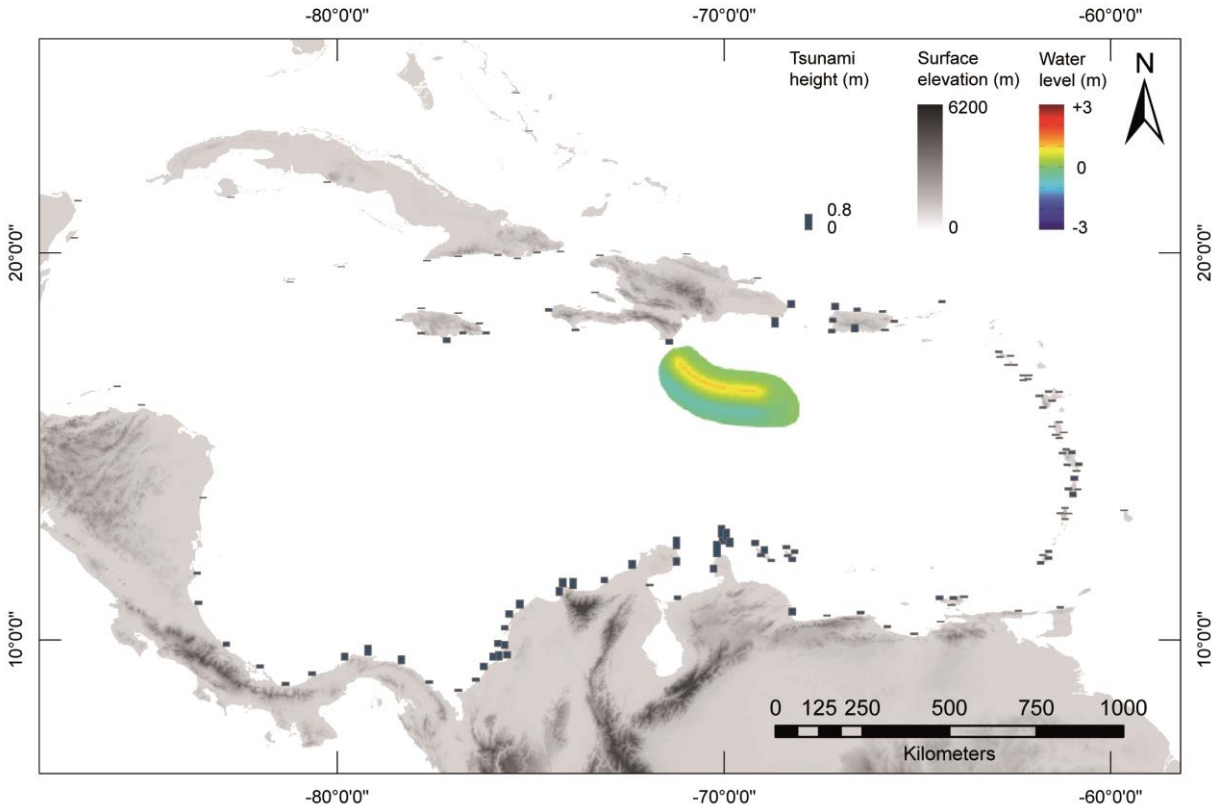
Tsunami height (m)
0.8
0
Surface elevation (m)
6200
0
Water level (m)
+3
0
-3
N
0 125 250 500 750 1000
Kilometers
-80°0'0"
-70°0'0"
-60°0'0"
20°0'0"
10°0'0"

Fig. 6

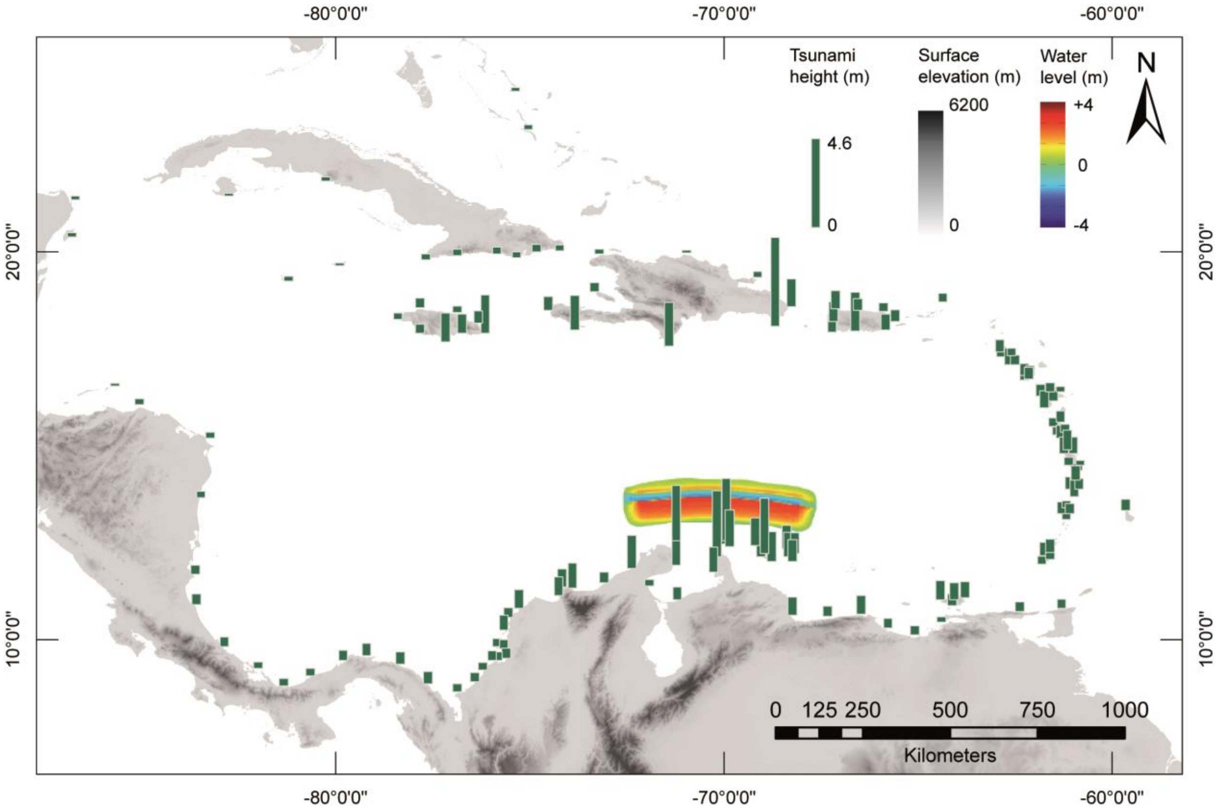
-80°0'0"
-70°0'0"
-60°0'0"
20°0'0"
10°0'0"
Tsunami height (m)
4.6
0
Surface elevation (m)
6200
0
Water level (m)
+4
0
-4
N
0 125 250 500 750 1000
Kilometers

Fig. 7

2206

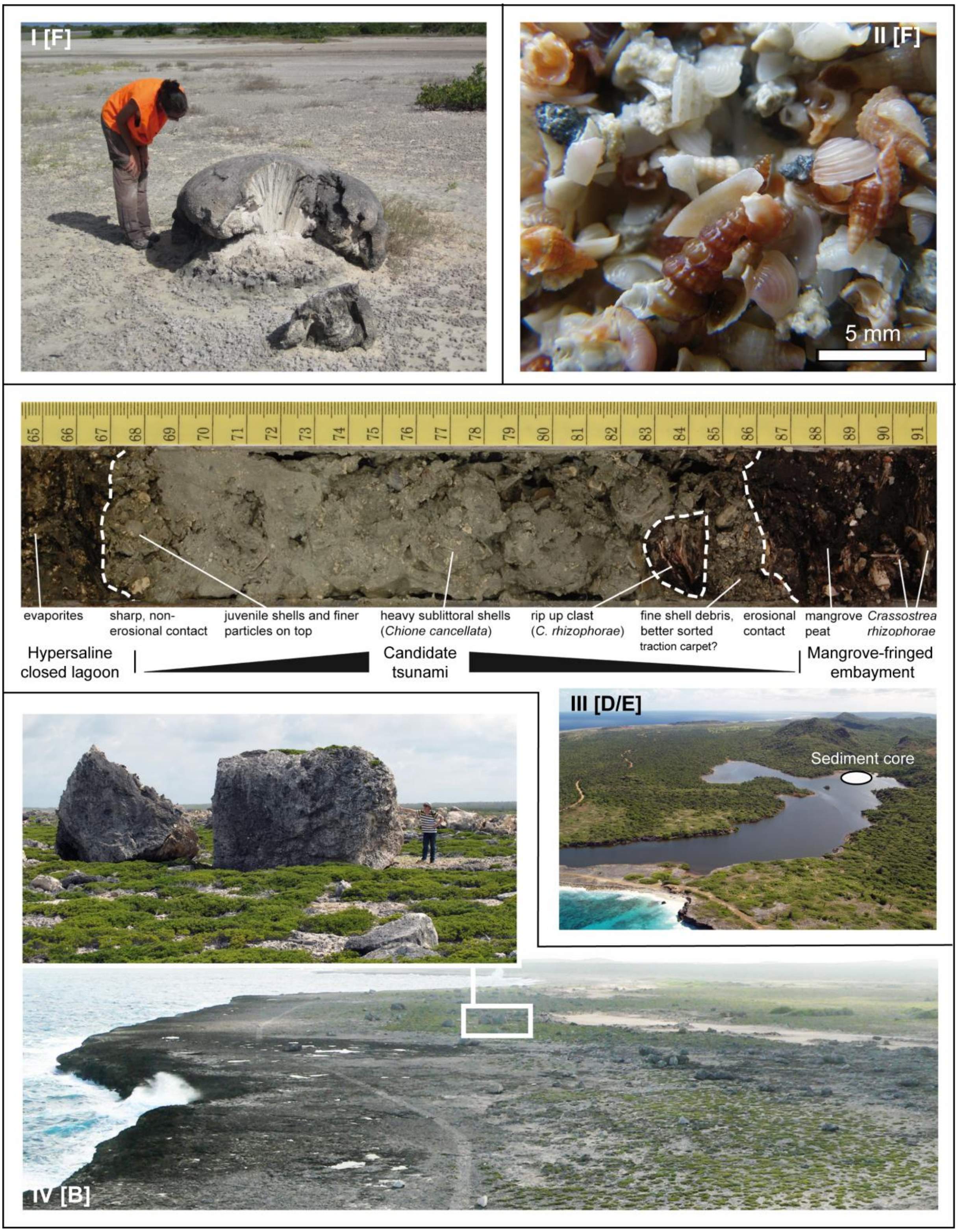

2207 Fig. 8

2208

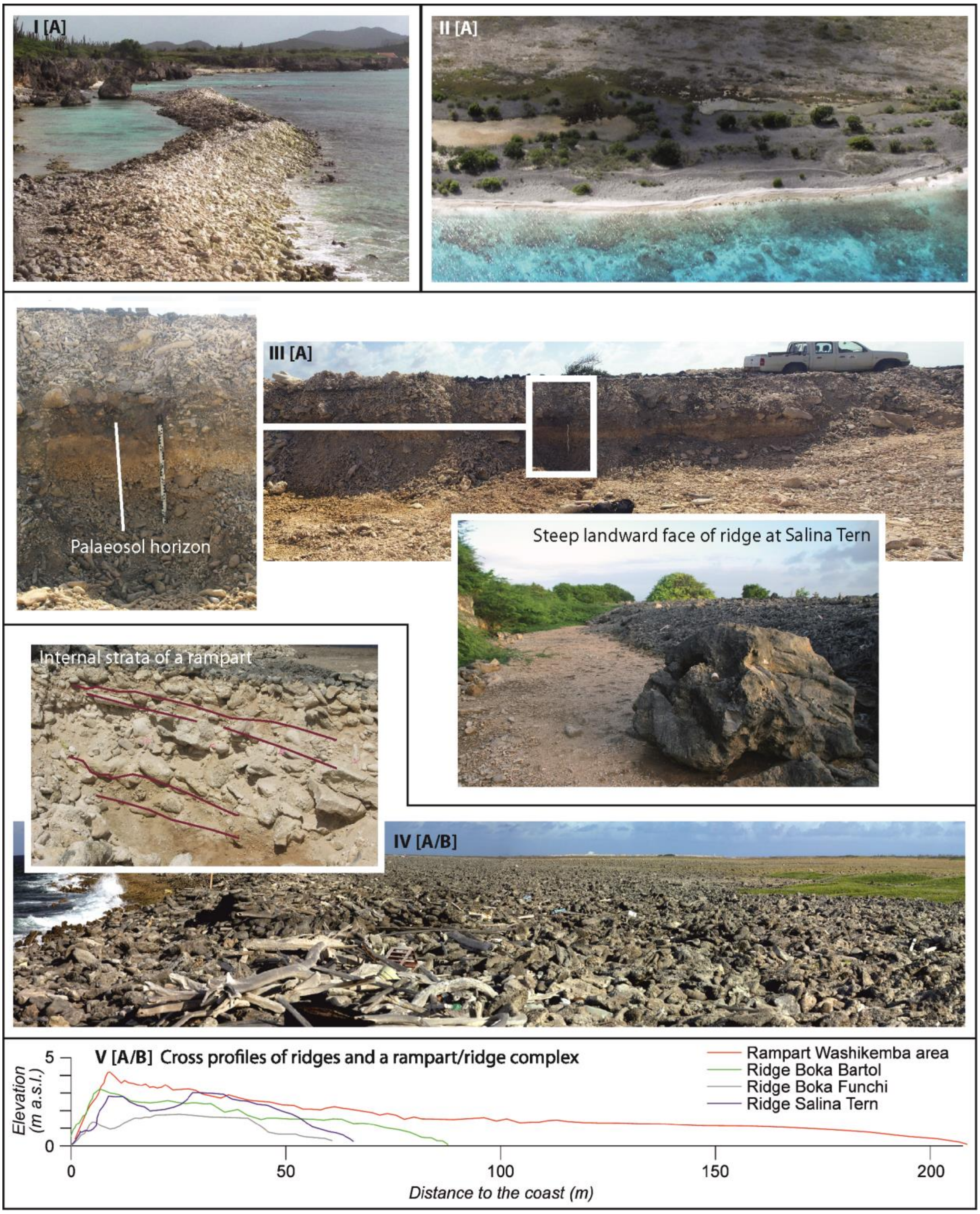

2209

2210 Fig. 9

2211

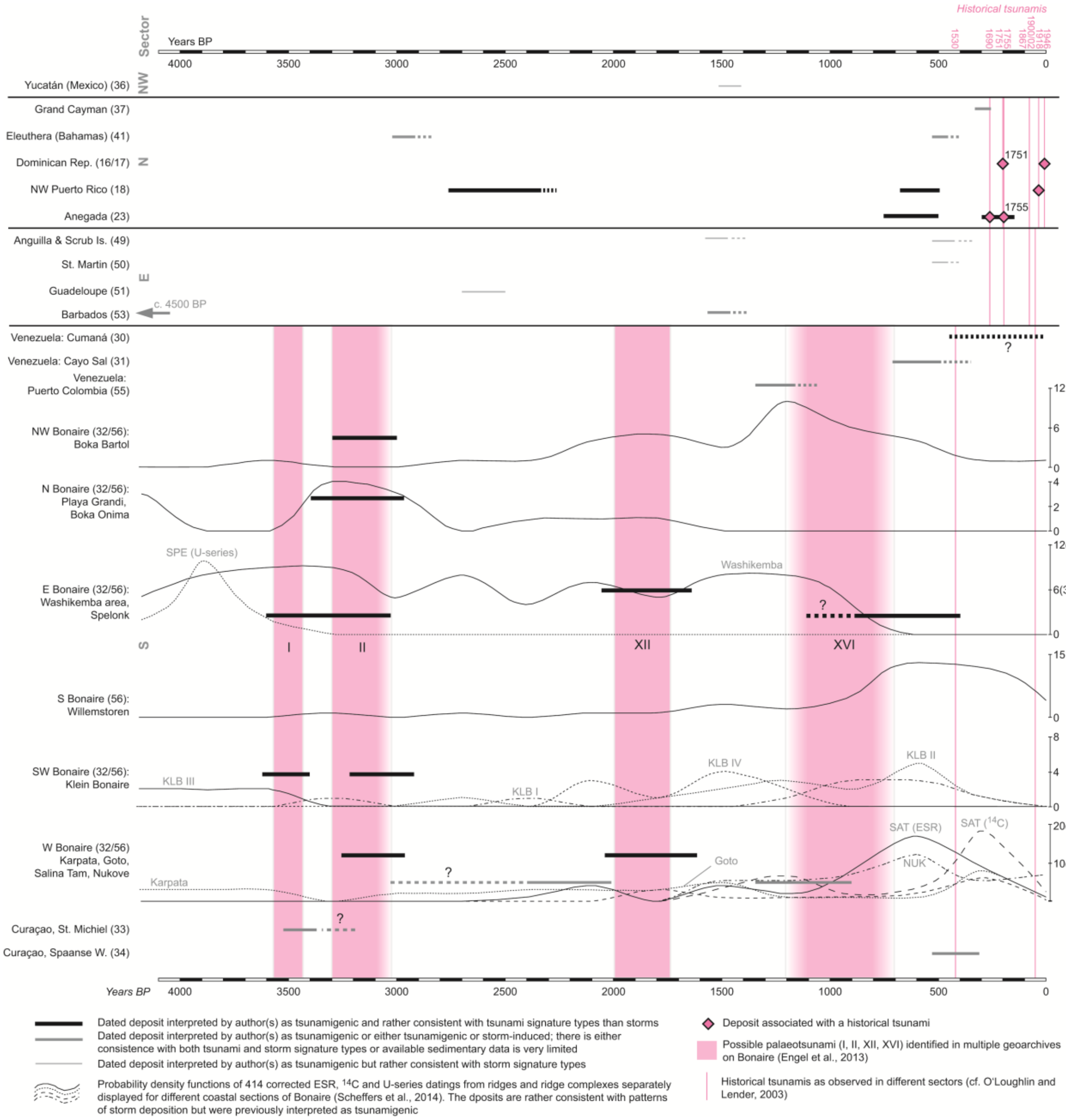
Historical tsunamis
1530
1690
1751
1755
1867
1900/02
1918
1946
Sector
Years BP
4000
3500
3000
2500
2000
1500
1000
500
0
NW
Yucatán (Mexico) (36)
N
Grand Cayman (37)
Eleuthera (Bahamas) (41)
Dominican Rep. (16/17)
NW Puerto Rico (18)
Anegada (23)
1751
1755
E
Anguilla & Scrub Is. (49)
St. Martin (50)
Guadeloupe (51)
Barbados (53)
c. 4500 BP
S
Venezuela: Cumaná (30)
Venezuela: Cayo Sal (31)
Venezuela: Puerto Colombia (55)
NW Bonaire (32/56): Boka Bartol
N Bonaire (32/56): Playa Grandi, Boka Onima
E Bonaire (32/56): Washikemba area, Spelonk
SPE (U-series)
Washikemba
I
II
XII
XVI
S Bonaire (56): Willemstoren
Age frequency
SW Bonaire (32/56): Klein Bonaire
KLB III
KLB I
KLB IV
KLB II
W Bonaire (32/56) Karpata, Goto, Salina Tam, Nukove
Karpata
Goto
SAT (ESR)
SAT (14C)
NUK
Curaçao, St. Michiel (33)
Curaçao, Spaanse W. (34)
12
6
0
4
2
12(6)
6(3)
15
8
20(12)
10(6)
?
Dated deposit interpreted by author(s) as tsunamigenic and rather consistent with tsunami signature types than storms
Dated deposit interpreted by author(s) as tsunamigenic or either tsunamigenic or storm-induced; there is either consistence with both tsunami and storm signature types or available sedimentary data is very limited
Dated deposit interpreted by author(s) as tsunamigenic but rather consistent with storm signature types
Probability density functions of 414 corrected ESR, 14C and U-series datings from ridges and ridge complexes separately displayed for different coastal sections of Bonaire (Scheffers et al., 2014). The dposits are rather consistent with patterns of storm deposition but were previously interpreted as tsunamigenic
Deposit associated with a historical tsunami
Possible palaeotsunami (I, II, XII, XVI) identified in multiple geoarchives on Bonaire (Engel et al., 2013)
Historical tsunamis as observed in different sectors (cf. O'Loughlin and Lender, 2003)

Fig. 10